Chronic liver infections: New *in-situ* insights into the dynamic regulation of exhausted CD8+ T cell subsets

Von der Fakultät für Lebenswissenschaften

der Technischen Universität Carolo-Wilhelmina zu Braunschweig

zur Erlangung des Grades eines

Doktors der Naturwissenschaften

(Dr. rer. nat.)

genehmigte

D i s s e r t a t i o n

von Kingsley Gideon Kumashie
aus Sasieme / Ghana

1. Referentin oder Referent: Prof. Dr. Susanne Engelmann
2. Referentin oder Referent: Prof. Dr. Dagmar Wirth

eingereicht am: 19.02.2020

mündliche Prüfung (Disputation) am: 20.05.2020

Druckjahr 2020

Vorveröffentlichungen der Dissertation

Teilergebnisse aus dieser Arbeit wurden mit Genehmigung der Fakultät für Lebenswissenschaften, vertreten durch die Mentorin der Arbeit, in folgenden Beiträgen vorab veröffentlicht:

Tagungsbeiträge

1. Elucidating the mechanisms underlying early fate decision making of T cells upon hepatic antigen recognition (Poster), 13th Spring School on Immunology, Ettal Germany (5.10.2017 - 10.03.2017)
2. T cell responses to high antigen density in the liver is regulated by NK and Kupffer cells (Poster), 47th DGfi meeting on Immunology, Erlangen Germany (12.09.2017 - 15.09.2017)
3. The role of CXCR5+ T cells in chronic liver infection (Talk), 12th German Meeting on Immune regulation, Berlin Germany (28.05.2018 - 30.05.2018)
4. Cytotoxic T cell response to chronic liver antigen consists of stem-like CXCR5+ T cells with potent memory properties (Poster), XIII World Immune regulation Meeting, Davos Switzerland (06.04.2019 - 09.04.2019)
5. Cytotoxic T cell response to chronic liver antigen consists of a fraction of potent memory-like CXCR5+ T cells (Poster), 1st Immunology and Inflammation meeting, Berlin Germany (24.02.2019 - 26.02.2019)
6. Host conditioning with CpG potentiates differential proliferation of exhausted CD8 T cell subsets and improves cytotoxicity (Poster), II Joint Meeting of DGfi and SIICA, München Germany (10.09.2019 - 13.09.2019)
7. Kupffer cell independent mechanism regulate T cell function in the liver (Poster), HZI PhD Retreat, 2017
8. Remodeling T cell responses to high antigen expressing hepatocytes (Talk), HZI PhD Retreat, 2018
9. Chronic liver infection: Do CXCR5+ T cells play a role? (Talk), HZI PhD retreat, 2019
10. Elucidating the mechanisms underlying early fate decision making of T cells upon hepatic antigen recognition (Poster), HZI PhD symposium, 2016
11. Remodeling T cell responses to high antigen expressing hepatocytes (Talk), HZI PhD symposium, 2017

12. The role of tissue resident CXCR5+ T cells in chronic liver infection (Talk), HZI PhD symposium, 2018

Table of contents

Abstract

Chronic hepatotropic viral infections represent a major challenge in current medicine. Chronic infections are a consequence of dysfunctional CD8+ T cell responses which impair effective viral clearance. Dysfunction in CD8+ T cells, as a result of T cell exhaustion, lift the break on viral replication, thereby promoting the development of liver diseases. Currently, immunomodulatory strategies are being explored as an attractive option to reinvigorate exhausted T cells in chronic infection as well as in cancer. However, the dynamic regulation of exhausted T cells as well as the mechanisms enforcing reinvigoration of exhausted T cells in the liver are not clearly defined. In this study, an OvaXCre transgenic mouse model characterized by antigen expression specifically in the liver was used to elucidate the dynamic differentiation and reinvigoration of exhausted T cells in the liver. The expression of antigen in a fraction of hepatocytes mimics persisting antigen situation in chronic liver infections. In this regard, it was observed that host conditioning with CpG oligodeoxynucleotides (CpG ODN), which modulates the liver environment, translates into eradication of chronic Ova-antigen from the liver by the action of cytotoxic T cells, probably as a result of exhausted T cell reinvigoration. Interestingly, antigen clearance was accompanied with an extreme loss of antigen specific T cells and T cell stemness. In depth characterization of exhausted T cells in liver revealed two distinct T cell subsets, identified by presence or absence of the chemokine receptor CXCR5. CXCR5+ and CXCR5- T cells exhibit profound differences in cytotoxic, effector and memory functions, with all these functional capacities skewed towards CXCR5+ T cells in the liver. The CXCR5+ T cells are follicular-like and liver resident cells by virtue of upregulation of the transcription factors Bcl6 and LFA-1. Robust and efficient mitochondria activities were manifested in CXCR5+ T cells, which was in contrast to CXCR5- T cells. Importantly, CXCR5+ T cells demonstrated a significant nutrient acquisition advantage and show enhanced recall responses and self-maintenance *in vivo*. In sum, these data show that CpG ODN immunomodulation reinvigorates exhausted T cells. While heterogeneity exists in the intrahepatic pool of exhausted T cells, the CXCR5+ T cell subset plays a major role in eliminating chronic antigen expression in liver. Therefore, this subset may be of interest for the development of novel immune based therapeutic strategies against chronic liver infections.

Graphical summary

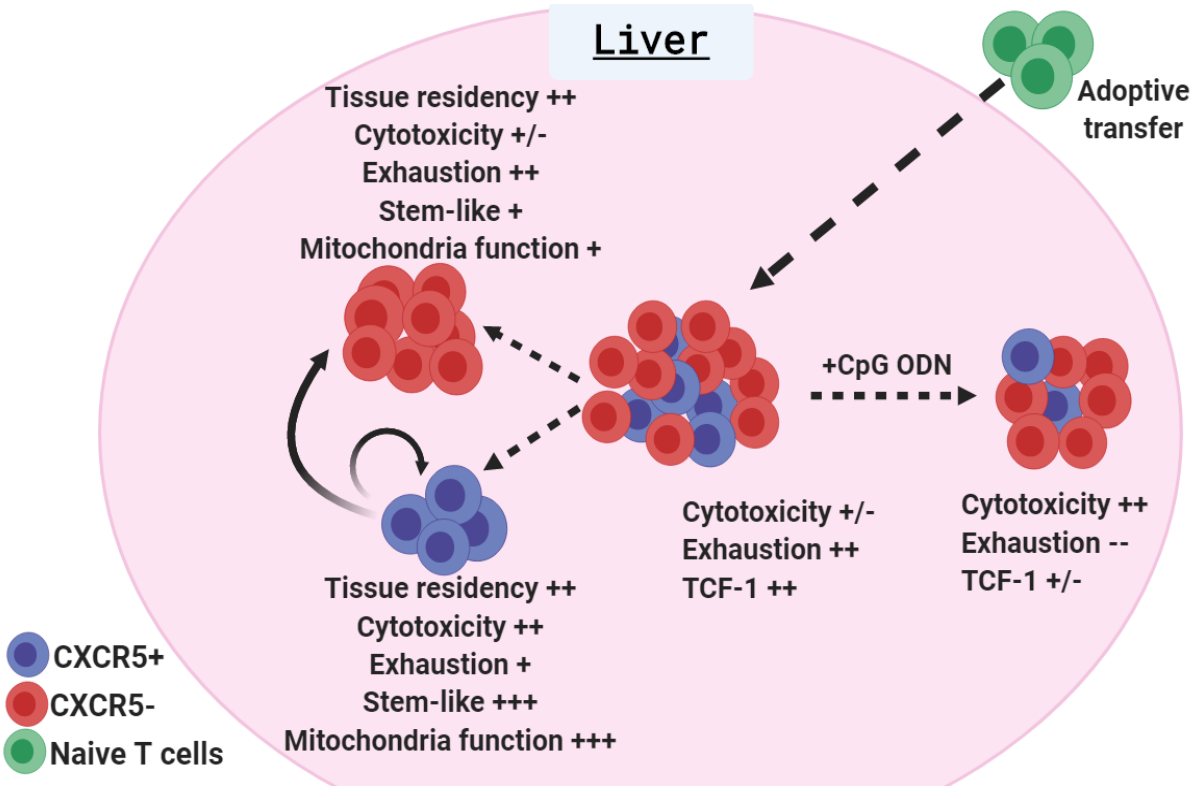

Highlights

- *CD8+ T cells differentiate into CXCR5+ and CXCR5- T cells during chronic antigen stimulation.*
- *CXCR5+ T cells undergo self-renewal, enhanced self- maintenance and differentiate into CXCR5- T cells.*
- *Improved mitochondria function is restricted to CXCR5+ cells in the pool of exhausted T cells*
- *Enhanced cytotoxic T cell function in the liver is associated with CXCR5+ T cells*
- *CXCR5+ and CXCR5- T cells are bona fide tissue resident T cells*
- *Host conditioning with CpG ODN possibly reinvigorate exhausted CD8+ T cells leading to antigen eradication.*
- *Host conditioning with CpG ODN reduces the expression of TCF-1 and CXCR5 on antigen specific CD8+ T cells.*

1 Introduction

1.1 Immune response to vaccination, acute and chronic viral infection

When pathogens breach the mucosal or epithelia barriers, professional antigen presenting cells (APCs) can phagocytose, process and present pathogen specific antigens via the major histocompatibility molecule (MHC) I or MHC II antigen presentation pathway. These events are key to establishing a potent immune response through facilitated CD8+ or CD4+ T cell activation, respectively. During acute virus infection or vaccination, naïve CD8+ T cells recognize antigen displayed on MHC I. Of note, vaccination entails the use of attenuated viruses, which mimics the natural course of acute infection. After antigen recognition, CD8+ T cells undergo differentiation and clonal expansion to generate effector T cells (Teff) (**Figure 1.1**). Clonal expansion produces a sizeable numbers of antigen specific CD8+ T cells which control pathogen[1,2]. Control of pathogen is mediated by expression of effector molecules perforin, granzyme B (GZMB), interferon gamma (IFN-γ) and tumor necrosis factor (TNFα). In addition, CD8+ T cells express chemokines and homing receptors which foster migration into peripheral tissues[1–3]. All these processes help to contain pathogens. The differentiation process of T cells post-activation is associated with epigenetic, metabolic and transcriptional changes. After antigen clearance, most effector cells undergo apoptosis leaving ca. 5 - 10%, which differentiate into memory CD8+ T cells (Tmem)[3] (**Figure 1.1**). Tmem downregulate effector programs and upregulate stem-like properties, which ordain long-term maintenance in the absence of antigens and rapid response to previously encountered pathogens[1,2,4]. In some cases, these responses cannot give rise to efficient pathogen clearance as a result of chronic infection, characterized by persistent antigen presentation. Indeed, contrary to acute infection or vaccination, in chronic infection or cancer, efficient Tmem fail to develop leading to the establishment of T cell exhaustion[5,6](**Figure 1.1**). Tex are characterized by loss of effector function, upregulation of inhibitory receptors (IRs), and deranged epigenetic, metabolic as well as transcriptional profile. The insights into Tex were initially obtained from mouse model of lymphocytic choriomeningitis virus (LCMV) infection[3,6–8]. It is now well documented that Tex occurs in chronic human infections such as hepatitis B virus (HBV) and hepatitis C virus (HCV), which target the liver. Of note, the liver plays important roles in physiological function necessary for efficient homeostasis, however chronic HBV and HCV infection compromises these functions.

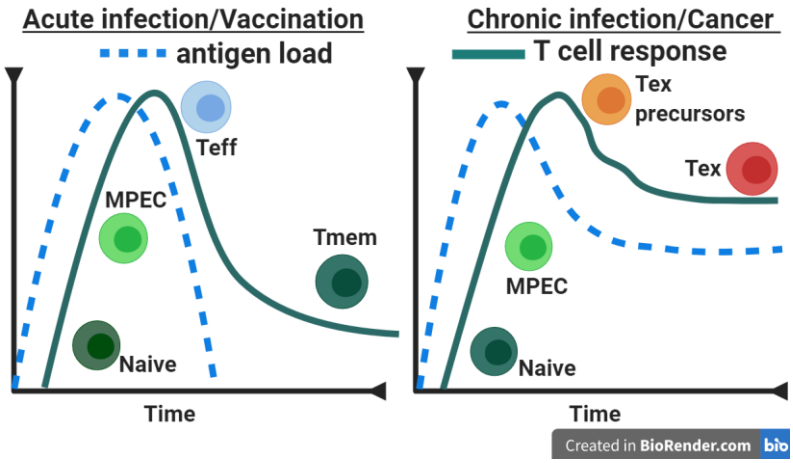

Figure 1.1: T cell response to acute infection or vaccination and chronic infection or cancer

Naïve T cell activation results in differentiation into memory precursor T cells (MPECs), which transition into fully differentiated Teff to eradicate antigen (in vaccination or acute infection) or exhausted T cell (Tex) precursor. In the settings of acute infection and vaccination, most effector cells undergoes apoptosis at the end of the immune response and the remaining cells differentiate into Tmem. These cells can either become tissue resident or peripheral memory T cells. In chronic infection or cancer, precursor Tex fail to eradicate antigen and gradually develop into full exhausted cells. Tex in most cases undergo apoptosis resulting in the loss of specific T cells in the presence of antigen[ℜ].

1.2 Liver function

The liver is a unique organ, which functions as a physiological sink for blood supply from gut and the circulatory system. It is critical for the production acute phase proteins (e.g. complement proteins), metabolism and sequestration of toxins[9,10]. The liver is made up of repetitive units – hepatocytes and liver sinusoidal endothelial cells (LSECs) (**Figure 1.2**). Blood entering the liver flows at a slow pace due to the capillary like sinusoids[11]. The hepatic sinusoids are lined by LSECs, which contain fenestrations (**Figure 1.2**). These fenestrations provide a gateway for blood into the underlying hepatocyte[12]. Apart from the hepatocytes and LSECs, which make up ca. 78 - 80%[13] of the liver, the liver consists of immune cells including APCs (innate immune cells) such as macrophages (known as Kupffer cells; KCs) and dendritic cells (DCs), as well as natural killer cells (NK) cells. The adaptive immune cells are made up of T cells, B cells and NKT cells[14,15]. The infinitesimal flow rate of blood in the liver vasculature enhances pathogen capture by APCs[9,16]. Indeed, the positioning of the liver relative to the gut, in itself, implicates the importance of the liver as an important organ for removing pathogens which might breach the gut

[ℜ] Figure by author

epithelium[17,18]. Hepatocytes are separated from the blood stream by LSECs, and the space between hepatocytes and LSECs is referred to as the space of Dissé. In the space of Dissé are stellate cells (**Figure 1.2**)[12,19]. The presence of high numbers of diverse immune cells in the liver reinforces the notion that immunity can be induced in the liver and this may be tightly regulated.

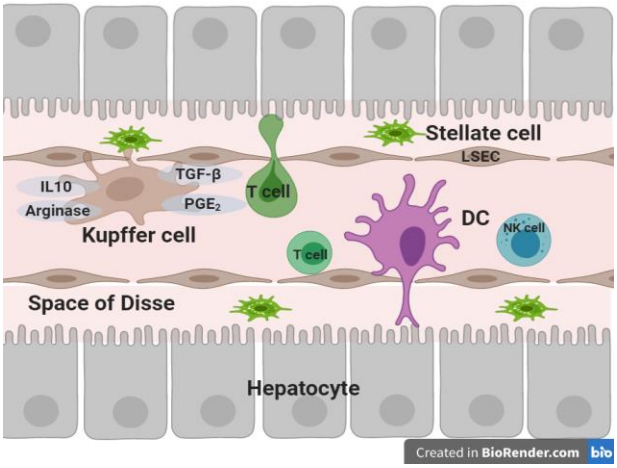

Figure 1.2: Architectural organization of the liver

Blood is supplied to the liver via the hepatic artery and the portal vein and circulating cells may carry pathogen derived molecules, nutrients and oxygen into the liver. In the liver, the blood flow becomes infinitesimally slow and pressure drop. This facilitates enough bathing of Kupffer cells and LSECs, thereby allowing them to sequester pathogens from the blood. Under appropriate conditions, LSECs and Kupffer cells can initiate or activate T cell response. In addition, T cells in the liver have the potential to scan hepatocytes for possible antigen via fenestrations in LSECs. Between LSECs and hepatocytes is the so-called space of Dissé, in which hepatic stellate cells reside[∞].

1.2.1 Induction of immunity and tolerance in the liver

The liver is not considered as a classical secondary lymphoid organ, but it has the potential to induce functional adaptive immunity[10,20,21]. In spite of the plethora of APCs in the liver and the ability to recruit different immune cells, the generation of coordinated adaptive immunity in the liver is not an efficient process. This inefficiency is particularly due to the physiological function of the liver – a frontline filter for self and non-self-antigens[21–23]. Thus, liver immune responses are orchestrated to maintain a balance between tolerance to self-antigens and immunity to non-self-antigens. Although liver APCs are capable of inducing T cell responses, at physiological condition they have a default program to mediating tolerance[13,15,24,25]. The priming of T cells by these tolerant APCs drives compromised antigen specific cytotoxic T cell expansion. This hypo-immune

[∞] Figure by author

responsiveness in the liver is exemplified by the success of allogeneic transplantation and the exploitation of the liver environment by HCV and HBV, causing persistent infection[21,24]. At baseline level, KCs, LSECs, DCs and hepatocytes suppress immunity as a result of low expression of MHC, low or lack of co-stimulation, high programmed death ligand (PD-L) 1 and galectin 9 as well as constitutive expression of anti-inflammatory cytokines transforming growth factor (TGF)-β and interleukin (IL)-10[21,24,26–28].

1.2.2 Hepatocytes and liver sinusoidal endothelial cells

LSECs can function as professional APCs due to efficient cross-presentation of exogenous antigen in MHC I and MHC II context. In this fashion, LSECs can activate and tolerize T cell subsets to blood and gut derived antigens[29,30] (**Figure 1.3**). In addition to LSECs, hepatocytes which make up ~80 % of liver, can also function as APCs[31]. They can detect, and present pathogen associated antigens to CD8+ T cells. Indeed, they possess the MHC I antigen processing machinery and also express costimulatory molecules, which foster T cell activation[32,33]. Current observation indicate that naïve T cells interact with hepatocytes in an intracellular adhesion molecule 1 and MHC-dependent fashion, resulting in T cell activation[21,22,31]. A more recent study demonstrated that CD8+ T cells crawl along the liver vasculature, actively patrolling and extending protrusions through the fenestrations in the sinusoid (**Figure 1.2**)[34]. This facilitates the ability to scan hepatocytes for possible antigen. Although hepatocytes are known to constitutively express MHC I, under inflammatory condition, they can express MHC II[31].

1.2.3 Dendritic and Kupffer cells

DCs in the liver also possess a default tolerizing capacity. They are broadly divided into two categories, plasmacytoid DCs (pDCs) and myeloid-derived DCs (mDCs)[15,21,26,31]. Studies have demonstrated that they efficiently present endogenous antigen, but poorly prime T cells compared to DCs from other tissues[24]. The inefficient priming of T cells is partly due to potent anti-inflammatory mediators IL-10 and indole-amine 2, 3-dioxygenase (IDO) production[22,24,35] (**Figure 1.3**). These anti-inflammatory mediators alongside constitutively high levels of PD-L1[31] (**Figure 1.3**) attenuate T cell responses.

KCs are arguably the most profound APCs in the liver. They form a large chunk of liver macrophage, constituting 80 - 90% of liver macrophage population. KCs are non-motile, positioned strategically to sequester antigens and pathogens from blood[24,36]. Continual exposure

of KCs to low levels of gut derived pathogen associated molecular patterns (PAMPs) such as lipopolysaccharide (LPS) dampens KCs' lymphocyte activation property[37–39]. The failure to induce immunity to gut derived antigens may be pre-ordained to protect the host from unwarranted inflammation. Although KCs poorly induce potent T cell activation, the presence of PAMPs such as Toll-like receptors (TLR) 3 and 9 as well as inflammatory cytokines can switch KC towards a potent inducer of T cell activation[24,31,40].

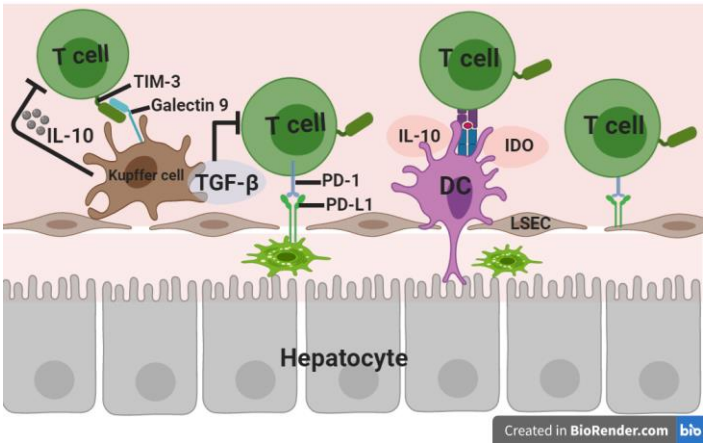

Figure 1.3: Mechanisms inducing tolerance in the liver

Multiple layers of immune regulatory mechanisms are present in the liver. IDO is expressed at high levels and is responsible for amino acid metabolism, thereby depriving T cells from essential amino acid needed for function. IL-10 produced by Kupffer cells dampens local proliferation and efficient T cell reactivity to infection. Several inhibitory ligands expressed by immune and non-immune cells in the liver also diminishes T cell response by ligating corresponding receptors on T cell. These events may also generate tolerant T cell in the liver, even in the presence of liver infection[∂].

1.3 Chronic HBV and HCV infection

HBV and HCV are enveloped hepatotropic viruses, which can be transmitted parenterally. They are only permissive in human liver and can establish long lasting infection. In HCV patients, the frequency of infected hepatocytes is ca. 1 - 54% and the frequency correlates with serum viral load[41,42]. In HBV, up to 100% of hepatocytes can be infected[10,21,42]. Contrary to the well-known concept of professional APCs priming antiviral CD8+ T cell response, a growing body of evidence suggest that infected hepatocytes can prime antiviral CD8+ T cell responses[24]. CD8+ T cells are central to hepatotropic viral control. This proposal was based on the findings that in acute infection,

[∂] Figure by author

direct correlation exist between virus clearance and emergence of antigen specific CD8+ T cells in the liver and peripheral blood of infected chimpanzees[43,44]. Also, lack of CD8+ T cells enhanced prolonged viremia in acute HBV and HCV infection in chimpanzees[44].

In persistent HBV and HCV, despite CD8+ T cell priming, infection progresses to end-stage liver disease – liver fibrosis and ultimately carcinoma. End-stage liver disease is exacerbated by T cell exhaustion and subsequent attrition of Tex[45,46]. In fact, studies evaluating T cell function in HBV and HCV infected patients demonstrate reduced proliferation and antiviral properties – a hallmark of Tex[8,21,46,47]. These effects were closely linked to co-expression of T cell IRs such as PD-1, cytotoxic T-lymphocyte antigen 4 (CTLA-4), T cell immunoglobulin molecule 3 (TIM-3), or 2B4 (CD244)[7,48]. Numerous factors have been suggested to drive T cell exhaustion in HBV and HCV infection including antigen load and inhibitory receptor signaling in T cells (discussed in **1.4**).

1.3.1 Clinical prospects for chronic liver infection

Direct acting antivirals (DAAs) drugs are now available in the clinics for treating chronic HCV infection. Sadly, treatment with DAAs are limited due to the high cost intensiveness[49]. Also, reinfection can occur after successful therapy, despite reports of partial reinvigoration of exhausted T cells[50]. In HBV infection, treatment with antiviral nucleoside and nucleotide analogues have shown success in suppressing viral replication. This facilitate progressive restoration of HBV specific T cell responses[51]. Nonetheless, HBV cannot be eradicated, due to the presence of covalently closed circular DNA in the cell. Currently, there is a general lack of immune mediated strategies which can elicit robust responses against HBV and HCV, which in addition boost the development of an efficient memory T cell pool. This has prompted, in recent years, the exploitation of strategies to restore T cell response in chronic HBV and HCV infection. These consist of direct (discussed in **1.5**) and indirect approaches. The indirect approaches entails the use of TLRs, which modulate T cell function via other immune cells[52]. Indeed, application of TLR7 agonist (GS-9620), which has been suggested to boost DC priming, facilitated the expansion of HBV specific T cells in patients. In spite of TLR7's modulatory effect on T cells, this treatment failed in phase II clinical trials in chronic HBV infection[52]. In addition, TLR9 agonist, also known as CpG oligodeoxynucleotide (CpG ODN) has been tested in mouse model of chronic liver infection[40]. This treatment has been shown to inure T cell function, via the formation of myeloid structures in the liver[40].

1.4 Factors driving T cell exhaustion

The initial developmental pathway of T cell exhaustion is currently not well understood. However, the general three-signal model of T cell activation could provide a useful structure for examining Tex development[3](**Figure 1.4).** The three-signal model integrates signals from antigen loaded on MHC (signal 1), negative co-stimulation from IR (signal 2) and signal 3 is mediated via inflammatory mediators[3](**Figure 1.4**). Repetitive antigen stimulation of T cells is a core driver of T cell exhaustion, but other factors are involved. A well-known event which was suggested to promote T cell exhaustion in chronic viral infection and cancer is the lack or poor help from CD4+ T cells[53].

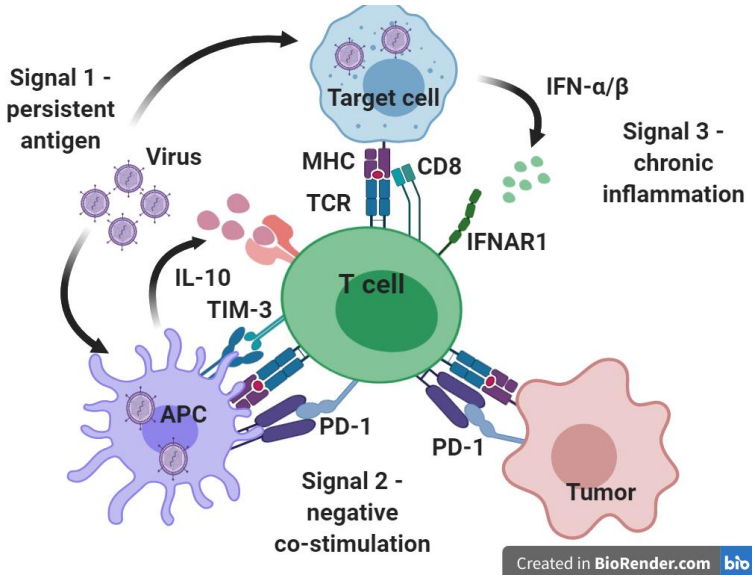

Figure 1.4: Signaling model for the development of T cell exhaustion

Signal 1 is mediated by persistent antigen from tumor or chronic virus infection, and it drives overwhelming activation of T cells, which subsequently results in the expression of inhibitory markers. These inhibitory markers are ligated by their corresponding ligand on APCs, target or tumor cells which provides negative co-stimulation signal (signal 2) in T cells. This prevents optimal Teff function, and in response to persistent antigen, APCs, tumor or target cells contribute to the establishment of chronic inflammation by producing pro- (IFNα/β) and anti-inflammatory (IL-10) cytokines (signal 3). These further potentiate the development of exhaustion[3].[§]

1.4.1 Persistence and duration of antigen exposure

A key feature of human and animal models of chronic viral infection and cancer is persistent antigen exposure to T cells[8,54–56]. Chronic viral infection such as LCMV, HBV, HCV and human

[§] Figure by author

immunodeficiency virus (HIV) are characterized by extreme T exhaustion, which is consistent with high antigen stimulation[57–59]. But the duration of exposure also contributes to severe T cell exhaustion. In fact, in adoptive transfer studies, CD8+ T cells primed during chronic virus infection within two weeks can recover and develop into memory cells if the primed cells were transferred into uninfected mice[60,61]. This suggest that duration of persistent antigen exposure drives T cell exhaustion. Also, in chronic viral infection, CD8+ T cell responses erode gradually with time, reinforcing the notion that exhaustion severity is gradual and is linked to the antigen burden as well as the duration of exposure[3].

1.4.2 Cytokines promoting T cell exhaustion

T cell activation and differentiation is shaped by the cytokine and inflammatory milieu[62]. High level of inflammatory cytokines (e.g. IFN-α/β) during chronic viral infections and cancer regulates the expression of regulatory cytokines (such as IL-10 and TGF-β), and T cell inhibitory receptors and ligands, which usually contribute to T cell exhaustion[4,63]. Of note, these inflammatory cytokines alone do not drive exhaustion[63]. IL-10 and TGF-β may impact on T cell function directly or indirectly via APCs or both[64,65].

1.4.3 Alteration in metabolic program

In response to activation and changing environmental cues, lymphocytes have a trademark feature of undergoing metabolic plasticity. After activation in acute viral infection, CD8+ T cells transition from their dependence on mitochondrial oxidative phosphorylation (OXPHOS) to glycolysis[66]. This is necessary to meet the bioenergetics demand of activation. Changes in metabolism is, at least partly a consequence of T cell receptor (TCR) mediated signaling via phosphoinositide 3-kinase (PI3K) and mammalian target of rapamycin (mTOR)[66]. After the peak of effector differentiation, precursor memory cells shift their metabolic state back to OXPHOS, but can also utilize fatty acid oxidation[67,68].

Transcriptionally, Tex display significant alteration in metabolic and citric acid cycle genes[56]. This observation suggests that exhaustion facilitates metabolic dysregulation. *In vivo* studies showed that exhausted T cells display a dysfunctional metabolism such as suppressed cellular respiration, reduced glucose uptake and deregulated mitochondria bioenergetics[69]. Peroxisome proliferator-activated receptor γ coactivator 1α (PGC-1α) and Fox-head box O1 (FoxO1) are key pathways

implicated in defective metabolism in exhausted T cells. Indeed, PD-1 signaling regulated early glycolytic and mitochondria alterations and represses PGC-1α transcriptional coactivator[70].

1.5 Modulating T cell exhaustion – potential therapeutic targets

Sustained expression of IRs is a hallmark of exhausted CD8+ T cells. IRs are mostly induced upon T cell activation or antigen recognition, suggesting that IRs are also expressed on functional Teff, albeit transient[5]. Tex usually co-express other IRs alongside PD-1, providing synergistic inhibitory effect. Currently, therapeutic modulation of exhaustion is largely focused on PD-1 and CTLA-4[5,71]. Although therapeutic agents for modulating other IR pathways such as leukocyte activation gene (Lag)-3 and TIM-3 exist.

1.5.1 PD-1

PD-1 is transmembrane protein receptor with a cytoplasmic region consisting of immunoreceptor tyrosine-based inhibitory motif (ITIM) and immunoreceptor tyrosine-based switch motif (ITSM). PD-1 ligation promote the phosphorylation of tyrosine in ITIM and ITSM motifs[72]. This drives the recruitment of Src homology 2 domain-containing tyrosine phosphatase 2, which attenuates proximal and distal mediators of T cell activation such as PI3K-Akt and Ras-MEK-ERK pathways[73,74]. In Tex, PD-1 promoter is always accessible, even in the absence of antigenic stimulation, unlike in Tmem cells[75,76]. Of note, lack of PD-1 does not prevent T cell exhaustion, demonstrating that development of exhaustion is independent of PD-1 signaling. Strikingly, lack of PD-1 potentiate severe exhaustion and poor maintenance of Tex[77,78]. These data suggest that PD-1 is involved in antagonizing TCR signaling, thereby limiting severe exhaustion.

Blockade of PD-1 pathway rejuvenates Tex cells via reshaping their metabolism, promoting proliferation and increasing the expression of effector molecules[8]. In mouse models of cancer and chronic infection as well as in non-human primate of HCV infection, PD-1 blockade reduces tumor growth and improves viral control[8,79]. These observations revealed two facts about Tex: (1) Tex are not terminally dysfunctional and (2) Tex are not anergic or unable to initiate TCR signaling. Indeed, blocking PD-1 rewired the anabolic metabolism and glycolysis in an mTOR dependent manner in Tex[79]. In addition, there was an increased uptake of glucose, largely by PD-1 low subset of exhausted T cell, the so called ’stem-like’ Tex subset[70].

1.5.2 CTLA-4

CTLA-4 competes with the positive CD28 costimulatory molecule, by binding to CD80/86 (B7) which may recruit phosphatases that shutdown TCR/CD28 signaling[80]. CTLA-4 blockade antibody was first used to treat advanced melanoma[81]. Subsequent studies showed higher efficacy when combined with PD-1 blockade. Indeed, PD-1 blockade failed to restore functionality in CTLA-4+PD-1+ CD8+ T cells, however CTLA-4 and PD-1 therapy reinvigorated HCV specific CD8+ T cells *in vitro*[82].

1.5.3 Co-stimulatory molecules

Currently there is a conscious effort to target positive co-stimulatory signals to improve exhausted T cell function[83]. CD28 is a major T cell costimulatory molecule, and positive CD28 signal interference by PD-1 and CTLA-4 is a testament to the fact that targeting CD28 may be beneficial to exhausted T cells[3,5]. Positive co-stimulation of CD28 amplifies TCR signaling; upregulating IL-2 and B cell lymphoma (Bcl)-2 expression. These modulates epigenetics, survival and metabolism of T cells[84,85]. CD28 dependent signaling is necessary for virus specific T cell reinvigoration following PD-1 blockade[86]. Thus, loss of CD28 on Tex hindered the expansion of virus specific T cells in the presence of PD-1 blockade[86] (**Figure 1.5**). A similar observation was made in tumor models suggesting that the CD28/B7 signaling pathway may be a determinant of PD-1 blockade success in cancer patients[5] (**Figure 1.5**). However, direct CD28 targeting to improve immunotherapy may be problematic due to the spectrum of CD28 expression on immune cells coupled to immuno-toxicity observed in clinical trials with CD28 super-agonist[5].

TNF receptor family co-stimulatory molecules OX40, CD27, and 4-1BB are being exploited in cancer therapy[4]. These play important roles in clonal expansion, differentiation and survival of effector cells. Agonist targeting 4-1BB synergizes with PD-L1 blockade in rejuvenating Tex[87]. Interestingly, continuous CD27 signaling results in severe Tex[88]. The molecular underpinnings of why TNFR signaling pathways function dichotomously on T cells are not clearly understood.

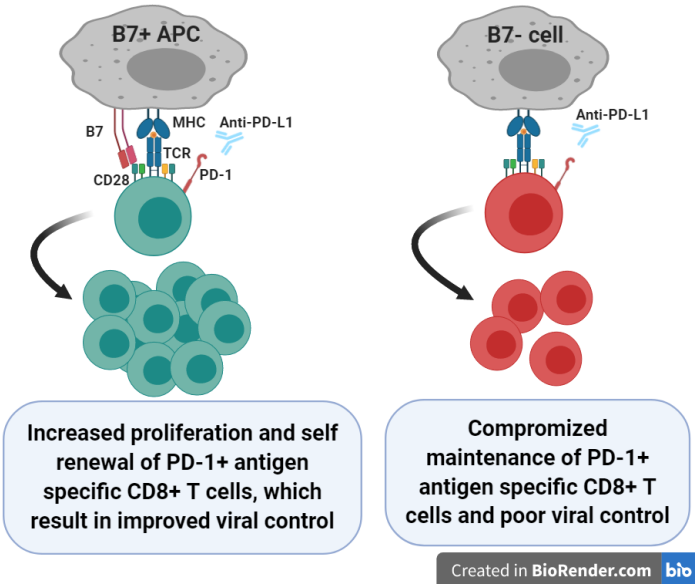

Figure 1.5: Reinvigorating exhausted T cells in PD-1 immunotherapy is CD28 dependent

B7 is a co-stimulatory ligand expressed on antigen presenting cells, and this mediates signaling in T cells for efficient T cell expansion and function. The corresponding receptor for B7 on T cells is CD28. During PD-L1 therapy, B7 mediates signaling which promote expansion and self-maintenance of Tex. In the absence of B7, immunotherapy with PD-L1 fails to achieve full potential of expansion and maintenance of Tex. Both CD28 signaling and PD-L1 blockade improves T cell function to controlling chronic virus infection compared to PD-L1 blocked without CD28 signaling.[δ]

1.6 Transcriptional and epigenetic regulation of exhausted T cells

1.6.1 T-bet, Eomes and TCF-1 regulation in exhausted T cells

Integrated transcriptional and network analyses show altered expression pattern of key transcription factors in exhausted T cells[89,90]. T-box factors (T-bet), Eomesodermin (Eomes) and T cell factor 1 (TCF-1) regulate Teff and Tmem, however in exhausted T cells the same transcription factors are altered and have distinct transcriptional circuit[89,90]. T-bet and Eomes play critical roles in Tmem and Teff CD8+ cell development[91]. In acute infections, T-bet drives Teff and KLRG-1+ terminal Teff development while Eomes foster Tmem development[92–94]. However, in chronic infection, T-bet and Eomes have distinct functions. Indeed, efficient T cell responses can be mounted in the absence of T-bet and Eomes in acute infection but this is not feasible in chronic viral infections[89]. Analysis of transcriptional circuits showed that Eomes was involved in distinct transcriptional networks in Tmem and Teff compared to Tex[90].

[δ] Figure by author

Initiation of T cell development in the thymus is TCF-1 regulated. It is also re-used in Tmem where TCF-1 orchestrate Eomes-IL2Rβ circuitry[95]. TCF-1 plays a similar role in Tex, as in Tmem, by maintaining stemness[96]. Furthermore, TCF-1 and Bcl6 have been suggested to co-operate in order to antagonize type 1 interferon pro-exhaustion effect, favoring stemness in Tex[97].

1.6.2 Epigenetic landscape of T cell exhaustion

Advances in genome profiling using ATACseq[98] have revealed the underlying epigenetic landscape in Tex. This technology allows for the analysis of accessible chromatin in Tex, and has revealed that distinct epigenetic signatures regulate Tex, Teff and Tmem[99,100]. These epigenetic signatures consist of alterations in IRs, transcription factors and genes modulating TCR signaling pathways, co-stimulatory, cytokine and metabolic signaling[99,100]. These unique epigenetic landscapes were similar for Tex in chronic human and mice infections[99–101]. The close association of epigenetic changes to Tex have significant repercussions for immunotherapy. Indeed, anti-PD-L1 treatment has the potential to restore some function in Tex, however the rejuvenated CD8+ T cells show minute epigenetic changes[100]. In concordance, after withdrawal of immunotherapy, the original epigenetic state was restored[100]. A more recent study reported that DNA methyltransferase 3A (DNMT3A) is essential for establishing exhaustion specific epigenetic landscape. DNMT3A initiates *de novo* DNA methylation[102].

1.7 Differentiation dynamics of exhausted CD8+ T cells

During chronic virus infection and cancer, it is now accepted that Tex undergo progressive and dynamic developmental processes. Recent data suggest that Tex are made up of distinct heterogeneous lineages. However, the precise level of heterogeneity is still a subject of intense investigation, but the underlying phenomena suggests a hierarchical proliferation necessary for long term maintenance of Tex. In chronic viral infections and probably in cancer, Tex develop from precursor KLRG-1^{lo} effector CD8+ T cells, which are known precursors of Tmem in acute infection[60]. Importantly, senescent KLRG-1+ effector T cells do not give rise to Tex[60], indicating that exhausted and senescent T cells emerge from distinct differentiation pathways. PD-1 and CD44 levels were the first markers exploited in distinguishing between subsets of Tex with distinct functions[3]. A careful examination of Tex shows the presence of PD-1^{hi} and PD-1^{int} cells[71]. Furthermore, the antigen specific PD-1^{hi}CD44^{int} cell subset was more functionally exhausted compared to the PD-1^{int}CD44^{hi} counterpart[71] (**Figure 1.6**). Also, the PD-1^{int} subset was more

responsive to PD-1 blockade, whereas PD-1^{hi} cells largely failed to response to PD-1 blockade therapy, suggesting terminal exhaustion[71] (**Figure 1.6**). Follow up studies demonstrated that the PD-1^{int} cell population was largely Eomes^{lo} (**Figure 1.6**)[89]. PD-1^{int}Eomes^{lo} function as [12]progenitors which give rise to PD-1^{hi}CD44^{int}Eomes^{hi} terminal Tex[89](**Figure 1.6**). In sum, these studies identified heterogeneity in Tex, identified stem-like Tex, and defined the pool of Tex mediating responses to immunotherapy.

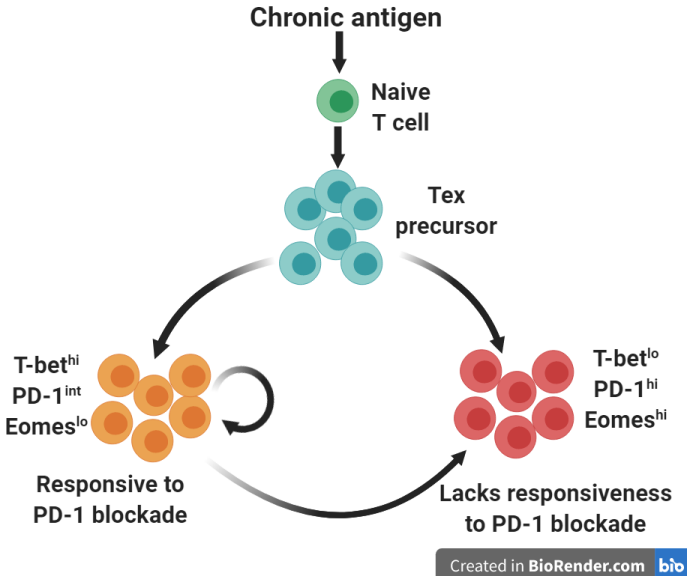

Figure 1.6: Differentiation subsets of exhausted T cells

In chronic antigen stimulation, T cells differentiate into exhausted precursor T cells. The precursor Tex diverge into two subsets of exhausted T cells: PD-1^{hi} and PD-1^{int} subset. The PD-1^{int} cells exhibit characteristics of self-renewal and responsiveness to PD-1 immunotherapy compared to PD-1^{hi} cells, which are terminally exhausted[ץ].

1.7.1 CXCR5+ CD8+ T cells in chronic viral infection

In recent years, more studies set-out to refine and understand the heterogeneity of Tex subsets. These studies used the chemokine receptor CXCR5[103–106], and slamf6[107] as well as the transcription factor TCF-1[96,97]. According to literature, CXCR5+ antigen specific CD8+ T cells which are TCF-1+TIM-3- have been observed in chronic LCMV infection. This subset of cell is stem-like and it is highly responsible to PD-1 blockade pathway, and has the potential to generate terminally exhausted CXCR5-TCF-1-TIM-3+ T cells[103,104]. Furthermore, the antigen specific CXCR5- CD8+ T cells which are TCF-1-TIM-3+ are less responsive to PD-1 therapy, and do not have the potential

[ץ] Figure by author

to differentiate into CXCR5+ T cells. Interestingly, no expression difference in T-bet and Eomes was observed for the progenitor CXCR5+TCF-1+ T cell subset and terminally exhausted CXCR5-TCF-1- cells[103]. This indicates that there may be further heterogeneity in the pool of PD-1^{hi} and PD-1^{int} cells previously described (**1.6**). The progenitor CD8+ T cells were driven by TCF-1/Bcl6 transcriptional network with gene expression profile synonymous to precursor memory CD8+ T cells and follicular helper T cells (Tfh)[97,108,109]. On a mechanistic level, TCF-1 is critical for the CXCR5+ T cell population, which is also in-line with high Tcf-7 (mRNA) expression in PD-1^{int}CD44^{hi} cells[71,90]. CXCR5+ and CXCR5- T cell subsets express PD-1, however, the stem-like CXCR5+ T cells express little to no 2B4 and TIM-3 and possess high expression levels of CD28 and ICOS costimulatory receptors[103,104].

Of note, differences in tissue distribution and localization for these two subsets of CD8+ T cells (**Figure 1.7**) have been described. The stem-like CXCR5+ T cells were localized in the secondary lymphoid organs, whereas the terminal CXCR5- T cells were profoundly found in infected tissues – peripheral tissues and lymphoid organs[104,109]. Strikingly, different localization of stem-like T cells in the secondary lymphoid organ have also been reported. Thus, in the B cell follicle[104] or T cells zone[103], where they are closely in contact with DCs (**Figure 1.7**)[103].

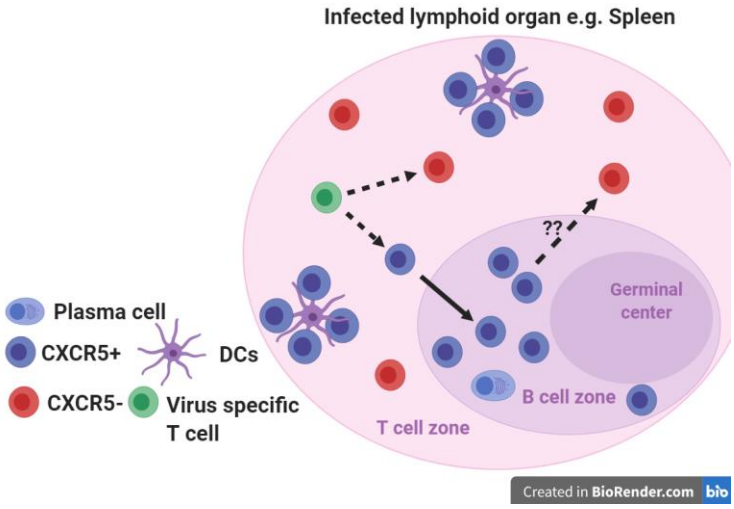

Figure 1.7: A model of CXCR5+ T cell localization in the spleen in chronic LCMV infection

During chronic infection, antigen specific T cells differentiate into CXCR5+ and CXCR5- T cells. CXCR5+ T cells may co-localize with DCs in the T cell zone or migrate into the B cell zone. These processes help to maintain the stem-like property of CXCR5+ T cells. In the B cell zone, CXCR5+ T cells can also generate CXCR5- T cell, which can migrate into the T zone, where they induce pathogen control.[104,109Ψ]

Ψ Figure by author

These observation lead to two hypotheses about stem-like CXCR5+ T cells: (1) Constant interaction with DCs may play a role in maintaining the stem-like nature by preventing excessive antigenic TCR stimulation (**Figure 1.7**)[103]. (2) Migration of stem-like cells into B cell follicles facilitates reduced inhibitory receptor signaling. This is due to the apparent low level of inhibitory ligands in B cell follicles (**Figure 1.7**)[104]. These two studies used a mouse model of chronic LCMV infection, which preferentially replicate in lymphoid organs. However, up to date little is known of the functional fate and differentiation pattern of CXCR5+ and CXCR5- T cells in viral infection which target the liver – a non-lymphoid organ (**Figure 1.8**).

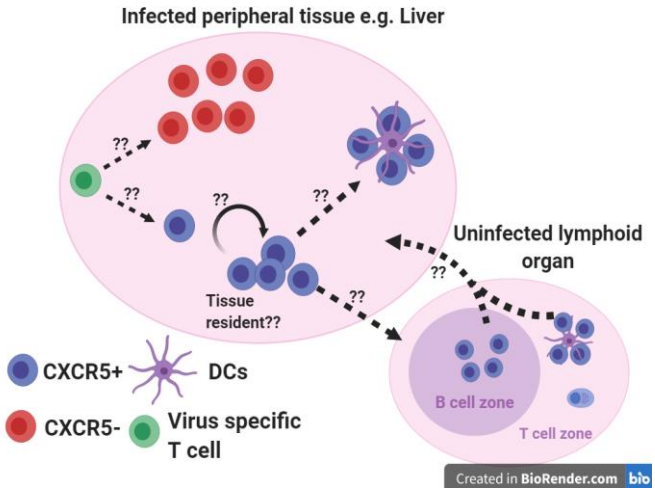

Figure 1.8: A model of CXCR5+ T cell generation in chronic peripheral tissue infection

During chronic liver infection, possibly CXCR5+ and CXCR5- T cells are generated. These may possess characteristics described in chronic LCMV infection; however, it is not clear if CXCR5+ T cells reside in the liver or recirculate between the lymphoid organ and the liver[ϕ].

1.8 A genetic mouse model to study exhausted T cell subsets in the liver

To elucidate the function of exhausted T cell subset in the liver, a mouse model with hepatocyte specific Ova-antigen expression was used, called OvaXCre hereafter[110–112]. This model was chosen due to the lack of small animal models which faithfully reflect and mimics chronic hepatotropic viral infection (**Figure 1.9**). The model has two integrated transgenes, encoding part of intracellular ovalbumin (Ova) and the CreERT2 recombinase (Cre). In particular, the OvaXCre mice have a silent Ova cassette under the ubiquitous Rosa26 promotor and the tamoxifen (Tam)

[ϕ] Figure by author

inducible Cre recombinase under hepatocyte specific promotor albumin. The Ova cassette is oriented in an antisense direction under the Rosa26, and flanked by inversely oriented loxP sites[110–112] (**Figure 1.9**).

Upon induction with Tam, Cre translocates into the nucleus of hepatocytes to mediate a recombination event at the loxP sites, facilitating the flipping of Ova cassette into the sense direction to Rosa26 promotor[110–112]. The recombination mediated in the presence of Tam is reversible but abrogated upon clearance of Tam from circulation, resulting in a fixed Ova state (so called ON-state). Without Tam induction i.e. in naïve OvaXCre mice, Ova is expressed in about 10% of hepatocytes (basal expression)[110,111] probably due to the constitutive activity of Cre recombinase during embryogenesis[113]. Upon Tam administration, Ova-antigen can be processed and presented via the MHC I antigen presentation pathway on the surface of about 50% of hepatocytes. Importantly, the OvaxCre model allows for the study of T cell responses to Ova-antigen presented by hepatocytes without innate immune contribution[110,114]. The OVA antigen presented on MHC-I molecule results in the initiation of T cell responses upon transfer of transgenic T (OT-1) cells, which express a TCR specific for Ova in the context of MHC-I[110]. In addition, intramuscular vaccination with adenoviral vector encoding Ova (hereafter referred to as AdOva) results in the generation of antigen specific T cells which respond to the presented Ova-antigen in the liver[114].

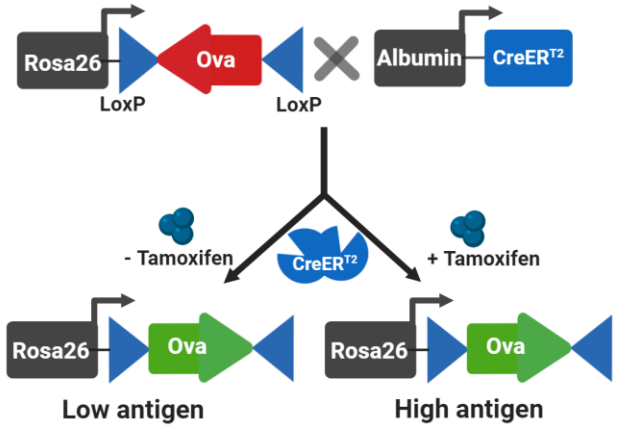

Figure 1.9: Transgenic mouse model with hepatocyte specific Ova antigen expression

Schematic representation of hepatocyte specific, Ova inducible transgenic mouse model OvaXCre. The Ova antigen is inversely oriented under the Rosa26 promoter and flanked by inversely oriented loxP sites. The Tam dependent Cre recombinase is under the control of the hepatocyte specific albumin promotor. Without Tam induction ca. 10 % (Low antigen) of hepatocytes express Ova while upon Tam induction the frequency increases to ca. 50 % (High antigen) of Ova expressing hepatocytes.

1.9 Aim and Objectives of the study

Currently the impact of hepatotropic viral infection on *in situ* CD8+ T cell functionality remains to be fully elucidated. This is partly a consequence of the lack of appropriate mouse infection models. In fact, most studies evaluating exhausted T cell response in chronic hepatotropic viral infection in patients rely heavily on the analysis of T cells from the peripheral blood, in spite of viral replication exclusively in the liver. Findings from these studies do not necessarily recapitulate the functionality of T cells at the site of antigen exposure[52]. Indeed, a growing body of evidence in mouse studies so far have underscored the necessity to understand immunity of resident T cells at the site of infection[115,116], which rapidly respond to, and guard tissues from infection.

Furthermore, despite the tremendous successes achieved by immunotherapeutic strategies (i.e. PD-1 pathway blockade) in cancer, these same strategies fail to broadly achieve efficacy in majority of patients infected with hepatotropic viruses. Although DAAs exist for HCV, these drugs are cost intensive and reinfection can occur after cessation. Hence, there is the need to fully comprehend CD8+ T cell responses in the liver, which may eventually proof key to rational design of immune-based strategies to chronic viral infection in the liver. Therefore, the aim of this study is to fully elucidate the functional dynamism of exhausted CD8+ T cell subsets in the well-controlled OvaXCre mouse model with chronic Ova antigen expression in the liver environment.

In this regard, the following goals were outlined to help elucidate the functional complexity of exhausted T cell in the liver:

- Are exhausted CD8+ T cells in the liver amenable to immunomodulation?
- Are there exhausted T cell subsets in the liver based on CXCR5 expression?
- Which functional characteristic could CXCR5- and CXCR5+ T cells possess in the liver?
- Is there possible differential cytotoxic function in CXCR5+ and CXCR5- T cells?
- Do CXCR5+ and CXCR5- T cells mediate distinct *in vivo* maintenance and differentiation?
- Are there dynamic metabolic differences in CXCR5+ and CXCR5- T cells?

2 Results

2.1 Low and high frequency of Ova-expressing hepatocytes in the liver induce different CD8+ T cell responses

In order to evaluate T cell responses to hepatocyte-restricted antigen, an experimental condition was established which facilitates the analysis of T cell responses in the liver. This experimental condition, which is attained using a transgenic OvaXCre mouse model, is outlined and described in **1.7.** Briefly, the OvaXCre model allows controlled expression of different frequencies of Ova-antigen expressing hepatocytes depending on the dose of Tam administered to the mice. Of note, naïve OvaXCre mice express basal level of Ova antigen with about 10% of expressing cells, termed as 'low antigen' and upon 50µg of Tam administration, an elevated (50%) frequency of Ova expressing hepatocytes are induced, referred to as 'high antigen'. Using this model, it was previously shown that the transfer of Ova-specific T cells (OT-1) cells into low antigen mice facilitate efficient antigen clearance[110]. In contrast, when the same experiment was performed under high antigen condition, antigen specific T cells get exhausted and completely fail to eradicate Ova antigen from the liver[110,114]. The lack of antigen clearance from the liver in high antigen setting was not due to the absence of antigen specific T cells in the liver[110]. These observations were also demonstrated for intramuscular vaccination of low and high antigen mice using the AdOVA viral vector, which elicits an endogenous antigen specific CD8+ T cell response against Ova in the liver[114]. Therefore, it was concluded that adoptive OT-1 transfer and AdOva vaccination strategies elicit similar T cell response to Ova antigen in the liver.

In order to properly dissect the dynamic regulation of antigen specific T cells to high antigen in the liver, it was asked if high antigen load impacts on the kinetics of antigen specific CD8+ T cells. In this regard, the frequency of antigen specific CD8+ T cells in the liver was monitored after AdOva vaccination of or transfer of OT-I cells in high antigen mice (**Figure 2.1a**). Upon vaccination, the number of non-parenchymal cells (NPC) and antigen specific T cells isolated from the liver increased to day 9 post vaccination (**Figure 2.1b, c**). Thereafter, the number of antigen specific T cells decreased drastically (**Figure 2.1c**). Furthermore, the frequency of antigen specific CD8+ T cells in the liver increased upon AdOVa vaccination and plateaued at ca. 8 % (**Figure 2.1d**). The antigen specific T cells which were present in the liver failed to eradicate Ova-antigen

from the liver (**Figure 2.1e**), and this is in line with previous data showing lack of antigen clearance and exhaustion of antigen specific T cells[110,114] .

These data correspond to the known phenomena of exhausted T cells in cancer and chronic LCMV infection, where tumor or virus specific CD8+ T cells decreases due to attrition of exhausted T cells[117]. However, the OvaXCre model allows for *in situ* visualization of these phenomena specifically in the liver environment, which has not been adequately elucidated. Taking together, these data demonstrate that adoptive transfer of OT-1 cells as well as AdOva vaccination of high antigen mice induces T cell exhaustion, which drives the depletion of antigen specific CD8+ T cells in the face of persistent antigen. Thus, OvaXCre mice represent a suitable model for the evaluate T cell response towards chronic antigen expression in the liver.

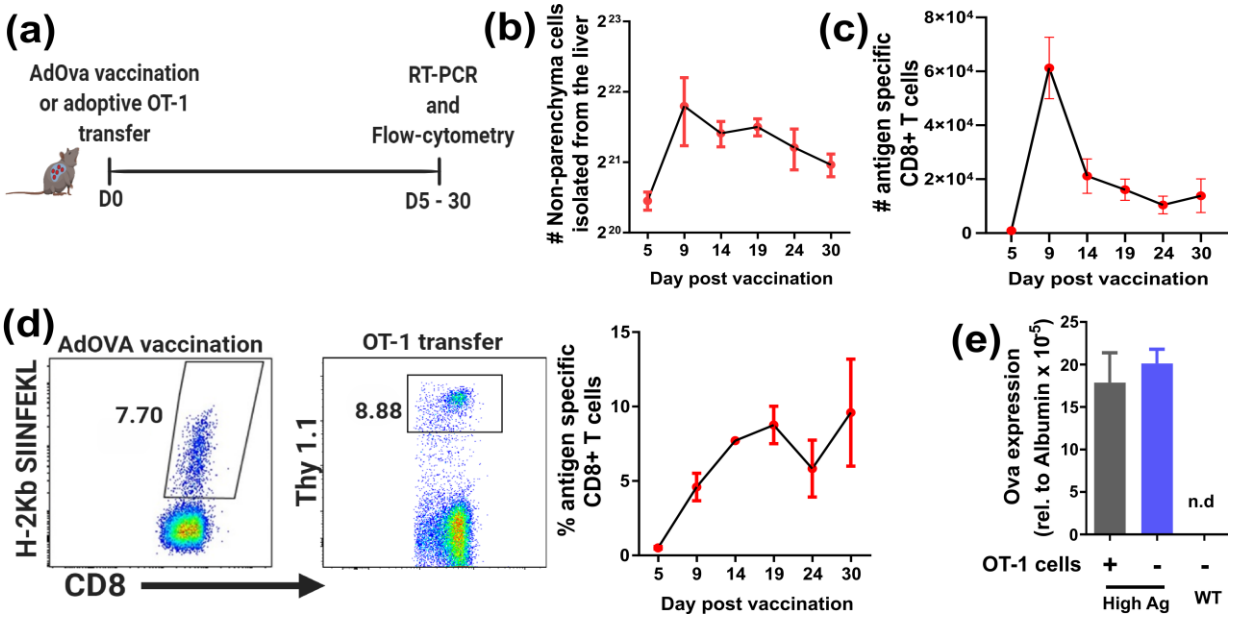

Figure 2.1: High Ova-antigen induces dysfunctional CD8+ T cell response in the liver

(a) Schematic representation of the experimental set-up. Ova expressing mice were either vaccinated with AdOva or adoptively infused with 3 – 5 x 10^6 OT-1 cells. NPCs were isolated from the liver of high antigen mice at various time points, phenotyped for antigen specific CD8+ T cells and analyzed by flow-cytometry. qRT-PCR was performed to assess antigen load D21 post OT-1 transfer.

(b) Absolute numbers of NPCs isolated from the liver from D5 to D30 after AdOva vaccination, from the experimental setup in (a).

(c) Absolute number of antigen specific T cells out of the pool of NPCs in the liver. NPCs isolated from the liver at each time point were stained with antibodies for CD8 and Ova-specific pentamer for flow cytometry.

(d) Representative dot plots of antigen specific T cells in the liver D21 post AdOva vaccination (left) and adoptive OT-1 cell transfer (right), and the kinetic of antigen specific T cells over 30 days period after AdOva vaccination. NPCs isolated from the liver at each time point were stained with antibodies for CD8 and Thy1.1 (in the adoptive

transfer experiment) or CD8 and Ova-specific pentamer (in the case of the AdOva vaccination experiment). Cells were then analyzed by flow cytometry.

(e) Relative Ova expression in the liver of high antigen mice transferred with OT-1 cells (black bar) and without OT-1 cell (blue bar) transfer. RNA was isolated from liver slices of the respective treated condition D21 post OT-1 transfer and subjected through quantitative RT-PCR. The quantified Ova expression was normalized to the hepatocyte specific (albumin) housekeeping gene. WT mice were used as negative control.

2.2 Host conditioning with CpG ODN reinvigorates exhausted CD8+ T cells in the liver

Cebula *et al*[114] have reported that host conditioning with CpG ODN during the initiation of naïve antigen specific T cell response to high Ova antigen in the liver overcomes the establishment of T cell exhaustion. Indeed, in the course of AdOva vaccination, CpG ODN administration during the effector T cell phase results in efficient antigen clearance. Based on this observation, it was asked if CpG ODN conditioning could rejuvenate already exhausted T cells in the liver, leading to the reduction of antigen level in the liver. In this regard, high antigen mice were transferred with OT-1 cells or vaccinated with the AdOVA viral vector. Day 35 post vaccination or adoptive OT-1 transfer, where T cells were fully exhausted, CpG ODN was administered 5x as shown in **Figure 2.2a**. Ova-antigen level was analyzed from the liver tissues 32 day post the first CpG ODN application. Data analysis suggests that CpG ODN treatment mediates efficient antigen clearance from the liver (**Figure 2.2b**). In addition, AdOva vaccination without CpG ODN application did not facilitate antigen clearance due to T cell exhaustion (**Figure 2.2b**). These observations suggest that CpG ODN host conditioning may be involved in remodeling the exhausted T cell responses to high antigen, resulting in probable improvement in cytotoxic T cell responses that finally leads to antigen clearance. To understand how CpG ODN impacts on exhausted antigen specific T cells, at the time when antigen was observed to be cleared from the liver, T cells were analyzed by flow cytometry from the mice which were conditioned with and without CpG ODN. Of note, analysis in CpG ODN treated mice was done 16 days post last CpG ODN application, when antigen was cleared. Thus, antigen specific CD8+ T cells with and without chronic antigenic stimulation in the liver were analyzed. There was a significant reduction in the frequency of antigen specific T cells in CpG ODN treated condition (**Figure 2.2c**), whereas the absolute number of antigen specific T cells in CpG ODN condition was also lower albeit not significantly (**Figure 2.2d**). This suggests that the functionality of T cells was improved by CpG ODN conditioning. Assessment of possible difference in activation marker CD69 expression showed a significant reduction in CD69

expression level on antigen specific T cells in CpG ODN treated condition (**Figure 2.2e, f**). CD69 is a late activation marker which is upregulated in response to antigenic mediated TCR stimulation. Therefore, the reduction in CD69 on T cells under CpG ODN treated condition is possibly due to no antigenic T cell receptor stimulation as a result of no antigen in the liver.

Recently, Danilo *et al*[118] showed that inflammatory cytokines largely drive effector T cell formation, while memory cells are formed efficiently in the absence of inflammatory cytokines[118]. In addition, the maintenance of long lived-memory cells (functional and exhausted) are shaped by TCF-1[96,107,109].

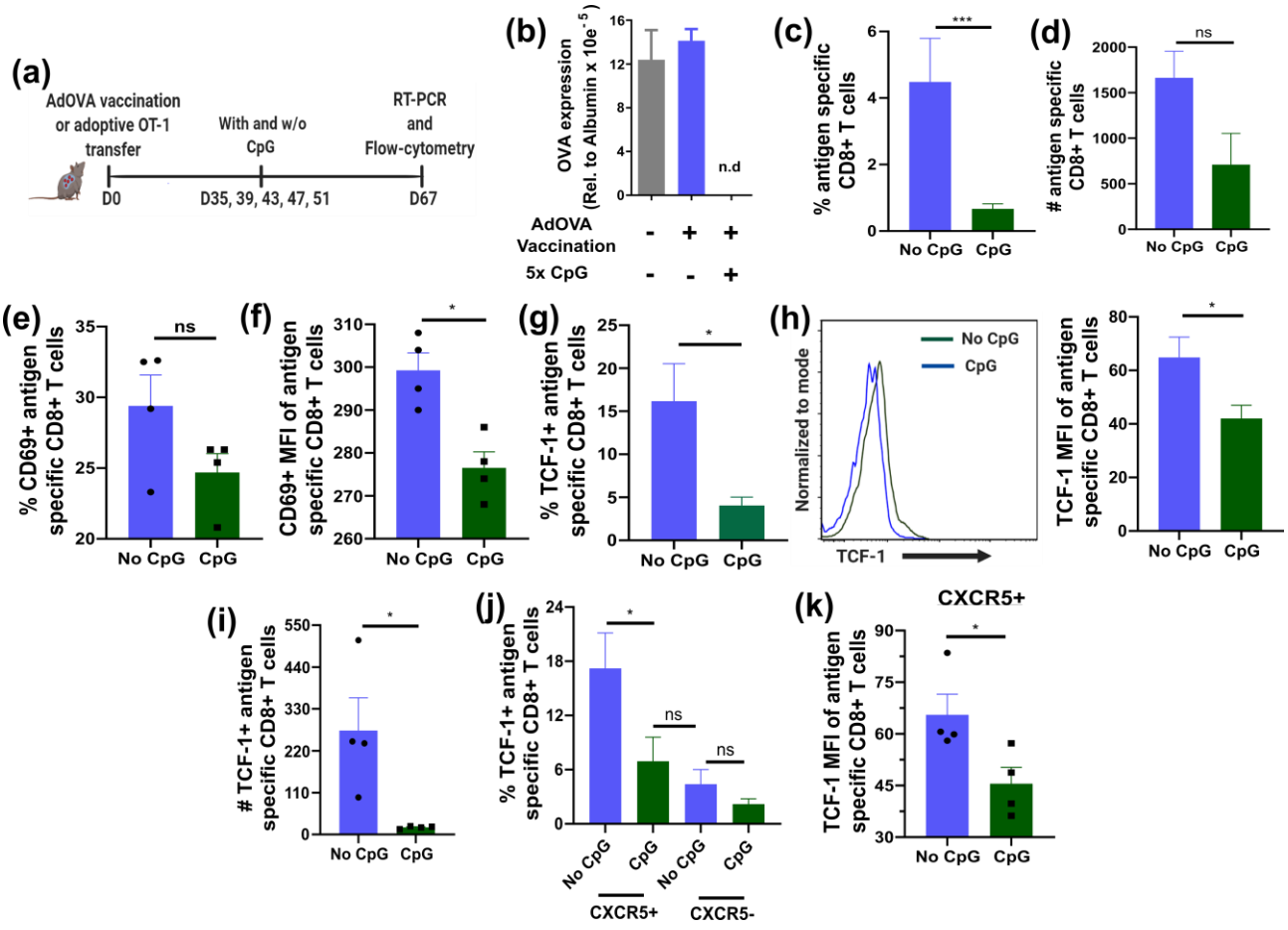

Figure 2.2: CpG ODN host conditioning remodels exhausted CD8+ T cell function in the liver

(a) Schematic representation of the experimental set-up. High antigen mice were vaccinated with AdOva or adoptively infused with 3 – 5 x 10^6 OT-1 cells. Day 35 post AdOva vaccination or OT-1 cell transfer, mice were treated with and without 40μg of CpG ODN intravenously as indicated. After day 67, Ova transcript levels were assessed by qRT-PCR. In addition, NPCs were isolated from the liver for flow cytometric analyses ***(Continuation on next page)***.

(b) Relative Ova transcript levels from the liver of high antigen mice with AdOva vaccination (light black bar), without AdOva vaccination (blue bar) and with AdOva vaccination plus CpG ODN (n.d). RNA was isolated from liver slices of the respective treated condition and Ova transcript levels were assessed by qRT-PCR analysis. The quantified Ova transcripts were normalized to hepatocyte specific (albumin) housekeeping gene.

(c) Frequency of antigen specific CD8+ T cells isolated from the liver with and without CpG ODN treatment. LNPCs were isolated from the liver D67 post adoptive OT-1 transfer and 5 x 10^5 LNPCs from each mouse were phenotyped for antigen specific CD8+ T cells. Data was collected and analyzed by flow cytometry.

(d) Absolute numbers of antigen specific CD8+ T cells recovered from the liver with and without CpG ODN host conditioning in (c).

(e) Frequency of T cell activation marker CD69+ CD8+ T cells in the liver with and without CpG ODN host conditioning from (c), analyzed by flow cytometry.

(f) Median fluorescence intensity (MFI) of CD69+ CD8+ T cells with and without CpG ODN conditioning from (e).

(g) Frequency of the T cell stemness marker TCF-1 expressing cells within antigen specific CD8+ T cells with and without CpG ODN conditioning, from (c).

(h) Representative histogram plot (left) and quantified MFI (right) of TCF-1 expression on antigen specific T cells under CpG ODN and non-CpG ODN host conditioned mice from (c).

(i) Estimated absolute numbers of TCF-1 expressing antigen specific T cells in the liver of mice with and without CpG ODN conditioning, from (c), analyzed by flow cytometry.

(j) Frequency of TCF-1 expression in CXCR5+ and CXCR5- T cells from mice with and without CpG ODN host conditioning. LNPCs were stained for antigen specific CXCR5+ and CXCR5- T cells expressing TCF-1 and data was analyzed by flow cytometry

(k) MFI of TCF-1 in CXCR5+ T cells from mice with and without CpG ODN conditioning in (j).

Data is representative of one of two independent experiments. Each group consists of 4 biological replicates, shown as dots if indicated. Data is depicted as Mean ± SEM. Significance was calculated by Mann-Whitney's test: *$p \leq 0.05$, **$p \leq 0.01$, $p \leq 0.001$; 'ns' indicates not significant.

In this study, the observed reduction of antigen specific CD8+ T cells frequency after CpG ODN conditioning (**Figure 2.2b**) raised the question if inflammation induced by CpG ODN[40] reshaped the stemness property of exhausted T cells. To this end, antigen specific T cells in the liver were analyzed for the stemness transcription factor TCF-1. Analysis showed reduced frequency and median fluorescence intensity (MFI) of TCF-1 expression in antigen specific CD8+ T cells under CpG ODN treated condition (**Figure 2.2g, h**). Instructively, the numbers of TCF-1 expressing cells in CpG ODN treated condition were also reduced (**Figure 2.2i**). Therefore, the reduced TCF-1 expression is possibly a consequence of CpG ODN host conditioning. Another marker which is known to identify stem-like exhausted T cells, CXCR5[104,109], was reduced (but not significantly) on antigen specific T cells in CpG ODN treated condition (**Figure 5S1a, b**). Since CXCR5 and TCF-1 are both considered as markers of stem-like memory cells, it was asked if CXCR5+ T cells preferentially express TCF-1. Indeed, TCF-1 assessment in CXCR5+ and CXCR5- T cells showed exclusively high TCF-1 localization in the CXCR5+ T cell compartment (**Figure 2.2j, k**). The

localization of TCF-1 in CXCR5+ T cells was significantly visible from mice without CpG ODN conditioning (**Figure 2.2j, k**). Strikingly, TCF-1 expression under CpG ODN conditioning out of the pool of CXCR5+ T cells were dramatically reduced (**Figure 2.2k**). Furthermore, the activation marker CD69 was increased on CXCR5+ T cells compared to CXCR5- T cells in both conditions (with and without CpG ODN) (**Figure 5S1c, d**). This suggest that in the presence and absence of antigen, CXCR5+ T cells have higher activation capacity by virtue of CD69 expression compared to CXCR5- T cells. Putting together, these data suggest that: (1) CpG conditioning probably rewires and reengages effector properties in exhausted T cells which may facilitates antigen clearance (2) CpG potentiates TCF-1 reduction in reinvigorated exhausted T cells, (3) loss of antigen specific CD8+ T cells after immunomodulation may be dependent on reduced TCF-1 mediated T cell maintenance and (4) CXCR5 could be used in this study as a marker to identify exhausted stem-like T cells.

2.3 Exhausted antigen specific CD8+ T cells harbor CXCR5+ T cells

Previous data showed the presence of CXCR5+ T cells in the liver, and TCF-1 are largely expressed in CXCR5+ T cells (**Figure 2.2**). An interesting proposition in literature about CXCR5+ antigen specific T cells in chronic LCMV infection is that CXCR5+ T cells are preferentially localized in secondary lymphoid organs, and not in non-lymphoid organs[104]. This suggestion raised the question of whether the CXCR5+ T cell subset observed in the liver – a non-lymphoid organ – are canonical CXCR5+ T cells and if they are resident in the liver tissue. In this regard, upon AdOVA vaccination, the frequency and absolute numbers of CXCR5+ antigen specific T cell were quantified in the liver over 42 days (**Figure 2.3a, b**). Although the absolute numbers of antigen specific CD8+ T cells were dramatically reduced with time (**Figure 2.1d**), ca. 20-30 % of CXCR5+ T cells were observed in the liver over time (**Figure 2.3a**). The estimated number of CXCR5+ T cells was slightly reduced over time (**Figure 2.3b**). Further, analysis of the splenic cells shows ca. 0.7 % of antigen specific T cells and 20-30 % of CXCR5+ T cells, whereas the absolute numbers of antigen specific T cells and CXCR5+ T cells were reduced with time (**Figure 5S2a - d**).

The chemokine CXCL13 is predominantly expressed in the lymphoid organ, and it is known to facilitate CXCR5+ T cell trafficking into the B cell zone[119]. Hence, the liver is not a classical natural niche for CXCR5+ T cell localization. Therefore, to ascertain the identity of CXCR5+ T cells in the liver and to rule-out possible artifact, it was asked if CXCR5+ T cells express the Tfh

transcription factor Bcl6. Bcl6 is a known regulator of CXCR5 expression[47]. Analyzed data of Bcl6 expression in CXCR5+ and CXCR5- T cells suggest that ~ 60-80 % CXCR5+ T cells express the Bcl6 transcription factor and the expression was exclusively restricted to CXCR5+ T cells (**Figure 2.3c, d**). Importantly, Bcl6 expression in CXCR5- and endogenous naïve T cells was comparable (**Figure 2.3c, d**). Analysis of Bcl6 expression in splenic CXCR5+ and CXCR5- T cells showed similar Bcl6 MFI and the frequency was restricted to CXCR5+ expressing CD8+ T cells (**Figure 5S2e, f**). In concordance with the observed CXCR5+ T cells in the liver, analysis of serum CXCL13 levels D14 post AdOva vaccination showed increased CXCL13 levels only in AdOva vaccinated high antigen mice (**Figure 2.3e**). Comparatively, AdOva vaccinated wildtype mice and unvaccinated high antigen mice showed similar levels of CXCL13 (**Figure 2.3e**). These data suggest that CXCL13 is induced upon antigen recognition in the liver and probably facilitates the retention of Tfh-like CXCR5+ T cells in the liver.

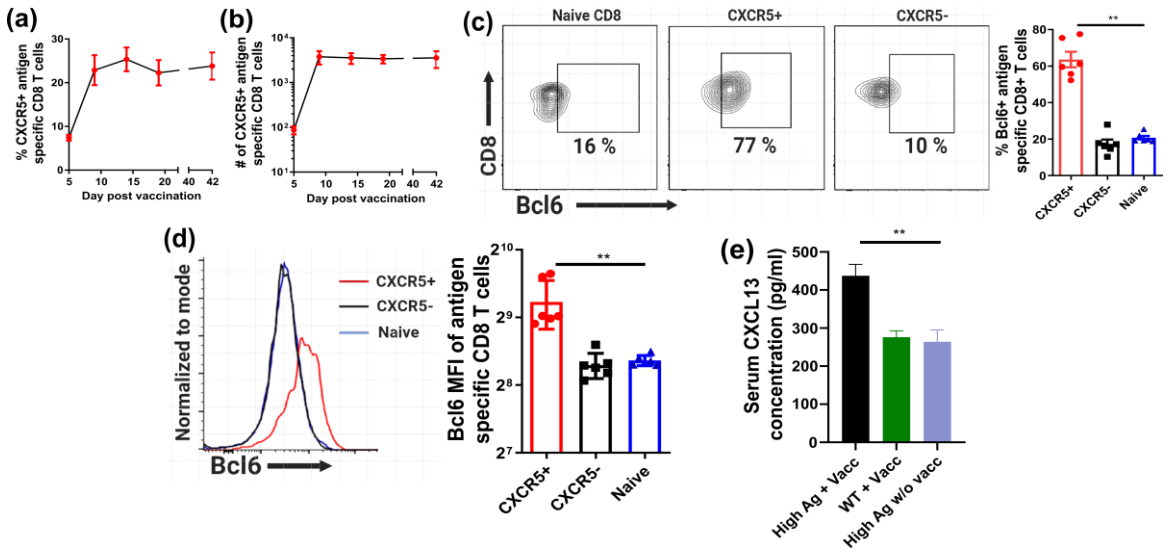

Figure 2.3: Exhausted antigen specific CD8+ T cells in the liver harbor CXCR5+ T cells

(a) Kinetic frequency of CXCR5+ antigen specific CD8+ T cells in the liver of high antigen mice vaccinated with AdOva. At each time point after vaccination, liver NPCs (LNPCs) were isolated, and 5 x 10^5 cells were phenotyped to identify CXCR5+ Ova specific CD8+ T cells. Stained cells were analyzed by flow cytometry.

(b) Absolute numbers of CXCR5+ antigen specific CD8+ T cells quantified in (a).

(c) Frequency of T follicular helper transcription factor Bcl6 staining in naïve CD8+ T cells, antigen specific CXCR5+ and CXCR5- CD8+ T cells for flow cytometry. Representative histogram plot (left) and summarized frequency (right) of Bcl6. LNPCs were isolated 21 days post AdOva vaccination, stained for Bcl6 in CXCR5+ and CXCR5- T cells, and analyzed by flow cytometry

(d) Expression level (MFI) of Bcl6 in naïve, antigen specific CXCR5+ and CXCR5- T cells in (c). Representative histogram overlay (left) and summary of MFI (right).

(e) Quantified serum levels of CXCL13 from AdOva vaccination of wildtype and high antigen mice, as well as high antigen mice without vaccination.

Data is representative of one independent experiment. Each group consist of 6 biological replicates, shown as dots. Data is depicted as Mean ± SEM. Significance was calculated by Mann-Whitney's test: *p ≤ 0.05, **p ≤ 0.01; 'ns' indicate not significant

2.4 CXCR5+ T cells in the liver possess tissue resident properties

To test liver residency or otherwise of CXCR5+ cells, CXCR5+ and CXCR5- T cells isolated from the liver 21 days post OT-1 transfer were phenotyped for the canonical liver residency marker LFA-1[120]. Interestingly, all CXCR5+ T cells express LFA-1, likewise CXCR5- T cells (**Figure 2.4a**). Further analysis of LFA-1 MFI revealed higher levels on CXCR5+ T cells compared to CXCR5- T cells (**Figure 2.4b**). These data suggest that CXCR5+ T cells may have higher activation, reduced senescence, enhanced stemness and proliferation properties compared to the CXCR5- T cell subset. Indeed, the regulation of exhausted T cell stemness is mediated by complex transcriptional network, with T cell factor 1 (TCF-1) playing a cardinal role[121]. Therefore, it was asked if TCF-1 was overly restricted to the CXCR5+ T cell subset. Assessment of TCF-1 expression suggests both frequency and MFI were higher in resident CXCR5+ T cell compartment compared to the CXCR5- T cells (**Figure 2.2g, h and 2.4c**).

Studies using chronic LCMV infection proposed preferential localization of CXCR5+ T cells in the B cell zone and/or co-localization to DCs in T cell zone. Accordingly, these localization favors reduced antigenic stimulation of CXCR5+ T cell[104]. Since the liver is not a lymphoid organ, it was asked if CXCR5+ and CXCR5- T cells were receiving similar signaling events through the TCR. To test this hypothesis, the surrogate TCR signaling transcription factor Nur77 was evaluated. Nur77 staining show similar expression frequency in CXCR5+ and CXCR5- T cell subset (**Figure 2.4d**). However, the MFI of Nur77 was not significant but slightly increased in CXCR5+ cells compared to CXCR5- T cells (**Figure 2.4e**). Furthermore, Nur77 has also been implicated in regulating the transcription networks enforcing the formation of tissue resident T cells[122–124], which further supports LFA-1 expression data (**Figure 2.4a, b**). Of interest is the lower Nur77 MFI in naive CD8 T cells compared to CXCR5+ and CXCR5- T cell subsets (**Figure 2.4e**), suggesting tonic signaling in CXCR5+ and CXCR5- T cells in the liver environment. Putting together, these data suggest that CXCR5+ T cells are stem-like cells residing (i.e. tissue resident T cells) in an

unconventional niche; the site of antigen recognition. Both CXCR5+ and CXCR5- T cells are liver resident T cells which may actively be involved in antigen recognition.

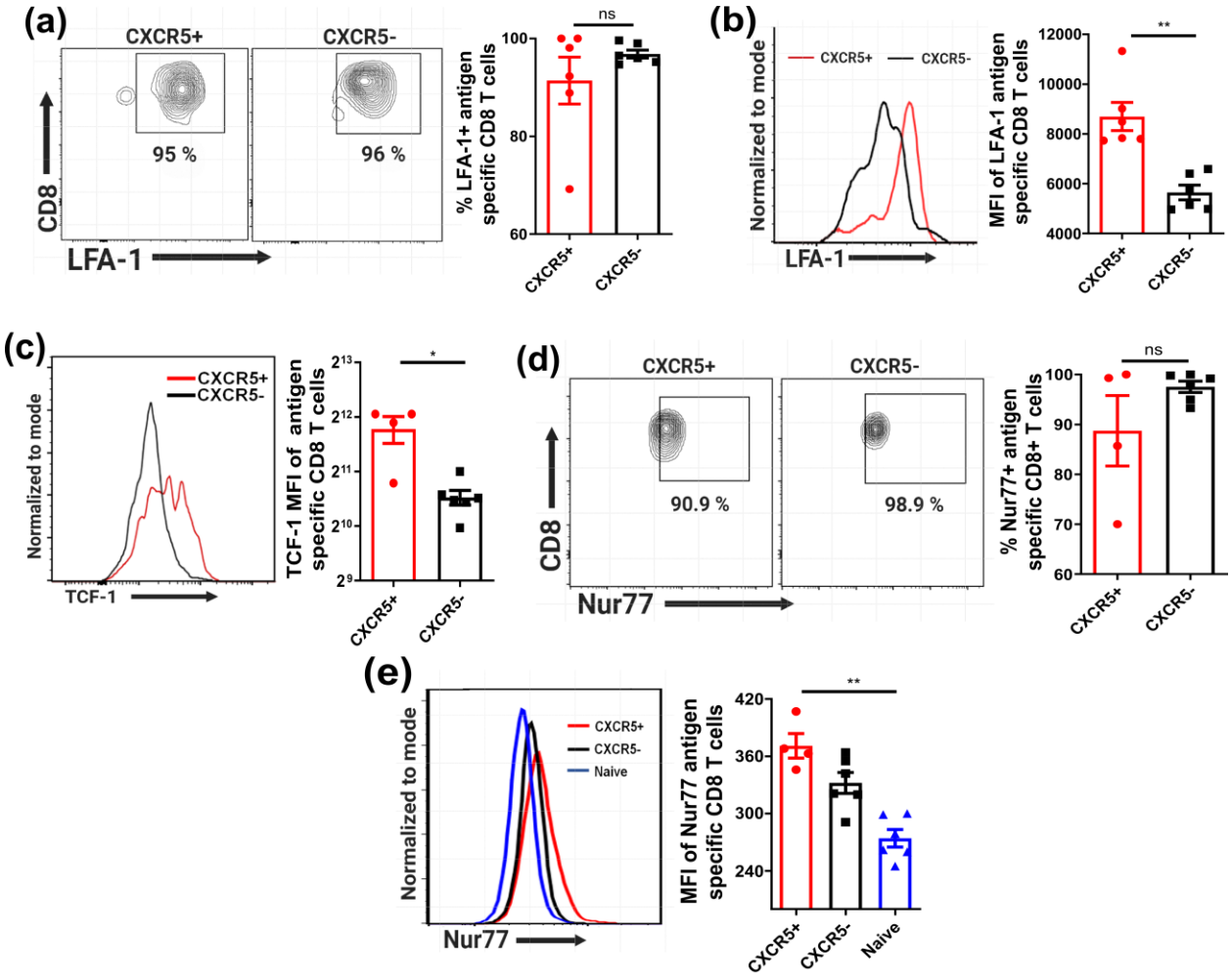

Figure 2.4: CXCR5+ T cells in the liver possess tissue residency capacity

5 x 10^5 LNPCs isolated from high antigen mice 21 days post AdOva vaccination or adoptive transfer of Thy1.1+OT-1 cells were phenotyped for antigen specific CXCR5+ and CXCR5- CD8+ T cells expressing LFA-1, TCF-1 and Nur77, and analysis was done by flow cytometry.

(a) Expression frequency of liver residency marker LFA-1 on CXCR5+ and CXCR5- T cells, D21 post 3 - 5 x 10^6 OT-1 transfer. Representative flow plots (left) and summary (right) of LFA-1 expression.

(b) MFI of LFA-1+ antigen specific CXCR5+ and CXCR5- T cells in (a). Representative histogram plot (left) and quantified MFI summary (right) of LFA-1 expression.

(c) MFI of the transcription factor T cell factor 1 (TCF-1) expression on antigen specific CXCR5+ and CXCR5- T cells, D21 post 3 - 5 x 10^6 OT-1 transfer. Representative histogram (left) and summarized MFI (right) of TCF-1.

(d) Representative flow plots (left) and summary (right) of the frequency of Nur77 expression in CXCR5+ and CXCR5- T cell, D21 post AdOva vaccination.

(e) Representative histogram plot (left) and summarized MFI (right) of Nur77 in naïve, CXCR5+ and CXCR5- T cell subsets in (d).

Representative data of one independent experiment. Each group consists of 4-6 biological replicates depicted as dots. Data is depicted as Mean ± SEM. Significance was calculated by Mann-Whitney's test: *p ≤ 0.05, **p ≤ 0.01; 'ns' indicate not significant

2.5 Liver resident CXCR5+ and CXCR5- T cells display distinct activation properties

Previous analyses showed two subsets of exhausted antigen specific CD8+ T cells in the liver, which are tissue resident and possess differential stemness property based on TCF-1 (**Figure 2.2h and 2.4c**). To dissect further properties of TCF-1 imprinted stemness on CXCR5+ T cells, the activation profiles of CXCR5+ and CXCR5- T cells were evaluated. The expression of the activation markers KLRG-1, CD44 and CD69 on T cells demonstrates T cell activation[8] and the expression level can distinguish exhausted T cells from fully functional T cells. Accordingly, these activation markers were analyzed on CXCR5+ and CXCR5- T cells D21 post AdOva vaccination. Although both subsets of T cells were exposed to the same microenvironment of the liver, there were observed differences in CD69, CD44 and KLRG-1 expression (**Figure 2.5a - e**). CXCR5+ T cells showed higher frequency and MFI of CD69 expression compared to CXCR5- T cells (**Figure 2.5a, b**). All subsets, i.e. CXCR5+ and CXCR5- T cell express CD44 (data not shown) however, the level of CD44 MFI was significantly higher on CXCR5+ T cells (**Figure 2.5c**). Likewise, the frequency of KLRG-1 expression was higher on CXCR5+ T cells (**Figure 2.5d**), but KLRG-1 MFI was not different between CXCR5+ and CXCR5- T cells (**Figure 2.5e**). The activation markers CD44, CD69 and KLRG-1 were also analyzed on splenic CXCR5+ and CXCR5- T cells D21 post vaccination (**Figure 5S3a-f**). The frequency and MFI of CD69 were higher on CXCR5+ T cells compared to CXCR5- T cells (**Figure 5S3a, b**). While $CD44^{hi}$ frequency were more restricted to the CXCR5- T cell compartment (**Figure 5S3c**), the MFI of CD44 was higher on the CXCR5+ T cell subset (**Figure 5S3d**). On the other hand, the frequency and MFI of KLRG-1 were similar in both subsets of cells (**Figure 5S3e, f**). Putting together, these data suggest a distinct activation profile of CXCR5+ and CXCR5- T cells in the same microenvironment.

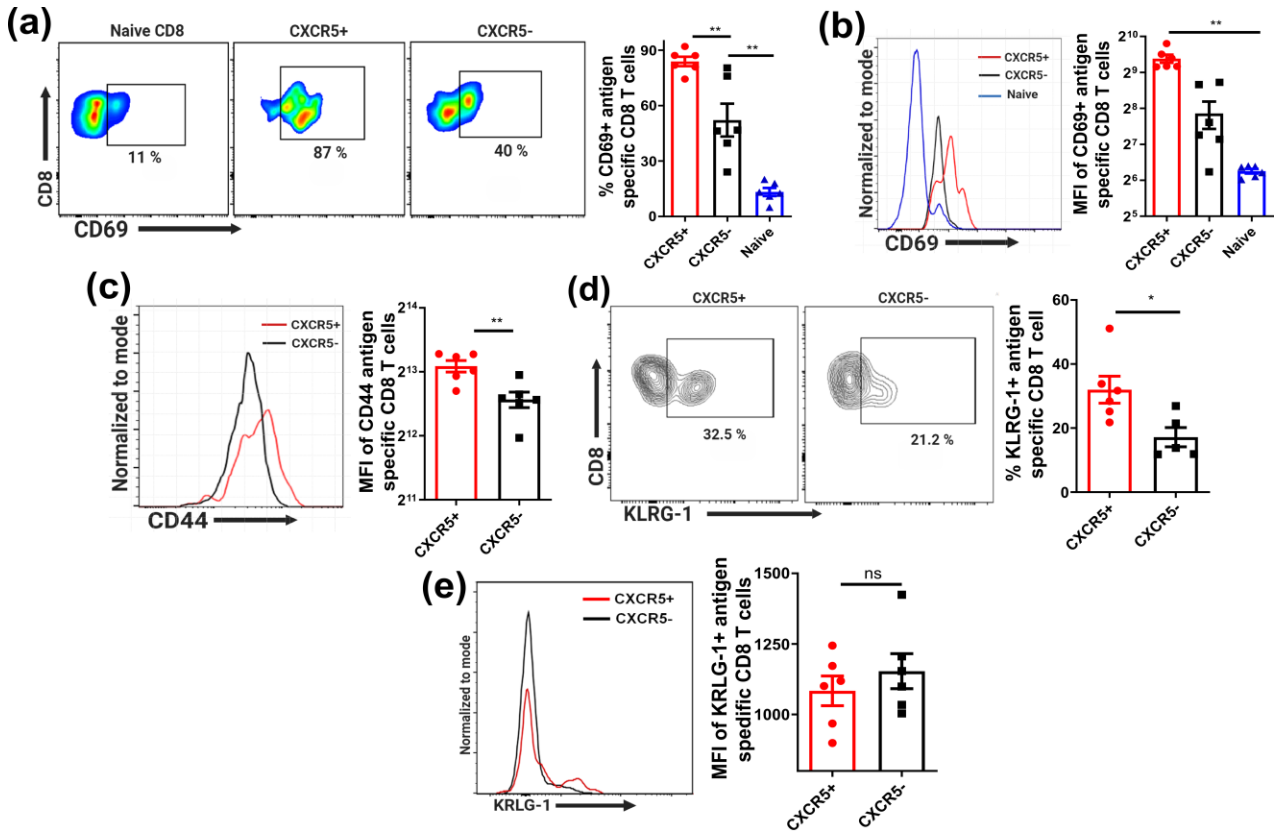

Figure 2.5: Liver resident CXCR5+ and CXCR5- T cells display distinct activation profiles

LNPCs from high antigen mice were isolated 21 days post AdOva vaccination or adoptive 3 - 5 x 10^6 OT-1 cell transfer, and 5 x 10^5cells were phenotyped for antigen specific CXCR5+ and CXCR5- T cells. The antigen specific CXCR5+ and CXCR5- CD8+ T cells were also phenotyped for the expression of activation markers CD69, CD44 and KLRG-1. Analysis was done by flow cytometer and representative data of AdOva vaccination experiments are shown.

(a) Frequency of CD69 expression on naïve, antigen specific CXCR5+ and CXCR5- T cells. Representative dot plot (left) and summarized frequency (right) of CD69 expression.

(b) Expression level of CD69 on naïve, antigen specific CXCR5+ and CXCR5- T cells in (a). Representative histogram overlay (left) and quantified MFI (right).

(c) Representative histogram plot (left) and summarized MFI (right) of CD44 on CXCR5+ and CXCR5- T cells.

(d) Frequency of KLRG-1 on Ova-specific CXCR5+ and CXCR5- T cell subsets. Representative dot plot (left) and summarized frequency (right).

(e) Quantified MFI of KLRG-1 expression on Ova-specific CXCR5+ and CXCR5- CD8+ T cells in (d). Representative histogram plot (left) and summary (right) of KLRG-1.

Data is representative of one of two independent experiments. Each group consist of 6 biological replicates, depicted as dots. Data is depicted as Mean ± SEM. Significance was calculated by Mann-Whitney's test: *p ≤ 0.05, **p ≤ 0.01, 'ns' indicate not significant

2.6 Liver resident CXCR5+ and CXCR5- T cells display distinct memory properties

CXCR5+ and CXCR5- T cells possess distinct activation statuses (**Figure 2.5**). Therefore, it was hypothesized that differences in activation status may also reflect on memory properties of CXCR5+ and CXCR5- T cells. To this end, the memory markers CD62L, CD127 and CCR7 were evaluated on CXCR5+ and CXCR5- T cell subset 21 days post vaccination. The memory marker CD62L was exclusively expressed on CXCR5+ T cells (**Figure 2.6a**) and CD62L MFI was higher on CXCR5+ T cells compared to CXCR5- T cell subset (**Figure 2.6b**). Furthermore, the frequency of CD127 and CCR7 were highly expressed on CXCR5+ cells compared to CXCR5- T cell (**Figure 2.6c, e**). Whereas MFI for CCR7 was similar between CXCR5+ and CXCR5- T cell subset (**Figure 2.6f**), CD127 MFI was higher on CXCR5+ T cells (**Figure 2.6d**). These memory markers were also analyzed on splenic antigen specific CD8+ T cells (**Figure 5S4a-f**). Out of the pool of antigen specific CD8+ T cells in the spleen, CXCR5+ T cells expressed higher frequency and MFI of CD62L compared to CXCR5- T cells (**Figure 5S4a, b**). Contrary to the liver, increased frequency of CD127 was associated with CXCR5- T cell in the spleen (**Figure 5S4c**), while the MFI was inversely correlated to the frequency (**Figure 5S4d**). Finally, CCR7+ cells were more on the CXCR5+ T cell compartment (**Figure 5S4e**) and MFI of CCR7 expressing CXCR5+ and CXCR5- T cells showed higher levels of CXCR5+ T cells (**Figure 5S4f**). Taking together, these data show-cased that in the liver microenvironment, the CXCR5+ and CXCR5- exhausted T cell subsets possess different memory properties.

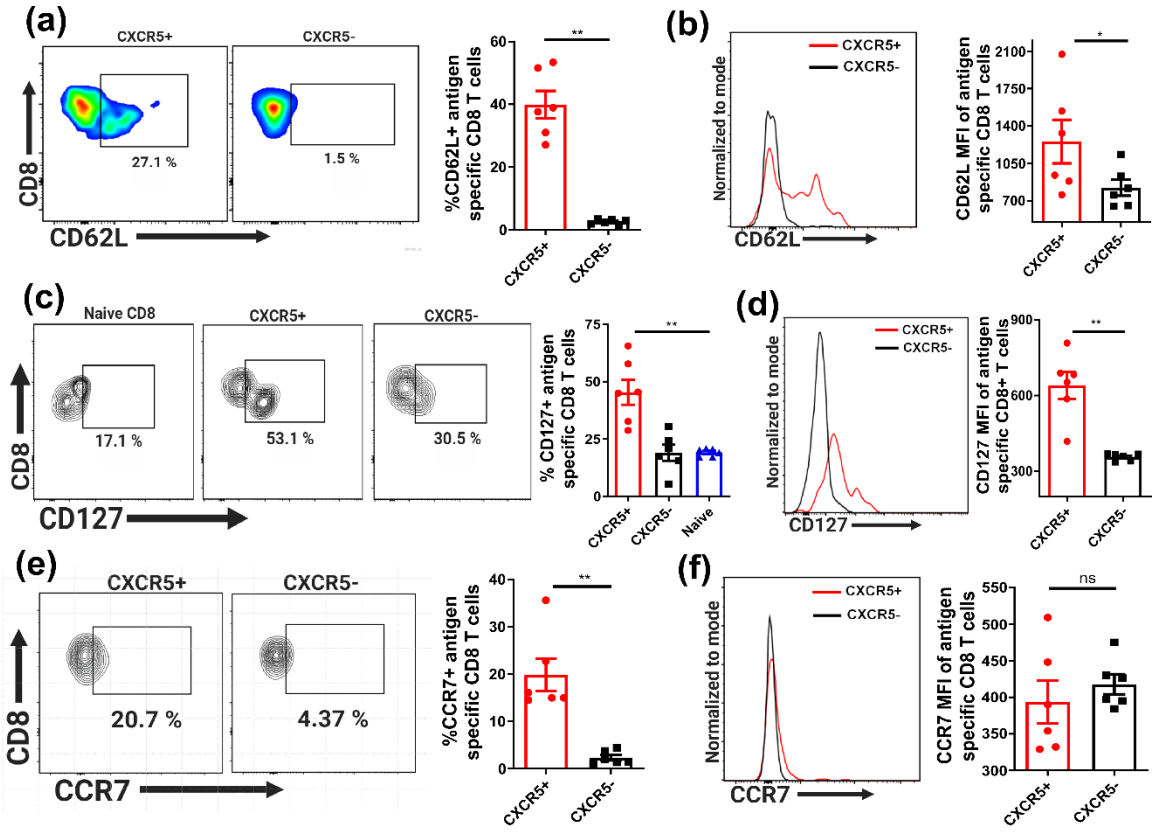

Figure 2.6: Liver resident CXCR5+ and CXCR5- T cells display distinct memory profiles

LNPCs from high antigen mice were isolated 21 days post AdOva vaccination or adoptive OT-1 transfer and 5 x 10^5 isolated LNPCs were phenotyped for antigen specific CXCR5+ and CXCR5- CD8+ T cells. The cells were also stained for memory markers CD62L, CCR7 and CD127 expression. Analysis was done by flow cytometer and representative data for AdOva vaccination experiments are shown.

(a) Frequency of CD62L+ Ova-specific CXCR5+ and CXCR5- CD8+ T cell subset. Representative dot plot (left) and summarized expression frequency (right) of CD62L.

(b) MFI of CD62L expression on Ova-specific CXCR5+ and CXCR5- T cell subsets in (a). Representative histogram plot (left) and quantified MFI (right) of CD62L.

(c) Frequency of CD127+ naïve, Ova-specific CXCR5+ and CXCR5- T cells. Representative dot plot (left) and summary (right) of CD127 expression.

(d) Quantified MFI of CD127+ Ova-specific CXCR5+ and CXCR5- T cells in (c). Representative dot plot (left) and summary (right) of CD127.

(e) Frequency of CCR7 expression on Ova-specific CXCR5+ and CXCR5- T cells. Representative dot plot (left) and summarized frequency (right) of CCR7.

(f) MFI of CCR7 expression on Ova-specific CXCR5+ and CXCR5- T cells in (e). Representative histogram plot (left) and quantified summary (right) of CCR7.

Representative data of one of two independent experiments are shown. Each group consist of 6 biological replicates depicted as dots. Data is depicted as Mean ± SEM. Significance was calculated by Mann-Whitney's test: *$p \leq 0.05$, **$p \leq 0.01$, 'ns' indicate not significant.

2.7 Distinct exhaustion profiles of exhausted CD8+ T cell subsets

So far, preceding data suggest that CXCR5+ and CXCR5- T cells possess different activation (**Figure 2.5**) and memory (**Figure 2.6**) properties. Based on these observations, it was hypothesized that there may as well be differences in exhaustion marker expression on CXCR5+ and CXCR5- T cells in the liver. To this end, 21 days post vaccination, CXCR5+ and CXCR5- antigen specific CD8+ T cells in the liver were phenotyped for the exhaustion markers CD244, TIM-3, Lag-3 and PD-1. Exhaustion marker expression on antigen experienced T cells defines a state of T cell dysfunctional in tumor and chronic viral infection[6]. The analysis of CD244, PD-1, Lag-3 and TIM-3 on CXCR5+ and CXCR5- T cells shows higher frequency of exhaustion markers on CXCR5- T cells compared to CXCR5+ T cells (**Figure 2.7a, c, e, and g**). Furthermore, analysis of antigen specific CD8+ T cells in the spleen, the site with no antigen expression, showed lower frequency of exhaustion marker on CXCR5+ T cells compared to CXCR5- T cell subsets (**Figure 5S5a, c, e, and g**). The MFI of exhaustion markers CD244, PD-1, TIM-3 and Lag-3 were however similar between CXCR5+ and CXCR5- T cell subsets in the liver (**Figure 2.7b, d, f, h**). In the spleen, CD244 and Lag-3 MFI were observed to be higher on CXCR5- T cells compared to CXCR5+ T cells (**Figure 5S5b, f**) but PD-1 and TIM-3 MFI remained similar between both subsets of cells (**Figure 5S5d, g**). Putting together, these data show differential exhaustion state of CXCR5+ and CXCR5- T cells in the liver, on the level of exhaustion marker expression.

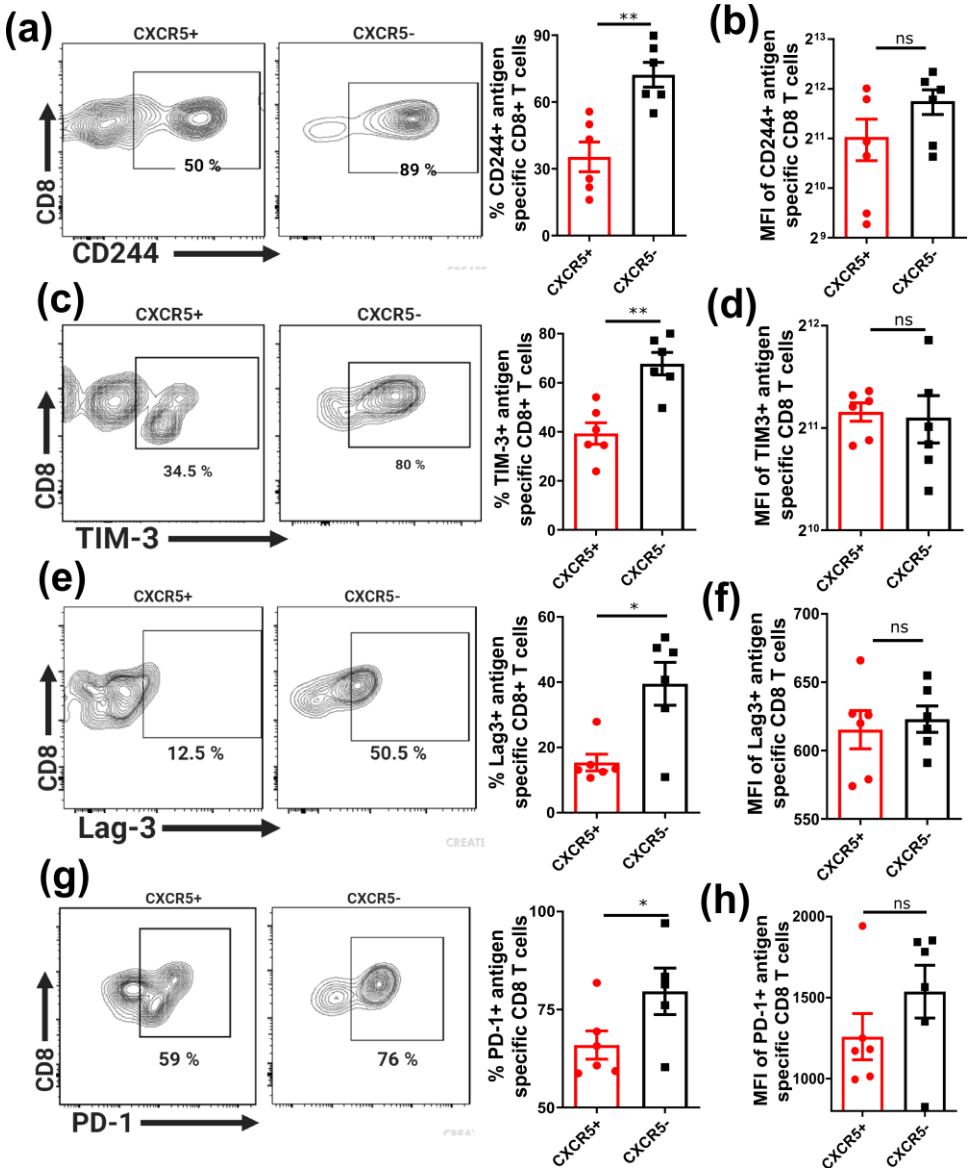

Figure 2.7: Liver resident CXCR5+ T cells display reduced exhaustion marker expression

D21 post AdOva vaccination of high antigen mice, LNPCs were isolated, and 5 x 10^5 cells were phenotyped for antigen specific CXCR5+ and CXCR5- CD8+ T cells. The cells were further stained for the exhaustion markers CD244, TIM-3, PD-1 and Lag-3 expression, and data was acquired and analyzed with flow cytometry

(a) Frequency of exhaustion marker CD244 on CXCR5+ and CXCR5- Ova-specific CD8+ T cells. Representative dot plot (left) and summary (right) of CD244 expressing CXCR5+ and CXCR5- T cells.

(b) MFI of CD244 on CXCR5+ and CXCR5- T cells analyzed in (a).

(c) Frequency of TIM-3 expression on Ova-specific CXCR5+ and CXCR5- T cells. Representative flow plot (left) and summarized frequency (right) of TIM-3.

(d) MFI of TIM-3 on antigen specific CXCR5+ and CXCR5- T cells analyzed in (c).

(e) Frequency of Lag-3 expressing Ova-specific CXCR5+ and CXCR5- T cells. Representative flow plot (left) and summarized frequency (right) of Lag-3.

*(f) Expression level of Lag-3 on Ova-specific CXCR5+ and CXCR5- T cells analyzed in (e). (**Continuation on next page**)*

(g) Frequency of PD-1 expressing CXCR5+ and CXCR5- Ova-specific CD8+ T cells. Representative dot plot (left) and summary (right) of PD-1 expression.

(h) *MFI of PD-1 on CXCR5+ and CXCR5- Ova-specific T cells in (g)*

Data is representative data of one independent experiment. Each group consist of 6 biological replicates, depicted as dots. Data was depicted as Mean ± SEM. Significance was calculated by Mann-Whitney's test: *p ≤ 0.05, **p ≤ 0.01, 'ns' indicate not significant.

2.8 Liver resident CXCR5+ and CXCR5- T cells exhibit distinct effector properties

The observed state of exhaustion (**Figure 2.7**) as well as activation (**Figure 2.5**) profile of CXCR5+ and CXCR5- T cells prompted the question if differential exhaustion and activation may have consequential implication on effector cytokine expression. In this regard, the frequency of effector cytokines such as GZMB, IFN-γ and TNF-α were analyzed on CXCR5+ and CXCR5- T cells, 21 days post AdOva vaccination. In agreement with differences in the exhaustion profile (**Figure 2.7**), CXCR5+ T cells were largely observed to express higher TNF-α, IFN-γ and GZMB (**Figure 2.8a, d, g**). Similar findings were made for antigen specific CD8+ T cells in the spleen, although there were no significant differences in IFN-γ expression between CXCR5+ and CXCR5- T cells (**Figure 5S6a, d, f**). In spite of the significant differences in the frequency of TNFα, IFN-γ and GZMB between CXCR5+ and CXCR5- T cells in the liver, it did not translate into MFI differences (**Figure 2.8a, d, g**). Assessment of antigen specific T cells in the spleen as well suggested no difference in MFI of TNFα, IFN-γ and GZMB in both CXCR5+ and CXCR5- T cells (**Figure 5S6b, e, h**). Importantly, analysis of the numbers of TNFα, IFN-γ and GZMB positive cells in the CXCR5+ and CXCR5- T cell compartment showed no significant differences, although CXCR5+ T cells made-up a minor fraction (~ 20 - 30 %) of the total pool of antigen specific CD8+ T cells in the liver (**Figure 2.8c, f, i**). Of note, regardless of the lack of statistical significance in the numbers of effector cytokines expressed by CXCR5+ and CXCR5- T cells, there was an observed tendency of higher numbers of TNFα, IFN-γ and GZMB in the CXCR5- T cell compartment (**Figure 2.8c, f and i**). In the spleen, the number of GZMB and IFN-γ were highly enriched in the CXCR5- T cell subset while the inverse was true for TNF-α numbers (**Figure 5S6c, f and i**). Taking together, this data suggests that CXCR5+ cells may possess an enhanced cytotoxic capacity compared to CXCR5- T cells in the liver.

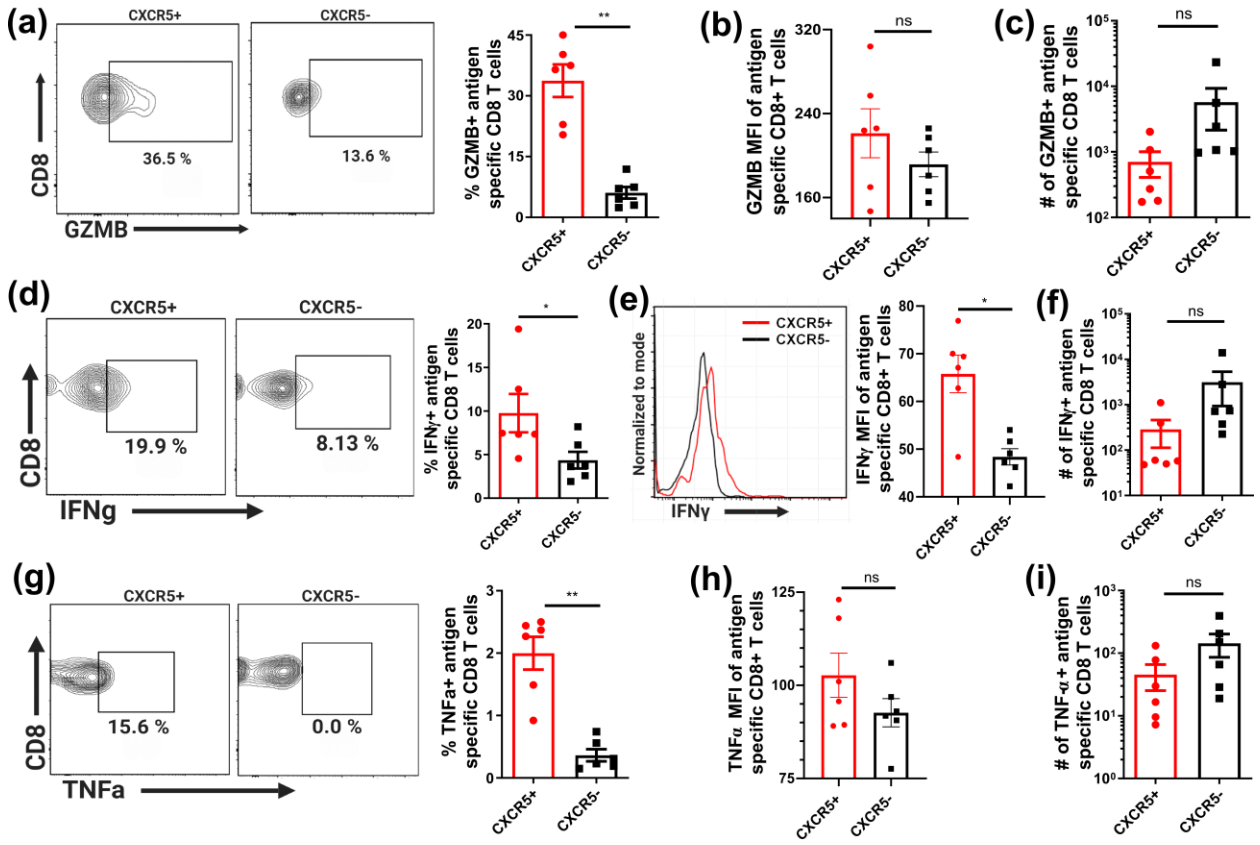

Figure 2.8: Liver resident CXCR5+ and CXCR5- T cells exhibit distinct effector properties

Day 21 post AdOva vaccination of high antigen mice, LNPCs were isolated, re-stimulated ex-vivo with PMA/ionomycin for 4-5h in the presence of Brefeldin A for the last 2h. The stimulated cells were, phenotyped for antigen specific CXCR5+ and CXCR5- CD8+ T cells expressing IFNγ, TNFα and GZMB and data was analyzed by flow cytometry

(a) Frequency of GZMB expression in Ova-specific CXCR5+ and CXCR5- T cells. Representative dot plot (left) and summary (right) of GZMB expression.

(b) MFI of GZMB+ Ova-specific CXCR5+ and CXCR5- T cells analyzed in (a)

(c) Absolute numbers of GZMB+ cells in the pool of CXCR5+ and CXCR5- T cell subset analyzed in (a).

(d) Frequency of IFNγ expression in CXCR5+ and CXCR5- T cells. Representative flow plot (left) and summary (right) of IFNγ expression.

(e) MFI of IFNγ+ CXCR5+ and CXCR5- T cells analyzed in (d). Representative histogram (left) and summarized MFI (right) of IFNγ.

(f) Absolute number of IFNγ expressing cells in Ova-specific CXCR5+ and CXCR5- T cells analyzed in (d).

(g) Frequency of TNFα expression in CXCR5+ and CXCR5- T cells. Representative flow plot (left) and summarized (right) TNFα expression.

(h) MFI of TNFα+ CXCR5+ and CXCR5- T cells analyzed in (g).

(i) Absolute number of TNFα expressing cells in Ova-specific CXCR5+ and CXCR5- T cells analyzed in (g).

Representative data of one of two independent experiment is shown. Each group consist of 6 biological replicates, depicted as dots. Data is depicted as Mean ± SEM. Significance was calculated by Mann-Whitney's test: *p ≤ 0.05, **p ≤ 0.01, 'ns' indicate not significant.

2.9 Liver resident CXCR5+ and CXCR5- T cells exhibit distinct cytotoxic functions

The increase in global effector cytokines, most importantly GZMB (**Figure 2.8**) by CXCR5+ T cells suggests that CXCR5+ T cells may also be enriched in the ability to produce T cell cytotoxicity molecule CD107a (Lamp1a). To test this proposal, the expression of CD107a was quantified in CXCR5+ and CXCR5- T cells. In spite of ca. 40 % of CXCR5+ T cells expressing GZMB (**Figure 2.8a**), almost all CXCR5+ cells express CD107a compared to ca. 50% in CXCR5- T cells (**Figure 2.9a**). Quantified MFI of CD107a further shows the enrichment of CD107a in the CXCR5+ T cell compartment (**Figure 2. 9b**). The absolute numbers of CD107a+ cells were higher for CXCR5- T cells compared to the CXCR5+ T cell subset (**Figure 2.9c**) nevertheless. In line with the observed CD107a profile in CXCR5+ and CXCR5- T cells in the liver, antigen specific CXCR5+ and CXCR5- T cells in the spleen largely followed similar trend. However, the MFI of CD107a was not different between CXCR5+ and CXCR5- T cells (**Figure 5S6j, k, and l**).

The increased expression of GZMB and CD107a in CXCR5+ T cells led to the hypothesis that CXCR5+ T cells may potentially exhibit enhanced cytotoxic function if compared to CXCR5- T cells. The validity of this proposal was tested using an *in vitro* T cell killing assay. To this end, naive OT-1 cells were transferred into mice expressing high antigen in the liver. D9 post transfer, CXCR5+ and CXCR5- T cells were sorted by flow cytometry and co-cultured with Ova-peptide pulsed EL4 target cells for 24h. D9 post transfer was chosen due to the recovery of highest numbers of antigen specific CD8+ T cells (**Figure 2.1e**) coupled to documented[110] evidence that D3 post OT-1 transfer, the T cell exhaustion trajectory has already been initiated. Effector target cell ratios of 2:1 and 5:1 were exploited for the *in vitro* killing assay. Data suggest enhanced killing of target cells by CXCR5+ T cells compared to CXCR5- T cells (**Figure 2.9d, e**). Effector target ratio of 2:1 killing capacity was not significant between CXCR5+ and CXCR5- T cells but showed a tendency of improved killing by CXCR5+ cells (**Figure 2.9d**). Taking together, these data suggest that antigen specific CD8 T cells responding to chronic liver antigen consist of CXCR5+ cells which are less exhausted and possess enhanced residual cytotoxic effector functions.

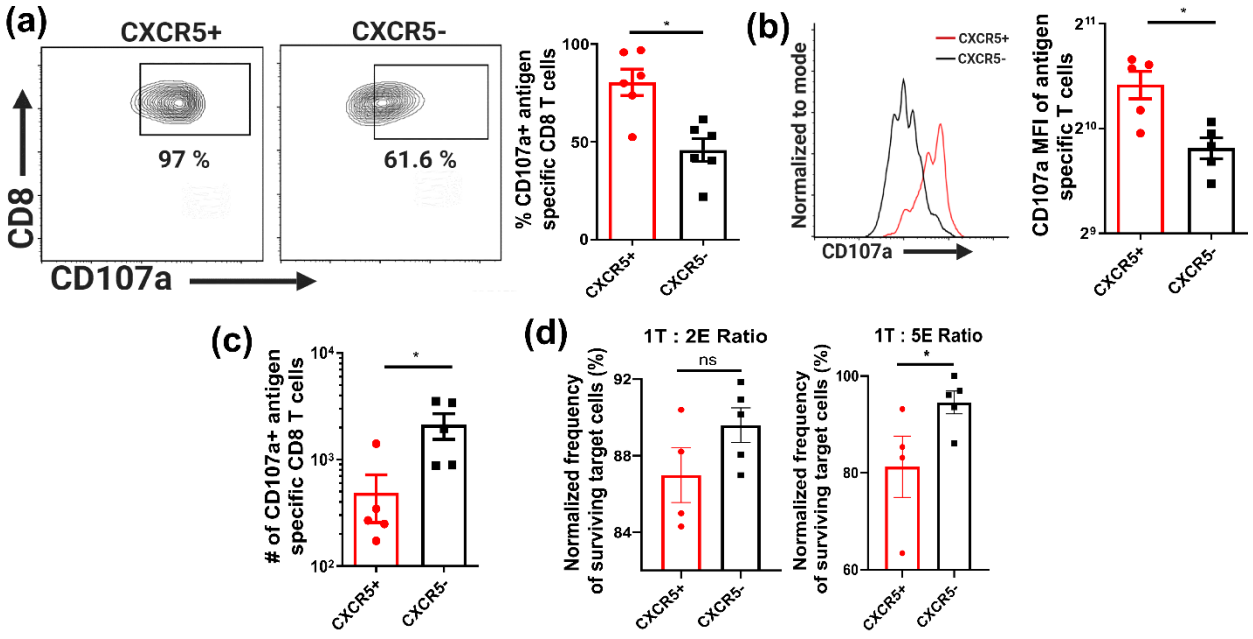

Figure 2.9: Liver resident CXCR5+ and CXCR5- T cells show distinct cytotoxic functions

Day 21 post AdOva vaccination of high antigen mice, LNPCs were isolated, re-stimulated ex-vivo with PMA/ionomycin in the presence of anti-CD107a for 4-5 h (a - c). The cells were harvested and phenotyped for Ova-specific CXCR5+ and CXCR5- CD8+ T cells, and data was analyzed by flow cytometer.

(a) Frequency of CD107a expression in Ova-specific CXCR5+ and CXCR5- T cells. Representative dot plot (left) and summarized frequency (right) of CD107a.

(b) Expression level (MFI) of CD107a in antigen specific CXCR5+ and CXCR5- T cells analyzed in (a). Representative histogram (left) and quantified MFI summary (right) of CD107a.

(c) Absolute number of CD107a+ antigen specific CXCR5+ and CXCR5- T cells analyzed in (a).

(d) D14 post adoptive transfer of 3 - 5 x 10^6 OT-1 cells, LNPCs were isolated and phenotyped for antigen specific CXCR5+ and CXCR5- T cells. The antigen specific cells were sorted (purified) by flow cytometer into CXCR5+ and CXCR5- T cell compartment. The CXCR5+ and CXCR5- T cells were co-cultured with EL4 cells pulsed with Ova-peptide for 24h in the ratios of 1 Target (T) : 2 Effector (E) and 1T:5E. The EL4 cells pulsed with peptide were normalized to EL4 cells which were not pulsed with peptide to determine the rate of antigen-specific T cell induced death of EL4 cells.

Data is representative data of one independent experiment. Each group consist of 4-6 biological replicates, depicted as dots. Data is depicted as Mean ± SEM. Significance was calculated by Mann-Whitney's test: *p ≤ 0.05, **p ≤ 0.01, 'ns' indicate not significant

2.10 Improved mitochondria fitness of exhausted T cells in the liver is associated with CXCR5+ T cells

Published data suggest that naïve T cell transitioning towards the generation of effector or memory cells is underpinned by changes in the metabolism, which is driven by mitochondria activity and dynamism[66,125]. In this study, exhausted CD8+ T cell subsets analyzed from the liver show distinct memory (**Figure 2.6**) and cytotoxic properties (**Figures 2.8 and 2.9**). These features prompted the

question that CXCR5+ and CXCR5- T cells may possess differential metabolic activities. Interestingly, a recent publication suggested that the purinergic receptor P2X7R drives the metabolic fitness and long-term survival of CD8+ T cells in viral infection[126]. Based on this publication, it was first asked if P2X7R was differentially expressed on CXCR5+ and CXCR5- T cells. Indeed, phenotypic analysis of P2X7R on CXCR5+ and CXCR5- T cells showed exclusive P2X7R expression on CXCR5+ T cells compared to CXCR5- and naive CD8+ T cells (**Figure 2.10a**). In addition, P2X7R MFI was higher on CXCR5+ T cells compared to the CXCR5- T cell subset (**Figure 2.10b**). CXCR5+ antigen specific T cells in the spleen also showed increased P2X7R frequency and MFI compared to CXCR5- T cells (**Figure 5S7a, b**).

The exclusive P2X7R expression (**Figure 2.10a, b**) on liver resident CXCR5+ T cells coupled to enhanced memory properties (**Figure 2.6**) led to the hypothesis that efficient mitochondria function may largely be restricted to the CXCR5+ T cell subset. Thus, the mass of mitochondria was quantified within CXCR5+ and CXCR5- T cells using the Mitotracker Green dye (MTG), 21 days post AdOva vaccination as well as upon adoptive OT-1 cell transfer. MTG is a mitochondrial potential insensitive dye, which incorporates into mitochondria regardless of mitochondria activity. Analyzed data showed that the mass of the mitochondria, which is determined by the MFI of MTG was higher in CXCR5+ T cells compared to the CXCR5- T cell subset (**Figure 2.10c**). More so, naive T cells showed reduced mitochondria mass compared to the CXCR5- T cell subset (**Figure 2.10c**). Antigen specific CXCR5+ T cells in the spleen also retained higher mitochondria mass compared to CXCR5- T cells (**Figure 5S7c**). Memory T cells are known to have higher mitochondria mass compared to effector T cells [127,128], therefore this data suggest that CXCR5+ T cells are memory-like cells and thus complement the memory data in **Figure 2.6**. Further aspect of the mitochondria activity such as the potential sensitivity and the expression of mitochondria ROS were measured for CXCR5+ and CXCR5- T cell subsets. Mitochondria membrane potential sensitivity was measured using two different potential sensitivity dye Tetramethylrhodamine ethyl ester, perchlorate (TMRE) and Mitotracker Deep Red (MTDR). TMRE and MTDR are potential sensitive dyes which accumulates into mitochondria depending on the potential gradient across the mitochondria membrane. Analysis of MTDR and TMRE data showed higher frequency of MTDR and TMRE in CXCR5+ T cell compartment (**Figure 2.10d, f**). Importantly, the MFI of mitochondria potential was highly reduced in the CXCR5- T cell subset compared to the CXCR5+

T cells (**Figure 2.10e, g**), suggesting compromised mitochondria membrane sensitivity in CXCR5- T cells.

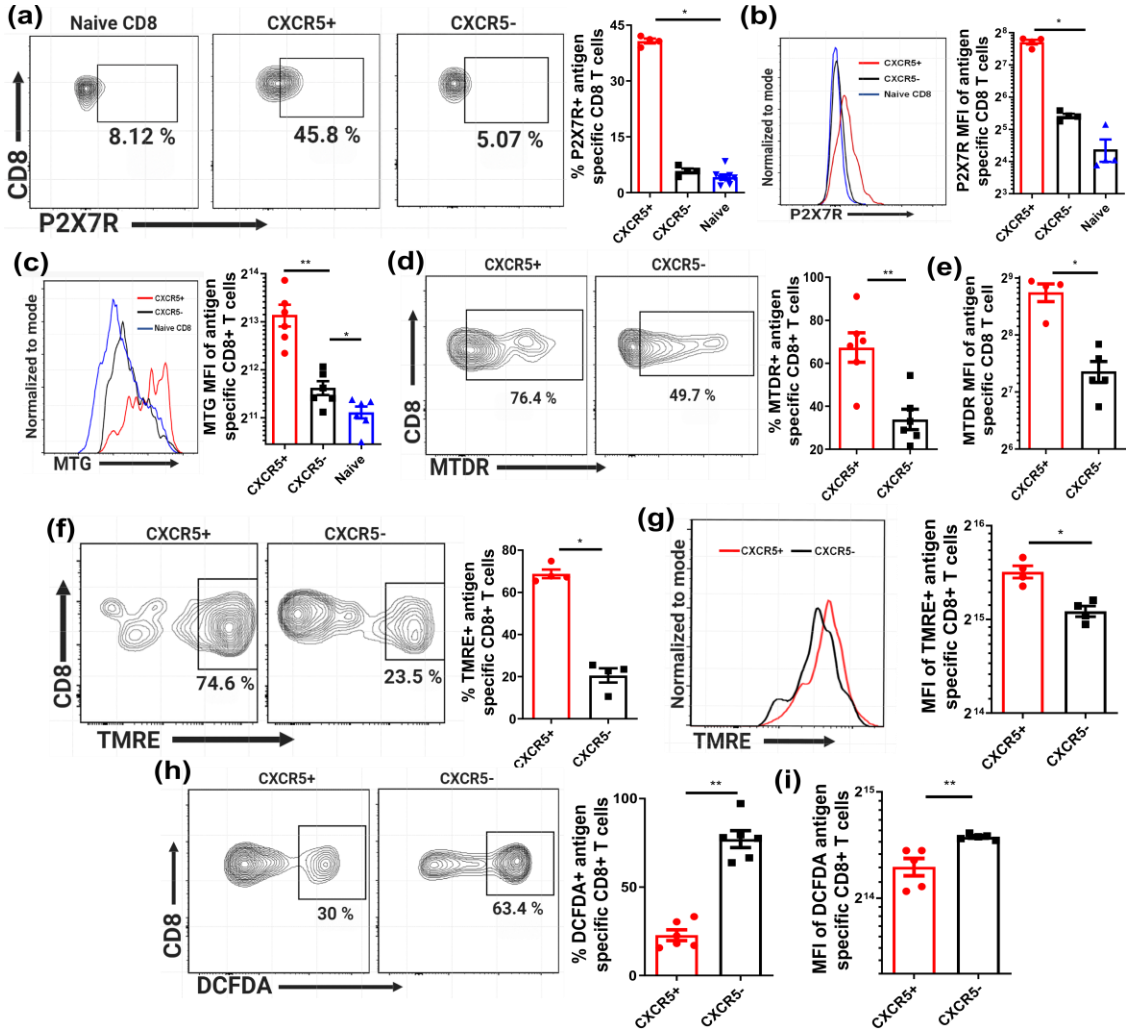

Figure 2.10: Improved mitochondria fitness of exhausted T cells in the liver is associated with CXCR5+ T cells

(a) Frequency of the purinergic receptor P2X7R expression on naïve CD8+ T cells, antigen specific CXCR5+ and CXCR5- T cells. Representative dot plots (left) and summary (right) of P2X7R expression. 5 x 10^5 LNPCs isolated from high antigen mice 21 days post vaccination were phenotyped for antigen specific CXCR5+ and CXCR5- T cells alongside P2X7R expression. Data was analyzed with flow cytometry.

(b) Expression level of P2X7R on naïve, CXCR5+ and CXCR5- T cells in (a). Representative histogram (left) and quantified MFI summary (right) of P2X7R expression.

(c – i) LNPCs from high antigen mice were isolated 21 days post AdOva vaccination or adoptive transfer of 3 - 5 x 10^6 OT-1 cells. 5 x 10^5 of the LNPCs were cultured with mitochondria sensitive dyes such as mitotracker green, deep red, TMRE and mROS dye DCFDA at 37°C for 15 – 30 min. Cells were the harvested and phenotyped for antigen specific CXCR5+ and CXCR5- CD8+ T cells. Analysis was by flow cytometry and representative data was from AdOva vaccination experiment unless otherwise stated. ***(Continuation on next page)***

(c) Expression level of mitotracker green (MTG; mitochondria mass) of CXCR5+ and CXCR5- T cells. Representative histogram plot (left) and quantified summary (MFI) of MTG.

(d) Expression frequency of mitotracker deep red (MTDR; mitochondria membrane potential) of CXCR5+ and CXCR5- T cells. Representative flow plot (left) and summarized frequency (right) of MTDR.

(e) Quantified MFI of MTDR in CXCR5+ and CXCR5- T cell subset analyzed in (d).

(f) Frequency of TMRE (mitochondria membrane potential) in CXCR5+ and CXCR5- T cells. Representative dot plot (left) and summarized frequency (right) of TMRE. Data is representative of OT-1 transfer experiment.

(g) Expression level (MFI) of TMRE in CXCR5+ and CXCR5- T cells in (f). Representative histogram (left) and quantified MFI summaries (right) of TMRE. Data is representative of adoptive OT-1 transfer experiment.

(h) Frequency of mitochondria ROS (DCFDA) expression in CXCR5+ and CXCR5- T cells. Representative dot plots (left) and summarized frequency (right) of DCFDA.

(i) MFI of DCFDA in CXCR5+ and CXCR5- T cells analyzed in (h).

Representative data of one of two independent experiment is shown. Each group consist of 4-6 biological replicates, depicted as dots. Data is depicted as Mean ± SEM. Significance was calculated by Mann-Whitney's test: *$p \leq 0.05$, **$p \leq 0.01$, 'ns' indicate not significant

The reduced mitochondria mass and compromised mitochondria sensitivity in CXCR5- T cells, raised the question of whether there is excessive mROS expression in CXCR5- T cells. mROS expression is known to trigger of T cell function[129], however, in some instances excessive mROS expression disrupts mitochondria function[130]. For this reason, mROS staining was performed on CXCR5+ and CXCR5- T cells, D21 post AdOva vaccination. Data suggest a striking phenomenon with ~90 % of CXCR5- T cells express mROS while a minority of CXCR5+ T cells express mROS (**Figure 2.10h**). Interestingly, mROS MFI was higher in CXCR5- T cells (**Figure 2.10i**). The state of mitochondria potential of CXCR5+ T cells in the spleen were observed to be reduced in CXCR5+ T cells compared to the CXCR5- T cell subset, taking into consideration the frequency and MFI (**Figure 5S7d, e**). Nevertheless, the accumulation of mROS was lower in the CXCR5+ T cells (**Figure 5S7f, g**). The specific differences in mROS from the liver data might be due to the quiescent nature of antigen specific CD8+ T cells in the spleen, in absence of antigen stimulation. Putting together, these datasets point to the possibility that CXCR5+ T cells may have efficient mitochondria function compared to the CXCR5- T cell subset, most especially in the liver where persistent T cell stimulation is ongoing.

2.11 Enhanced nutrient uptake by exhausted T cells is CXCR5+ T cell restricted

In this study, CXCR5+ T cells were found to be armed with efficient mitochondria (**Figure 2.10**) and effector function than CXCR5- T cells subset (**Figure 2.8 and 2.9**). The production of effector cytokine is largely coupled to bioenergetics and nutrient acquisition efficiencies of T cells[66,131].

Therefore, it was asked if the ability of CXCR5+ T cells to globally produce more effector cytokines is a consequence of a nutrient acquisition advantage. In this regard, exhausted T cells isolated from the liver D21 post AdOva vaccination or adoptive OT-1 transfer were phenotyped for glucose 1 transporter (Glut-1). Glut-1 is essential for importing glucose into the cell which helps to fuel the cellular and biological processes of T cells. Results obtained from Glut-1 staining showed a startling revelation where CXCR5+ and naive T cells were imprinted with higher frequency compared to the CXCR5- T cell subset (**Figure 2.11a**). Quantification of Glut-1 MFI further indicated higher protein level in CXCR5+ T cells compared to the CXCR5- T cell subset (**Figure 2.11b**).

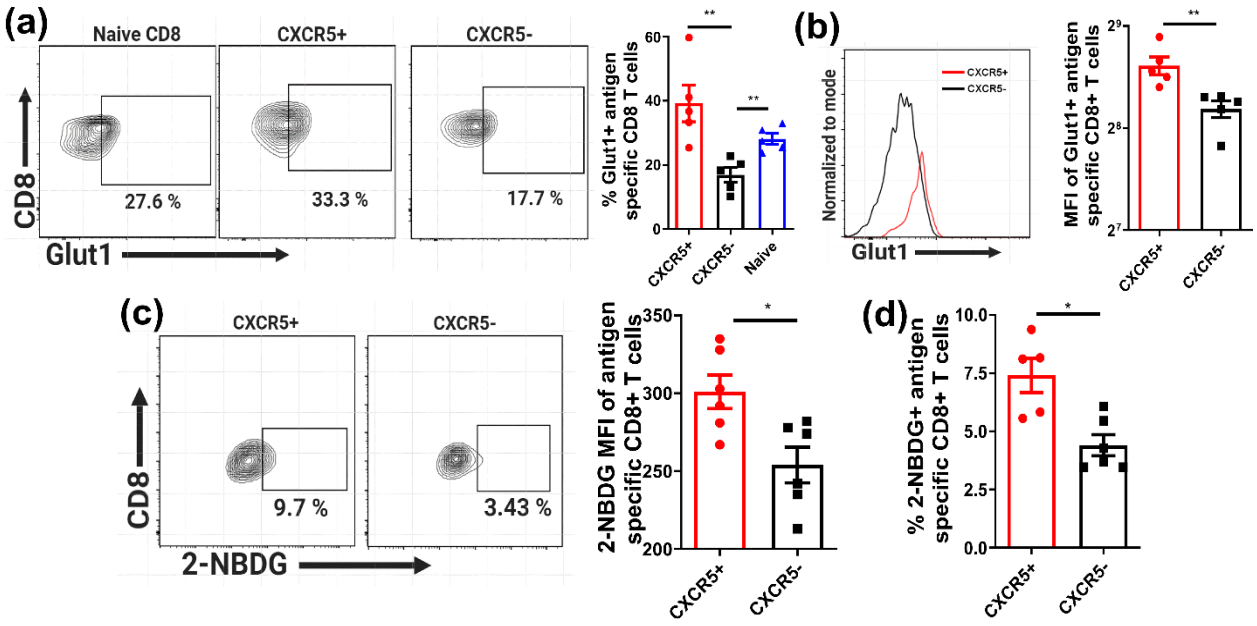

Figure 2.11: Enhanced nutrient uptake of exhausted T cells in the liver is restricted to the CXCR5+ T cell subset

(a) Frequency of glucose-1 (Glut-1) expression on naïve, antigen specific CXCR5+ and CXCR5- T cells. Representative dot plots (left) and summarized frequency (right) of Glut-1. LNPCs from high antigen mice were isolated 21 days post vaccination and 5 x 10^5 cells were phenotyped for Glut-1 expression intracellularly in antigen specific CXCR5+ and CXCR5- T cell subsets.

(b) Expression level of Glut-1 expression in CXCR5+ and CXCR5- T cells in (a). Representative histograms (left) and quantified MFI summary (right) of Glut-1 expression.

(c) Frequency of fluorescent glucose (2-NBDG) uptake in CXCR5+ and CXCR5- T cells. Representative dot plots (left) and summary (right) of 2-NBDG uptake. 5 x 10^5 cells of the LNPCs isolated from high antigen mice 21 days post vaccination were culture with 2-NBDG at 37°C for 30 min and analyzed for the uptake of glucose in antigen specific CXCR5+ and CXCR5- T cells with flow cytometry.

(d) MFI of 2-NBDG in CXCR5+ and CXCR5- T cell subsets analyzed in (c).

Representative data of one of two independent experiment is shown. Each group consist of 5-6 biological replicates, depicted as dots. Data is depicted as Mean ± SEM. Significance was calculated by Mann-Whitney's test: *$p \leq 0.05$, **$p \leq 0.01$, 'ns' indicate not significant

However, to test the functionality of Glut-1 expression by CXCR5+ and CXCR5- T cells, isolated NPCs from the liver were cultured with fluorescent glucose (2-NBDG). Detailed analysis suggests that the CXCR5+ T cells, in concordance to higher Glut-1 expression, showed higher frequency of 2-NBDG uptake (**Figure 2.11c**) as well as the MFI of 2-NBDG (**Figure 2.11d**). In addition, taking a look at the quiescent antigen specific CD8+ T cells in the spleen, the frequency of Glut-1 on CXCR5+ T cells were relatively higher, but the MFI showed no difference in CXCR5+ and CXCR5- T cells (**Figure 5S8a, b**). The functional assessment of the Glut-1 expression by splenic resident antigen specific T cells showed higher frequency of 2-NBDG uptake in CXCR5+ T cells (**Figure 5S8c**). Although CXCR5+ T cells take up more glucose, the MFI of glucose uptake remained similar between CXCR5+ and CXCR5- T cells (**Figure 5S8d**). Taking all together, these data suggest that efficient oriented mitochondria function of exhausted CD8+ T cells in the liver is tightly associated with tissue resident memory-like CXCR5+ T cells.

2.12 Enhanced proliferation and co-stimulatory markers in CXCR5+ T cells

Enhanced nutrient acquisition advantage endowed in CXCR5+ T cells (**Figure 2.11**) suggest that the acquired nutrients might be needed to drive rapid proliferation and other cellular processes of CXCR5+ T cell subset. In this regard, it was hypothesized that CXCR5+ T cells may have a distinct proliferation status compared to CXCR5- T cells. Therefore, the cell cycle marker Ki67 was assessed 21 days post AdOva vaccination in CXCR5+ and CXCR5- T cell subset. All cells in the CXCR5+ and CXCR5- T cell compartment was positive for Ki67 (data not shown), however a careful examination showed a higher frequency of CXCR5+ T cells expressing high Ki67 ($Ki67^{hi}$) (**Figure 2.12a**). In accordance to higher frequency of $Ki67^{hi}$ expressing CXCR5+ T cells, the MFI of Ki67 was similarly higher in CXCR5+ T cell subset compared to CXCR5- T cells (**Figure 2.12b**), suggesting that CXCR5+ T cells may undergo enhanced proliferation compared to the CXCR5- T cell subset. Also, antigen specific CD8+ T cells analyzed from spleen showed similar observations made from the liver, where higher expression level of Ki67 were restricted to CXCR5+ T cells (**Figure 5S9a, b**).

Enhanced proliferation marker expression on CXCR5+ T cells points to the probability that CXCR5+ T cells might also possess improved co-stimulatory marker CD28. Indeed, signaling through the TCR alongside the costimulatory molecule CD28 has been demonstrated to improve T cell function and proliferation. Therefore, it was next queried if the observed difference in cell cycle protein expression correlates with the expression of the T cell costimulatory receptor CD28. Costimulatory receptor CD28 was analyzed and all CXCR5+ T cells express CD28, whereas ~50 % of CXCR5- T cells express CD28 (**Figure 2.12c**). In addition, quantification of CD28 MFI showed much higher (2-fold) expression level of CD28 on CXCR5+ T cells compared to CXCR5- T cell subset (**Figure 2.12d**). Taking together, these data are suggestive of possible proliferation improvement and *in vivo* maintenance of CXCR5+ T cells as opposed to CXCR5- T cells.

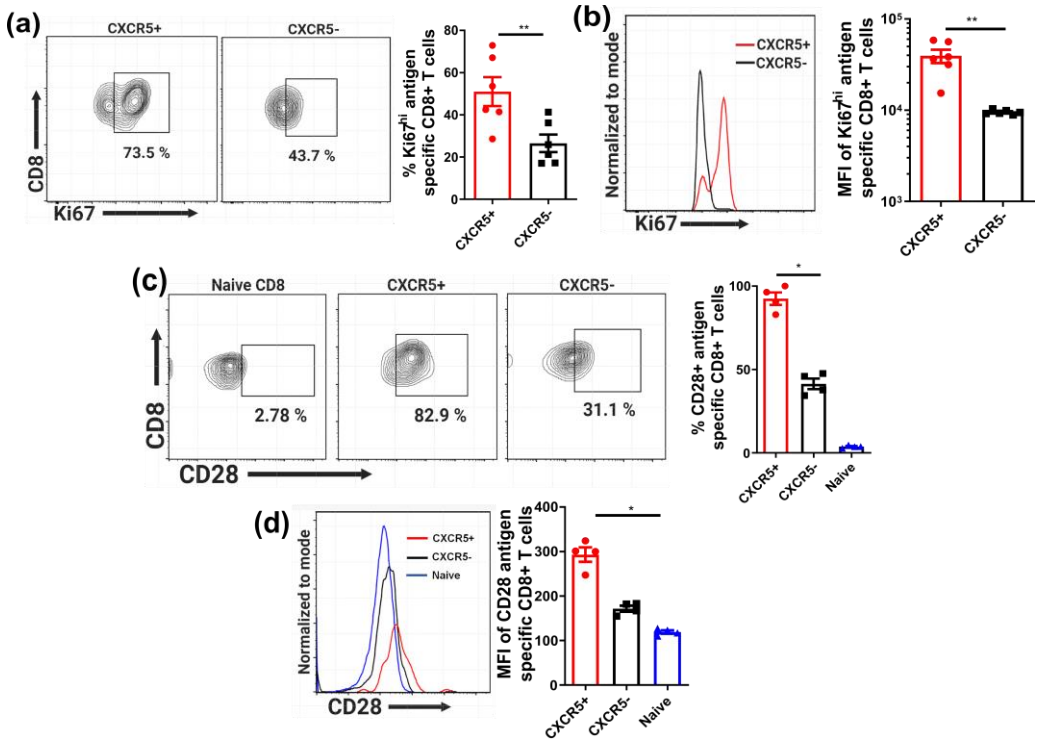

Figure 2.12: Different level of proliferation and costimulatory marker in exhausted T cell subsets in the liver

(a) Frequency of Ki67^{hi} expression in CXCR5+ and CXCR5- T cells. Representative dot plots (left) and summarized frequency (right) of Ki67^{hi}. D21 post AdOva vaccination of high antigen mice, 5 x 10^5 LNPCs isolated were phenotyped for Ki67 expression in antigen specific CXCR5+ and CXCR5- T cells. Data analysis was done with flow cytometry.

(b) Expression level of Ki67^{hi} in CXCR5+ and CXCR5- T cells as in (a). Representative dot plot (left) and quantified MFI summary (right) of Ki67^{hi} expression.

(c) Percent frequency of CD28 expression on naïve, antigen specific CXCR5+ and CXCR5- T cells. Representative dot plots (left) and summarized frequency (right) of CD28. 5 x 10^5 LNPCs isolated from high antigen mice 21 days post AdOva vaccination were phenotyped for CD28 expression on antigen specific CXCR5+ and CXCR5- T cells and analysis was done with flow cytometry.

(d) Expression level of CD28 on naïve, antigen specific CXCR5+ and CXCR5- T cell subset analyzed in (c). Representative dot plot (left) and quantified MFI summary (right) of CD28.

Representative data of one independent experiment is shown. Each group consist of 4-6 biological replicates, depicted as dots. Data is depicted as Mean ± SEM. Significance was calculated by Mann-Whitney's test: *$p \leq 0.05$, **$p \leq 0.01$, 'ns' indicate not significant

2.13 Exhausted liver resident T cell subsets exhibit differential *in vivo* maintenance

The differential glucose uptake (**Figure 2.11**), memory status as well as CD28 and Ki67 expression in CXCR5+ and CXCR5- T cells prompted the hypothesis that CXCR5+ and CXCR5- T cells may possess distinct *in vivo* maintenance and recall responses. To test this hypothesis, naive OT-1 cells were transferred into high antigen mice (**Figure 2.13a**). D9 post T cell transfer, CXCR5+ and CXCR5- T cells were sorted by flow cytometry and transferred into low antigen recipient mice (**Figure 2.13a**). D6 post transfer of CXCR5+ and CXCR5- T cells, LNPCs were isolated and phenotyped for flow cytometry analysis. Analyzed data showed higher frequency of antigen specific T cells in the liver of CXCR5+ T cells recipient mice compared to the CXCR5- T cell recipient mice (**Figure 2.13b**). Furthermore, quantification of the number of antigen specific T cells showed higher numbers in CXCR5+ T cell recipient mice (**Figure 2.13c**). Also, the differentiation pattern shows that antigen specific cells in CXCR5- T cell recipient mice remained largely CXCR5- while the CXCR5+ T cell recipient mice generate CXCR5- T cells as well as maintaining CXCR5+ T cell (**Figure 2.13d**). In sum, these data suggest that CXCR5+ T cells have a proliferation, self-maintenance and memory recall advantage over the CXCR5- T cell subset in the liver.

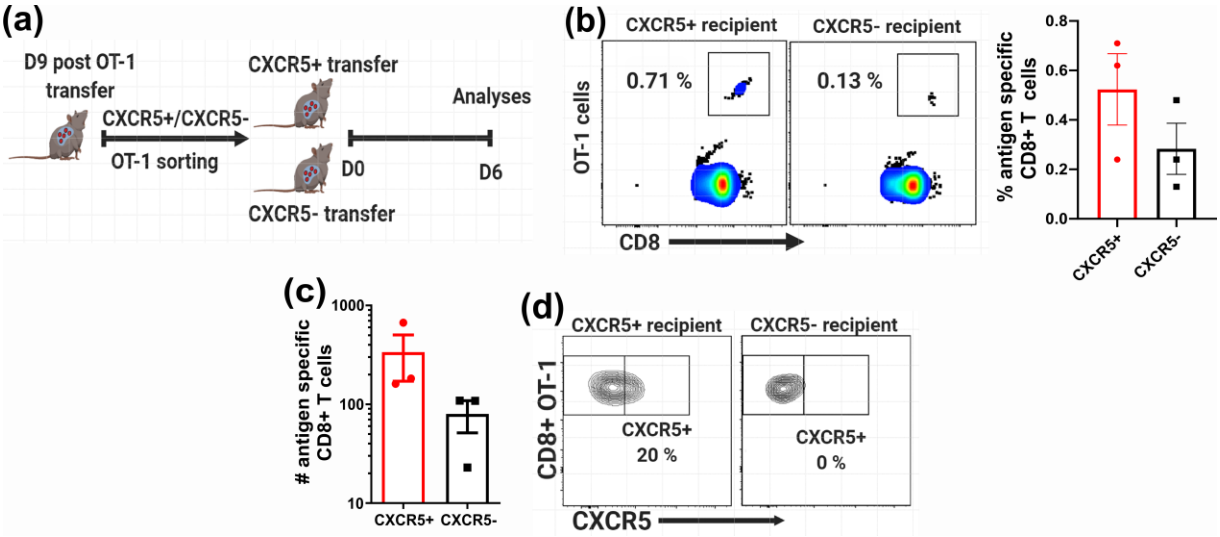

Figure 2.13: Distinct in vivo maintenance of the exhausted liver resident T cell subsets

D9 post transfer of naïve 3 - 5 x 10^6 DsRED+OT-1 cells into high antigen mice, LNPCs were isolated and phenotyped to identify antigen specific CXCR5+ and CXCR5- T cells. The stained cells were FACS sorted for DsRED positive CXCR5+ and CXCR5- T cells. The sorted cells (CXCR5+ and CXCR5-) were then transferred into respective low antigen recipient mice. D6 post transfer of CXCR5+ and CXCR5- T cells, LNPCs were isolated and phenotyped for antigen specific T cells in the liver.

(a) Schematic depiction of the experimental setup.

(b) Representative dot plots (left) and summary (right) of the frequency of antigen specific CXCR5+ and CXCR5- T cells in recipient mice.

(c) Absolute numbers of antigen specific CD8+ T cells in the liver of CXCR5+ and CXCR5- T cell recipient mice analyzed in (b).

(d) Representative dot plots of the differentiation pattern of CXCR5+ and CXCR5- T cells post transfer.

Representative data of one independent experiment is shown. Each group consist of 3 biological replicates, depicted as dots. Data was depicted as Mean ± SEM.

3 Discussion, Conclusion and Future perspective

3.1 Discussion

Hepatotropic viruses specifically infect and thrive in human hepatocytes, resulting in impaired T cell function. As such, there are currently no mouse adapted viruses which adequately and exclusively infect hepatocytes, to recapitulate the situation in HBV and HCV infection. This epitomizes a particular limitation in the pursuit of dissecting immunity to chronic liver infection. Indeed, this is due to the fact that the liver provides a unique environment, which is particularly different from other tissues and organs. The unique liver environment is known to be associated with high level of anti-inflammatory cytokines and mediators such as IL-10, TGF-β and prostaglandins due to its physiological function. In addition, the expression of high amount of IDO, which depletes essential amino acids and deprives T cells of amino acid, is an important key player that makes immune responses in the liver different from other organs. Therefore, the lack of small animal models presents a profound limitation on understanding *in situ* T cell dysfunction in the liver and for the development of immune based therapeutic approaches for treating liver infections. In this study, this limitation was partially circumvented with a transgenic mouse model (OvaXCre) in which a heterologous antigen (Ova) was intracellularly expressed in about 50% of hepatocytes as a consequence of Tam mediated recombination[110,112]. These mice are characterized by chronic expression of the intracellular antigen (Ova) exclusively in hepatocytes, thereby mimicking chronic antigen expression, a situation observed in chronic HBV and HCV infection, where viral antigens are displayed by hepatocytes. Upon AdOva vaccination, which results in priming of endogenous antigen specific T cells, or transfer of antigen specific OT-1 cells, antigen specific T cells accumulate and expands in the liver but fail to eradicate the Ova antigen. The lack of Ova antigen clearance is observed to be a consequence of T cell exhaustion[110,114]. This is accompanied by high inhibitory receptor expression and decreased effector functions of T cells in the liver[110]. These phenomena are consistent with human and mouse models of chronic viral infection such as HIV and LCMV infection respectively. In addition, it also recapitulate the phenotype of CD8+ T cell observed in liver cancer and chronic HBV and HCV infection, licensing the high antigen OvaXCre model as a tool to understand the dynamic regulation of T cell exhaustion and the impact of immunomodulation on exhausted T cells in the tolerogenic liver environment.

In this study, exhausted T cells in the liver were monitored in real-time, and they were observed to undergo extreme reduction as the duration of chronic antigen stimulation increased. However, host conditioning with CpG ODN, which is known to trigger the TLR9 signaling pathway and remodels the liver environment[40], facilitated the efficient clearance of Ova-antigen from the liver. This is probably due to rewiring of the effector functions in already exhausted T cells. The clearance of Ova antigen, and possibly rewiring of effector function in exhausted T cells may partly contribute to the reduced expression of the stemness transcription factor TCF-1.

Two subsets of exhausted T cells were identified out of the pool of exhausted T cells in the liver of mice without CpG ODN treatment. These subsets were delineated by the expression of the chemokine receptor CXCR5. Although the liver has not yet been described to be a habitat for CXCR5+ T cells, detailed analysis indicated that CXCR5+ T cells are *bona fide* CXCR5+ T cells due to the expression of Bcl6, the transcription factor governing CXCR5 expression. Intriguingly, CXCR5+ T cells show upregulated expression of the liver resident T cell marker LFA-1 and, are the major host for TCF-1 expression in the pool of exhausted T cells in the liver. Importantly, CXCR5+ and CXCR5- T cells are involved in antigen recognition as they upregulate the surrogate T cell receptor signaling pathway Nur77.

Furthermore, CXCR5+ T cells have the resemblance of tissue resident memory cells. In addition, the CXCR5+ cells generate both CXCR5+ and CXCR5- T cells and, are therefore referred to as progenitor CXCR5+ T cells. The CXCR5- T cells on the other hand are referred to as terminal exhausted CXCR5+ T cell due to their terminal differentiation state. The terminal differentiation state of CXCR5- T cells is characterized by lack of sufficient self-maintenance, high exhaustion and blunted effector properties. Importantly, in spite of their memory nature, CXCR5+ T cells are highly poised to mediate cytotoxic functions, possibly due to reduced exhaustion and accelerated effector function. In concord to the memory-like nature, CXCR5+ T cells exhibit improved mitochondria function and self-maintenance in vivo – a hallmark of memory cells.

In sum, these data indicate that host conditioning with CpG ODN can reshape exhausted T cell function. Moreover, they show that the pool of exhausted T cells in the liver consists of progenitor and terminal exhausted T cells which possess differential effector, memory-like, *in vivo* self-renewal and cytotoxic functions, and distinct mitochondria dynamics.

3.1.1 CpG ODN host conditioning remodels the functionality of exhausted CD8+ T cells

In recent years, immunomodulation with checkpoint blockade antibodies such as PD-L1 and CTLA-4 have gained tremendous success in chronic viral infection and cancer. These immune checkpoint blockade antibodies rejuvenate exhausted T cells, leading to remission of chronic infection and tumor[6,132]. However, there is a growing interest to as well exploit PAMPs such as TLR ligands to modulate T cell responses in cancer and chronic infections[133,134]. TLRs are conserved receptors expressed profoundly on innate immune cells such as monocytes and DCs, and ligation of TLR initiate maturation of immune cell, potentiating the secretion of inflammatory cytokines[40,114,133]. PAMPs which target innate immune sensors TLR1/2, TLR7 and TLR9 have shown promise in modulating T cell function *in vivo*[40,133]. For instance, immune cell maturation upon signaling via TLR9 results in upregulation of co-stimulatory molecules CD80/86 and OX40 and these are known to foster improved T cell function[40].

In this study, exhausted T cells were dramatically reduced in the liver with time (**Figure 2.1**), suggesting that the load of antigen and duration of exposure were possibly impacting on exhausted T cell maintenance in the liver. The apparent loss of antigen specific T cell may be a result of apoptosis-induced attrition accompanying severe exhaustion. The loss of antigen specific T cells may partly play a role, aside reduced effector function, in the lack of antigen reduction in the liver.

Previous studies from our lab and others have demonstrated the importance of modulating T cell response to chronic antigen via TLR9 ligation with CpG ODN. These studies show that CpG ODN host conditioning circumvents the development of T cell exhausted while fostering improved T cell function[40,114]. Improved T cell function as a result of TLR9 targeting, as demonstrated by one of the studies, was due to the formation of myeloid clusters[40]. These myeloid cells were shown to upregulate OX40 and CD80/86, which helps in sanctioning improved T cell blastogenesis and effector function[40]. Importantly, these studies relied on host conditioning with CpG during the initiation phase of effector T cell response.

In this present study, the impact of CpG ODN host conditioning (**Figure 2.2**) was evaluated in a late phase after OT-I transfer or after vaccination, when antigen clearance failed, and T cell exhaustion is fully established. Strikingly, host conditioning with CpG ODN facilitated efficient

antigen clearance, suggesting rejuvenation of already exhausted T cells. This may be due to CpG ODN mediated rewiring and reengagement of effector properties in exhausted T cells.

Indeed, a recent study posits that immunotherapy with PD-1 blockade rewired effector properties through reengaging effector specific transcriptional networks in exhausted T cells[100]. This reengagement improved effector functions of exhausted T cells, however this was transiently maintained due to the epigenetic stability of the exhausted T cell landscape[100,102]. Although this might occur under CpG treatment, it remains to be proven if CpG ODN treatment and PD-1 blockade reengages similar transcription factor networks in exhausted T cells.

After CpG ODN conditioning, antigen specific T cells were dramatically reduced in the liver. This effect may be linked to the imprinted effector properties imposed on exhausted T cells, which after antigen clearance may have undergone apoptosis. Indeed, it is known that the majority of effector cells undergo apoptosis at the end of an immune response[4,5]. Of note, the ability of CpG ODN to potentiate antigen clearance via possible rejuvenation of exhausted T cells supports the findings that exhausted T cells are not anergic, and that anergic and exhausted T cells develop from distinct transcriptionally regulated and differentiation pathways[8,79]. Further, inflammatory signaling potentiates the suppression of TCF-1[118], and the extreme loss of TCF-1 in residual T cells may possibly be a consequence of the inflammatory environment created by CpG ODN conditioning, thereby resulting in decreased self-renewal. Therefore, the depletion of antigen specific T cells after CpG ODN conditioning may partly be due to the loss of TCF-1 in antigen specific T cells.

During chronic viral infection, even though T cells get exhausted, they can be maintained life long without complete depletion[89]. The ability of exhausted T cells to undergo life-long maintenance is ascribed to TCF-1 mediated transcriptional regulation[96,135]. Indeed, in cancer as well as in chronic viral infection, lack of TCF-1 expression exacerbates severe exhaustion, extreme loss and apparent depletion of antigen specific T cells[136,137]. In concordance, the absence of CpG ODN host conditioning facilitated an improved maintenance of T cells, probably as a result of higher levels of TCF-1 expression compared to CpG ODN treated condition where TCF-1 is downregulated. Importantly, the number of TCF-1+ antigen specific T cells indicates that enhanced maintenance of antigen specific T cells may be linked tightly to TCF-1 expression. Furthermore, the reduced level of activation marker CD69 on antigen specific T cells after CpG ODN suggests that these T cells may be relatively quiescent as a consequence of the lack of TCR signaling. This is possibly

due to no antigen in the liver. Indeed, TCR signaling is tightly associated with the expression of activation markers on T cells.

3.1.2 Differentiation subsets of exhausted T cells in the liver

During chronic viral infection and cancer, hierarchical differentiation states have been alluded to, in the pool of exhausted T cells. This is currently the governing proposal guiding the dynamic understanding of T cell exhaustion[3,5]. Indeed, different studies have identified a particular heterogeneity in exhausted T cells using receptors such as CXCR5, PD-1, Slamf6[107] and CD44, and transcription factor TCF-1[3,5,138]. In a simplistic term, this heterogeneity can be categorized as progenitor and terminally exhausted T cell subsets. The progenitor subset of exhausted T cells have a self-renewing property, robustly responds to PD-1 immunotherapy and maintains the pool of exhausted T cells whereas the terminally exhausted T cells lack these properties[3,107].

Progenitor CXCR5+ T cells were first described in chronic LCMV infection and were shown to exclusively reside in lymphoid organs[109,139]. However, this observation may be due to the type of infection model used, and partly to enriched expression of chemokine CXCL13, the ligand for CXCR5+, in lymphoid organs[140]. Importantly, in this current study, CXCR5+ T cells were identified in the liver – the site of antigen expression, suggesting that other factors may contribute to retaining CXCR5+ T cells in conventional and unconventional niches (**Figure 2.3**). Although serum CXCL13 levels were found increased in response to antigen recognition in the liver, antigen may be a major contributing factor in retaining CXCR5+ T cells in the liver. Thus, CXCR5+ T cells may be retained in the liver as a result of antigen recognition, which facilitated increase in serum level of CXCL13. Increase in CXCL13 serum levels is possibly due to expression of CXCL13 from liver tissues as a consequence of antigen recognition in the liver. This may play a role, in addition to antigen, in enhancing the localization of CXCR5+ T cells in the liver. Indeed, a recent study suggests that high levels of CXCL13 in chronic HBV patients facilitates intrahepatic recruitment of CXCR5+ T cells[141].

The generated numbers of CXCR5+ T cells were relatively stable (**Figure 2.3**) in the liver as severity of exhaustion increases with time, indicating that CXCR5+ T cells may be undergoing self-maintenance, as previously suggested[104]. Interestingly, published data indicate that the transcription factors Bcl6 and TCF-1 co-operate in restraining the pro-exhaustion effect of IFN-1, thereby nurturing the stemness of exhausted T cells[97]. In line with this proposal, Bcl6 and TCF-1

were exclusive expressed in CXCR5+ T cells, suggesting that the TCF-1-Bcl6 transcription factor axis may potentially play a role in regulating multi-potency, cytotoxicity and exhaustion states of CXCR5+ T cells (**Figures 2.3 and 2.4**). Further, effector T cells are known to downregulate TCF-1 expression[118], and the lack or loss TCF-1 expression is indicative of probable effector potential of CXCR5- T cells.

To investigate if the CXCR5 cells reside in the liver or rather circulate it was tested if they express Nur77. Nur77 forms a part of the transcriptional circuits regulating tissue resident T cell formation[123]. In addition, it was recently shown that upregulation of LFA-1 supports the retention of T cells in the liver[120]. Therefore, the observed upregulation of LFA-1 and Nur77 is indicative of T cells residency and thus, CXCR5+ and CXCR5- T cells may be *bona fide* liver resident T cells (**Figure 2.4**). However, this claim remains to be validated exclusively using parabiosis studies, by surgically connecting the circulatory system of two congenic mice. This system is the proposed gold standard used in validating tissue residency of immune cells. Further, Nur77 expression is consequential on TCR signaling[142]. The expression of Nur77 in this study strongly supports the idea that exhausted T cells are not anergic, and it additionally demonstrates that exhausted T cells are capable of undergoing rejuvenation upon CpG ODN administration.

3.1.3 Cytotoxic function of exhausted T cell subsets

In chronic viral infection and possibly in cancer, exhausted T cells can control viral load and cancer metastasis to some extent. This effect is mediated by residual effector functions of exhausted T cells[143,144]. Until recently it was not well understood if a subset of exhausted T cells is responsible for mediating residual effector function. Although current understanding projects the presence of progenitor and terminal exhausted T cell subsets[96,101,107,109], there is an apparent lack of consensus on the subset of cells which are actively involved in inducing control of tumor or chronic viral infection. Indeed, in chronic LCMV infection progenitor exhausted T cells were shown to have classical memory-like properties and lack effector functions while terminal exhausted T cells were shown to mediate direct killing of infected cells[96]. On the contrary, in tumor models progenitor exhausted cells mediated direct killing of tumor cells[107]. This dichotomy may be a result of different tissue localization and disease models under which these two subsets were studied.

In this study, the CXCR5+ T cell subset were shown to have a memory-like phenotype (**Figure 2.5**). Although memory-like, they possess high cytotoxic function, a feature that is inconsistent

with classical memory T cells (**Figure 2.9**). In concordance, CXCR5+ T cells exhibit reduced exhaustion and enhanced effector cytokine expression if compared to CXCR5- T cells (**Figures 2.7 and 2.8**). Improved memory and effector functions coupled to the ability of CXCR5+ T cells to generate both CXCR5+ and CXCR5- T cells (**Figure 2.13**) further support the importance of the Bcl6-TCF-1 axis in maintaining multipotency and polyfunctionality of T cells[137]. The cooperativity of Bcl6-TCF-1 may also confer a survival advantage of CXCR5+ T cells over CXCR5- T cells. Indeed, CD127 is known to foster long-term survival of T cells[88,145] and its enriched expression suggests a predisposition to improved CXCR5+ T cell survival (**Figure 2.6**). In concert to enhanced survival predisposition, CXCR5+ T cells had improved *in vivo* maintenance compared to CXCR5- T cells. The level of Ki67 expression in CXCR5+ and CXCR5- T cells coupled to *in vivo* maintenance suggest that the extent of cell cycle progression may be linked tightly to the extent to which CXCR5+ and CXCR5- T cells are maintained *in vivo*.

The transcription factor networks regulating Teff and Tmem cells are dysregulated in exhausted T cells[3,5,6]. As such, the effector-memory bi-functional nature of CXCR5+ T cells may be due to atypical transcriptional and possibly epigenetic regulation in CXCR5+ T cells. Thus, exhaustion mediated transcriptional networks may sanction aberrant engagement of memory and effector transcription factors in CXCR5+ T cells. On the contrary, CXCR5- T cell subsets exhibit reduced effector and memory-like properties if compared to CXCR5+ T cells. This is probably due to the engagement of severely deranged transcriptional circuits. The memory and cytotoxic function of CXCR5+ T cells shown in the current study agrees with studies evaluating CXCR5+ T cells in chronic LCMV infection. Nevertheless, this is in contrast to studies where TCF-1+ was used as a reporter in studying subsets of exhausted T cells[96,136]. The divergence in these two subgroups of progenitor exhausted T cells (TCF-1+ vs CXCR5+) implies a possible heterogeneity in the CXCR5+ T cell subset.

Recently, CXCR5+ T cells were suggested to traffic either to the B cell zone[104] or to preferentially dock to DCs in the T cell zone[109] of lymphoid organs. Therefore, it was hypothesized that the improved cytotoxicity of CXCR5+ T cells in the current study might be due to the co-localization of CXCR5+ T cells to myeloid cells (i.e. DCs) in the liver. Probably, this is the strategy utilized by CXCR5+ T cells to retain enhanced cytotoxic functions and reduced exhaustion, however, this proposal warrants further investigation. This hypothesis stems from the fact that the liver is not a

classical lymphoid organ where germinal centers are formed, and thereby facilitating CXCR5+ T cell localization. In addition, signaling through CD28 improves the functionality of T cells[3,5]. Increased CD28 expression on CXCR5+ T cells coupled to possible interactions of CXCR5+ T cells with myeloid cells may be responsible for their enhanced cytotoxic function.

3.1.4 Mitochondria dynamics and its impact on exhausted T cell subsets

Mitochondria are referred to as the powerhouse of the cell[146,147]. They mediate multiple cellular and molecular homeostatic processes. After activation, T cell engages cellular metabolism to meet the increasing demand for metabolic products in the form of ATP and biomass needed for cell growth, differentiation, production of effector molecules and proliferation[147,148]. The supply of ATP within T cells is mediated by either glycolysis or oxidative phosphorylation (OXPHOS). During the lifetime of a T cell, mitochondria morphology changes dynamically, and these changes tightly regulate distinct metabolic pathways. Additionally, mitochondria dynamism facilitates mitochondria biogenesis, nurturing the formation of increased mitochondria mass, and this process is mediated by PGC-1α[147,148]. Indeed, after T cell activation, mitochondria in Teff cells undergo fragmentation, and rely on aerobic glycolysis for full function. Fragmented mitochondria result in an increased ROS generation, which may be important for Teff activation and enhanced mitophagy[147,148]. Intriguingly, in Tmem, fused and elongated mitochondria networks are enacted, which promote efficient electron transport chain (ETC) activity, facilitating robust OXPHOS. These arrangement fosters increased spare respiratory activity (SRC), which is the ability to produce energy under stressful conditions[147,148] – a hallmark of memory T cells.

Documented evidence suggests the expression of purinergic receptor on antigen specific T cells marks long-lived memory cells[126]. In the current study, CXCR5+ T cells exclusively express the purinergic receptor P2X7R, indicating that they may be long-term memory cells (**Figure 2.10**). Interestingly, the involvement of P2X7R in T cell metabolism is mediated via AMPK stimulation, OXPHOS, increased glucose and fatty acid uptake[126]. In concert, the mass of mitochondria in the CXCR5+ T cells, which shapes memory T cell development[149] was larger compared to CXCR5- T cells. This posits the likelihood that CXCR5+ T cells may possess enhanced ETC activity and depend more on OXPHOS for cellular function and maintenance while CXCR5- T cells may rely on glycolysis for their cellular activity. These characteristic features also agree with the improved maintenance and recall response of CXCR5+ T cells *in vivo*.

The mitochondria mass and the exclusive expression of Bcl6 in CXCR5+ T cells further suggest that CXCR5+ T cells may rely heavily on OXPHOS, since Bcl6 is known to negatively regulate glycolysis[148]. Thus, Bcl6 may possibly ensure reduced glycolytic activity in CXCR5+ T cells. Whereas the lack of Bcl6 expression in CXCR5- T cells might be indicative of exclusive reliance on glycolysis. These possibilities however remain to be fully validated by detailed analysis of the bioenergetics in CXCR5+ and CXCR5- T cells.

The improved mitochondria potential of CXCR5+ T cells and decreased ROS expression (**Figure 2.10**) also support the idea that CXCR5+ T cells may be characterized by efficient ETC. Efficient ETC formation and activity regulates ROS expression[148,149] and the extent of ROS expression in T cells may in turn drive mitochondria membrane infidelity[150,151]. The increased level of mROS in CXCR5- T cells is probably a consequential effect of fragmented mitochondria, which may have accounted for decreased mitochondria potential.

Upon T cell activation, Glut1 is upregulated. Usually upregulation of Glut1is needed by the cell to import glucose to drive growth, effector function and proliferation of T cells, most especially in Teff cells[147,148]. The imported glucose is injected into the glycolytic pathway, fueling cellular processes in effector T cells. In memory T cells however, there is a reduced reliance on glycolysis to fuel cellular maintenance[147,148]. Interestingly in this study, memory like CXCR5+ T cells showed higher upregulation of Glut1 and this translated into an improved uptake of glucose compared to CXCR5- T cells (**Figure 2.11**). This observation indicates that exhausted memory-like T cell may, alongside with OXPHOS, rely on glycolysis to fuel cellular metabolism. In this regard, it is possible that CXCR5+ T cells might depend more on utilizing glycolysis than CXCR5- T cells, if the rate of glycolysis is similar in CXCR5+ and CXCR5- T cells.

CXCR5+ T cells exhibit enhanced cytotoxic and effector functions; hence it is not completely surprising that CXCR5+ T cells might also utilize glycolysis to fuel the bioenergetics demand for their cytotoxic function. Of note, glycolysis generates 2 molecules of ATP per glucose molecule while OXPHOS churns out 32 molecules of ATP. As such, glycolysis is regarded as a metabolically inefficient way of generating ATP for the cell, although faster[147,148]. Thus, the possible engagement of glycolysis in CXCR5+ T cells may be necessary to rapidly fuel the energy needed for the expression of effector molecules, and this may probably be a hallmark of tissue resident memory cells.

During chronic infection and cancer, PGC-1α which programs mitochondria biogenesis, is progressively repressed fostering decreased effector functions[70,152]. Therefore, the relatively smaller mitochondria coupled to abrogated effector and cytotoxic functions (**Figure 2.10**) are suggestive of enhanced repression or the possible loss of PGC-1α in CXCR5- T cells compared to CXCR5+ T cells. However, it remains to be shown if PGC-1α is differentially expressed in CXCR5+ and CXCR5- T cell subsets. In addition, it is possible that exhausted memory-like CXCR5+ T cells upregulate glucose uptake and possibly engage glycolytic pathway to compensate for reduced T cell oxidative metabolism, as a consequence of reduced PGC-1α during persistent T cell stimulation.

3.2 Conclusion and Future perspectives

In this study, it has been demonstrated that expressing a high load of Ova-antigen in the liver models T cell function into a state of exhaustion. This observation is consistent with what is reported in chronic viral infection and cancer. Taking together, antigen load is a major player in driving exhaustion of T cells[110,114]. Exhausted T cells were remodeled with CpG ODN treatment, translating into antigen clearance. Future studies would be needed to clarify if CpG ODN has direct and/or indirect immunomodulatory effects on exhausted T cells. In addition, TCF-1 was reshaped after CpG ODN mediated host conditioning probably due to inflammation induced by CpG ODN. Therefore, elucidating the types of inflammatory cytokines induced, facilitating TCF-1 remodeling would guide novel strategies towards the usage of inflammatory cytokines for reverting Tex. This would facilitate a cleaner way of reinvigorating exhausted T cells than the application of CpG ODN which may induces undesirable side effects in the host. The rejuvenation of T cells in this study is congruent to studies evaluating inhibitory receptor blockade antibodies (i.e. PD-L1) in chronic infection. Hence, it will be interesting to understand the molecular mechanisms underlying the transcription and probably epigenetic remodeling imposed by CpG ODN treatment on exhausted T cells.

Further, subsets of exhausted T cells were elucidated from the liver. These subsets, which was delineated based on CXCR5 expression were somewhat unexpected, since CXCR5+ T cells were previously described to localize in lymphoid organs. Most importantly, their liver resident capacity contradicts the dogma that CXCR5+ T cells are trafficking along chemokine gradients into lymphoid tissues. In the current study, increase in CXCL13 levels coincide with antigen

recognition in the liver, indicating that the Ova-antigen and increased CXCL13 may partly be responsible for sustained presence of CXCR5+ T cells in the liver and thus overriding chemotactic trafficking of antigen specific CXCR5+ T cells into lymphoid organs. Although transcriptional regulation of CXCR5+ and CXCR5- T cells in this study may differ from those studied in the spleen, it would be interesting to compare cell subsets from these two organs. This would throw more light on tissue specific regulation of T cell exhaustion, and possibly tissue specific differentiation dynamics of exhausted T cell subsets. These would reveal important T cell intrinsic modulatory strategies which might be targeted to circumvent or remodel the development of T cell exhaustion.

This study showed that CpG ODN host conditioning rejuvenated exhausted T cells in the liver resulting in efficient antigen clearance. However, the mechanisms potentiating CpG ODN mediated rejuvenation remain to be elucidated. There are at least two possibilities by which CpG mediates rejuvenation of exhausted T cells: (1) CpG ODN may induce global proliferation and enrich cytotoxic functions in the pool of exhausted T cells (2) CpG ODN may potentiate preferential proliferation and enriched effector and cytotoxic function in a subset of exhausted T cells. To elucidate the underlying mechanism, it would be imperative to evaluate CpG ODN host conditioning upon adaptive transfer of CXCR5+ vs. CXCR5- T cells *in vivo* and assessing the proliferation dynamics as well as the expression of effector cytokines.

CXCR5+ T cells were observed to show features of progenitor cells, exhibiting potent cytotoxic functions. These phenomena might be due to preferential docking of CXCR5+ T cells to myeloid cells and/or CXCL13 expressing cells in the liver. In this regard, dissecting the possibility of CXCR5+ T cell docking to specific cell subsets in the liver would shed more light on how CXCR5+ T cells maintain reduced exhaustion state and better cytotoxic functions coupled to enhanced self-maintenance properties. In addition, assessing the possibility of lymphoid structure formation in the liver would be important to indicate in the liver any probable lymphoid structure formation in this study.

In sum, the differential cytotoxic property of progenitor exhausted CXCR5+ T cells and terminally exhausted CXCR5- T cells indicate that CXCR5+ T cells would primarily, to a large extent, mediate control of chronic liver infection. The specific cytotoxic and memory states they hold create an avenue to exploit these subsets of cells to combating chronic liver infections such as

HBV and HCV infections. A long standing but crucial question in the field is to understand the signaling circuits in progenitor exhausted T cells. This would create an avenue for dissecting the signaling pathways which can enhance long term maintenance of the progenitor cells. Thereby retaining the progenitor cells in their progenitor state, with minimal or no terminal differentiation. Indeed, a recent transcriptional and mechanistic studies have identified that cell intrinsic IL-27 signaling mediates sustained proliferation of progenitor exhausted T cells[153]. In addition, cell autonomous IFN1 blockade and IRF1 signaling was important for the generation and sustained expansion of CXCR5+ T cells in a mouse model with chronic LCMV infection[153]. Since this study was evaluated in chronic LCMV infections which target the spleen, tissue specific regulation could exist between the liver and the spleen. Thus, further studies would have to test if these observations are also relevant for liver specific infections. In addition, transcriptional profiling would be needed to identify specific gene signatures which are highly enriched or depleted and may play a role in CXCR5+ T cell maintenance in the liver. Based on these hits, genetic gain and/or loss of function studies can be carried out on naïve OT-1 cells to test which specific gene(s) are modulating the long-term maintenance and generation of high numbers of CXCR5+ T cells in the liver. These specific genes can then be forcefully reprogrammed and/or ablated in T cells, which may foster the generation of increased numbers as well as long term maintenance of CXCR5+ T cells for therapeutic application.

4 Supplementary Figures

Figure 5S 1: Exhausted T cell remodeling with CpG ODN potentiate reduced TCF-1 and CD69 expression in the liver

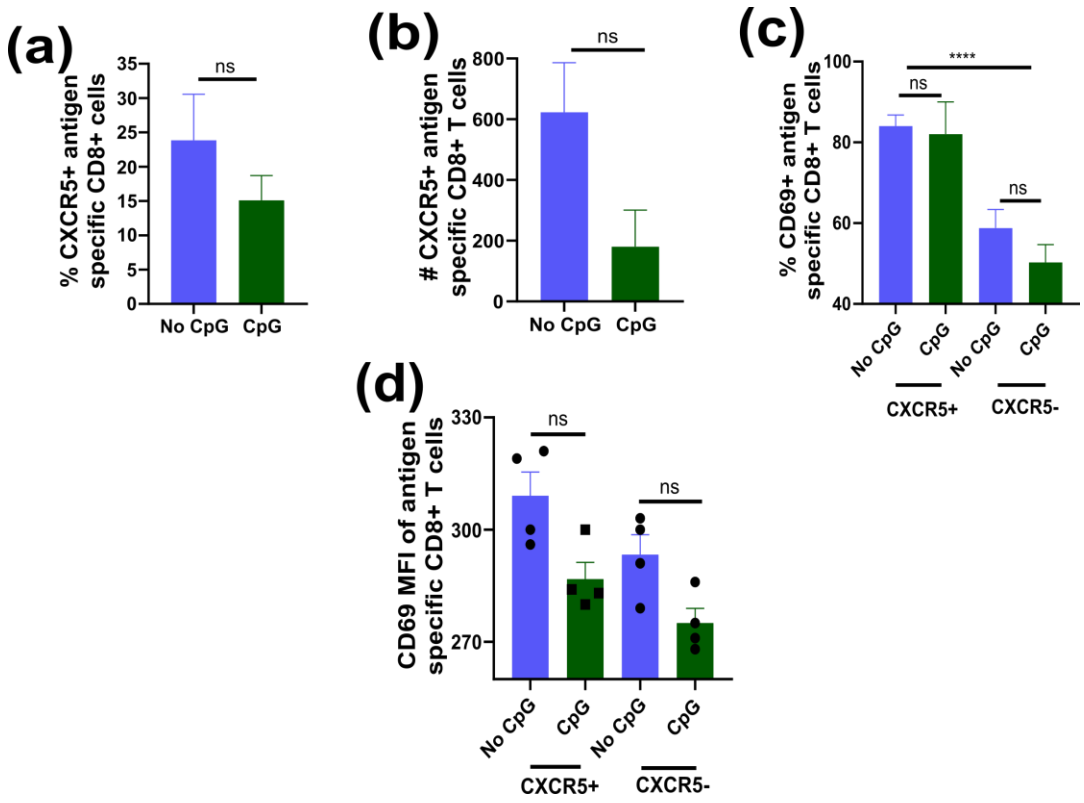

LNPCs were isolated from the liver D67 post adoptive OT-1 transfer in the presence or absence of CpG ODN host conditioning as indicated in Figure 2.2a. The LNPCs were phenotyped for CXCR5, CD69, and TCF-1 on antigen specific CD8 T cells.

(a) Frequency of CXCR5+ T cells with and without CpG ODN treatment

(b) Absolute numbers of CXCR5+ T cells with and without CpG ODN treatment

(c) Frequency of CD69 expressing CXCR5+ and CXCR5- T cells from mice with and without CpG ODN conditioning.

(d) Quantified MFI of CD69 expression on CXCR5+ and CXCR5- T cell subset in (c).

Figure 5S 2: Higher frequency of Bcl6 expression is localized in CXCR5+ T cells in the spleen

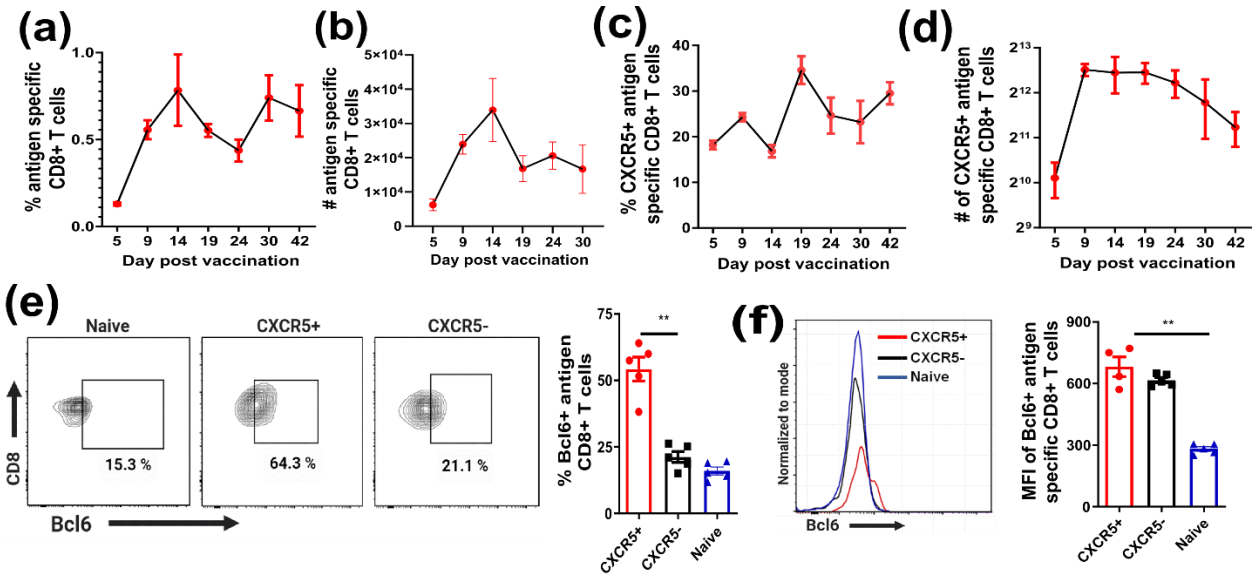

(a) Kinetics of the frequency of antigen specific CD8+ T cells. High antigen mice were AdOva vaccinated, and after each respective time point, splenocytes were stained with antibodies for CD8 and Ova pentamer. Analysis was done with flow cytometer.

(b) Kinetics of the absolute numbers of antigen specific CD8+ T cells in (a)

(c) Kinetic frequency of CXCR5+ T cells in the spleen

(d) Absolute numbers of CXCR5+ T cells in (c)

(e) Frequency of Tfh transcription factor Bcl6 expression in naïve, antigen specific CXCR5+ and CXCR5- T cells. Representative dot plot (left) and summarized frequency (right) of Bcl6 expression. Splenocytes isolated from high antigen mice after 21 days post vaccination, phenotyped for Bcl6 expression in antigen specific CXCR5+ and CXCR5- T cells and analysis was done by flow cytometry.

(f) Expression level of Bcl6 in naïve, antigen specific CXCR5+ and CXCR5- T cells in (c). Representative dot plot (left) and quantified MFI summary (right).

Figure 5S 3: CXCR5+ and CXCR5- T cells in the spleen display distinct activation profile

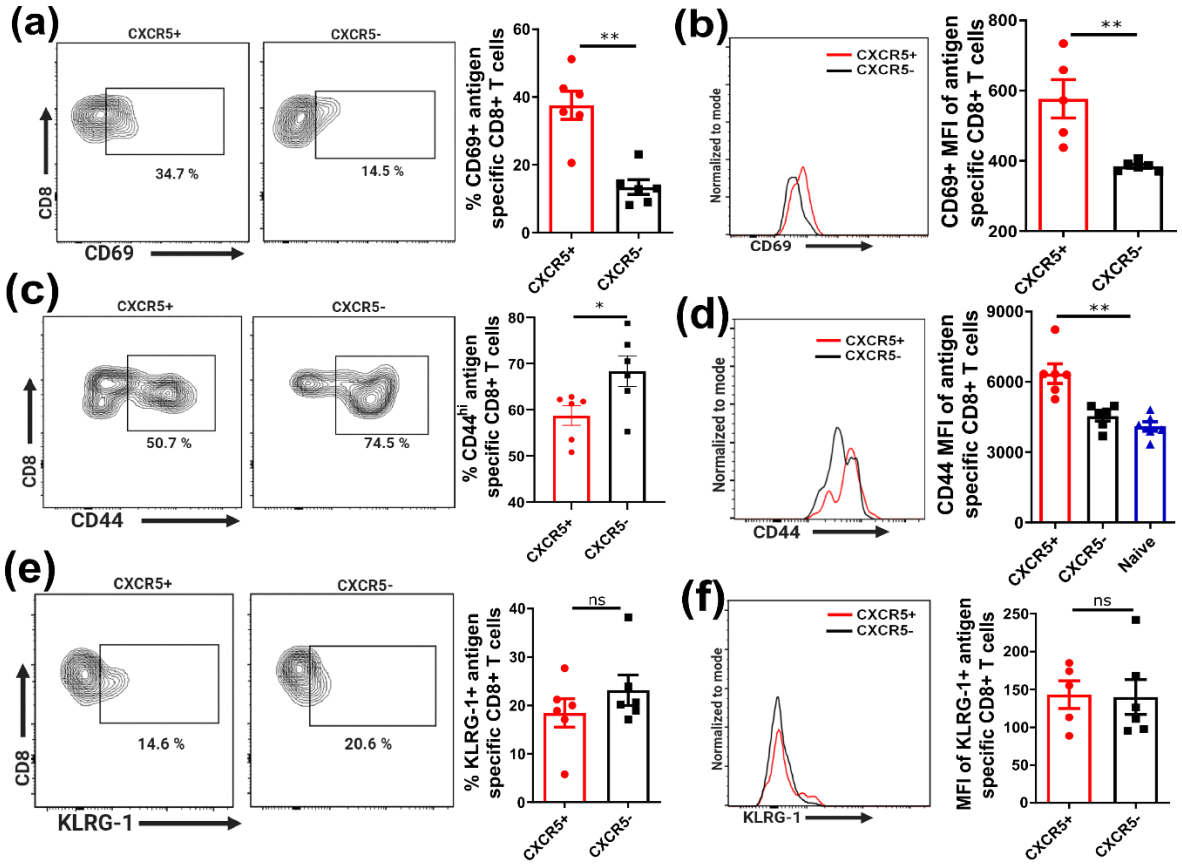

Day 21 post vaccination of high antigen mice, splenocytes were isolated and phenotyped for antigen specific CXCR5+ and CXCR5- CD8+ T cells expressing the activation marker CD69, CD44 and KLRG-1. Analysis was done with flow cytometry.

(a) Frequency of CD69 on antigen specific CXCR5+ and CXCR5- T cells. Representative dot plot (left) and summary (right) of CD69 expression.

(b) Quantified MFI of CD69 on naïve, Ova-specific CXCR5+ and CXCR5- T cells in (a). Representative dot plot (left) and summarized MFI (right) of CD69 expression.

(c) Frequency of $CD44^{hi}$ Ova-specific CXCR5+ and CXCR5- T cells. Representative dot plot (left) and summary (right) of $CD44^{hi}$ expression.

(d) MFI of $CD44^{hi}$ Ova-specific CXCR5+ and CXCR5- T cells in (c). Representative histogram plot (left) and quantified summary (right) of $CD44^{hi}$.

(e) Frequency of KLRG-1 on CXCR5+ and CXCR5- T cells. Representative dot plot (left) and summarized frequency (right) of KLRG-1.

(f) MFI of KLRG-1 on antigen specific CXCR5+ and CXCR5- T cells in (e). Representative histogram plot (left) and quantified summary (right) of KLRG-1 MFI.

Figure 5S 4: CXCR5+ and CXCR5- T cells in the spleen display distinct memory profile

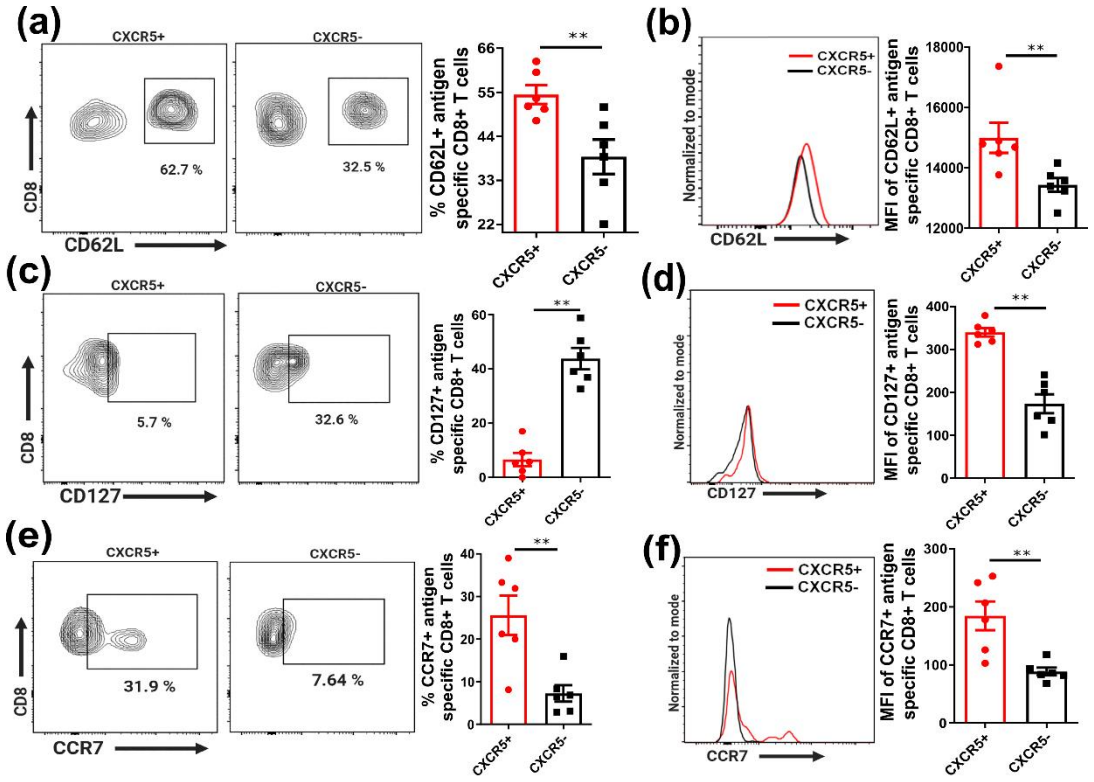

Day 21 post vaccination of high antigen mice, splenocytes were isolated and phenotyped for antigen specific CXCR5+ and CXCR5- CD8+ T cells expressing the memory markers CD62L, CD127 and CCR7 (g – l). Analysis was done with flow cytometry.

(a) Frequency of CD62L expressing Ova-specific CXCR5+ and CXCR5- T cells. Representative flow plot (left) and summarized frequency (right) of CD62L.

(b) Quantified MFI of CD62L expressing Ova-specific CXCR5+ and CXCR5- T cells in (g). Representative histogram (left) and summarized MFI (right) of CD62L.

(c) Frequency of CD127 expressing CXCR5+ and CXCR5- antigen specific T cells. Representative flow plot (left) and summarized frequency (right) of CD127 expression.

(d) Expression level of CD127 on CXCR5+ and CXCR5- antigen specific CD8+ T cells in (i). Representative histogram (left) and quantified MFI (right) of CD127.

(e) Frequency of CCR7 expressing CXCR5+ and CXCR5- antigen specific CD8+ T cells. Representative flow plot (left) and summarized frequency (right) of CCR7 expression.

(f) Expression level of CCR7 on antigen specific CXCR5+ and CXCR5- T cells in (k). Representative histogram plot (left) and quantified MFI of CCR7 expression on CXCR5+ and CXCR5- T cells.

Figure 5S 5: Splenic CXCR5+ and CXCR5- T cells have distinct exhaustion properties

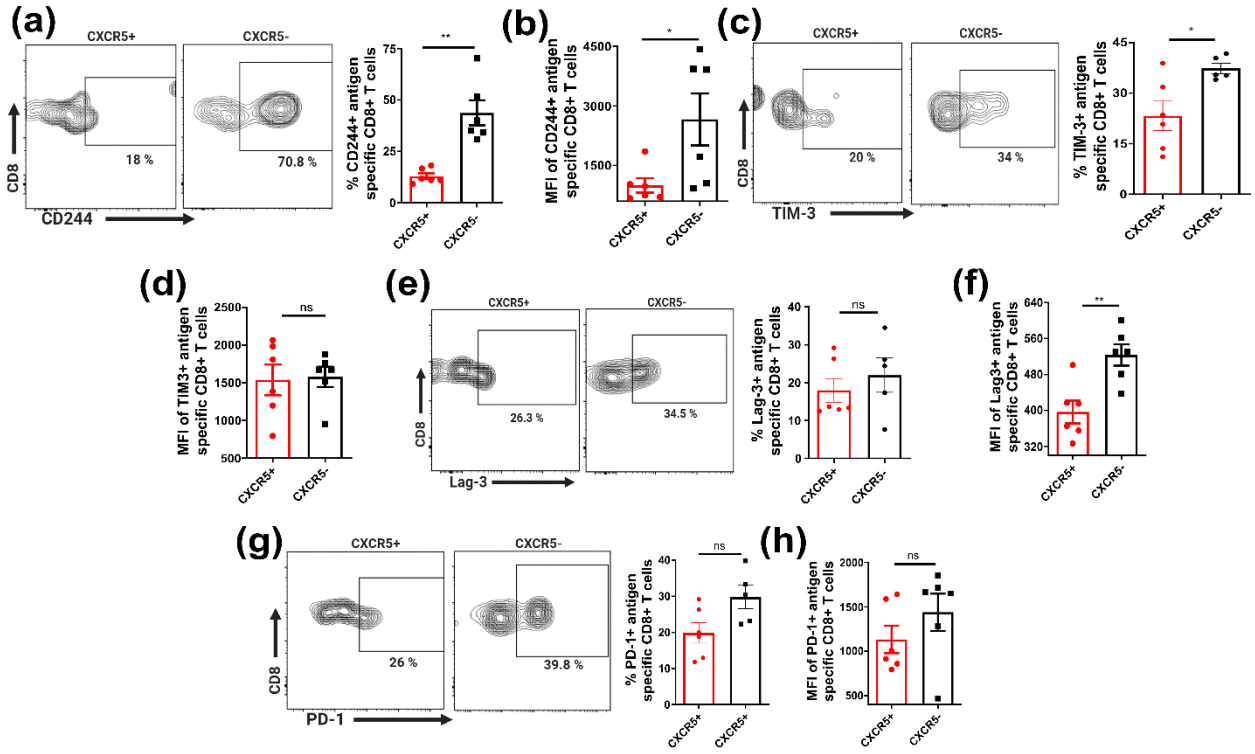

Splenocytes were isolated from high antigen mice 21 days post AdOva vaccination. The cells were phenotyped to identify Ova-specific CXCR5+ and CXCR5- CD8+ T cells expressing exhaustion markers CD244, TIM-3, PD-1 and Lag-3.

(a) Frequency of CD244 expression on CXCR5+ and CXCR5- T cells. Representative dot plot (left) and summarized frequency (right) of CD244.

(b) Quantified MFI of CD244 on CXCR5+ and CXCR5– T cell subset.

(c) Frequency of TIM-3 on CXCR5+ and CXCR5- T cells. Representative flow plot (left) and summarized frequency (right) of TIM-3.

(d) MFI of TIM-3 on CXCR5+ and CXCR5- T cells.

(e) Frequency of Lag-3 on CXCR5+ and CXCR5- T cells. Representative dot plot (left) and summarized frequency (right) of Lag-3 expression.

(f) MFI of Lag-3 on CXCR5+ and CXCR5- T cells.

(g) Frequency of PD-1 on CXCR5+ and CXCR5- T cells. Representative dot plot (left) and summary of the frequencies (right) of PD-1 expression.

(h) Quantified MFI of PD-1 on CXCR5+ and CXCR5- T cells.

Figure 5S 6: Splenic CXCR5+ and CXCR5- T cells have distinct effector properties

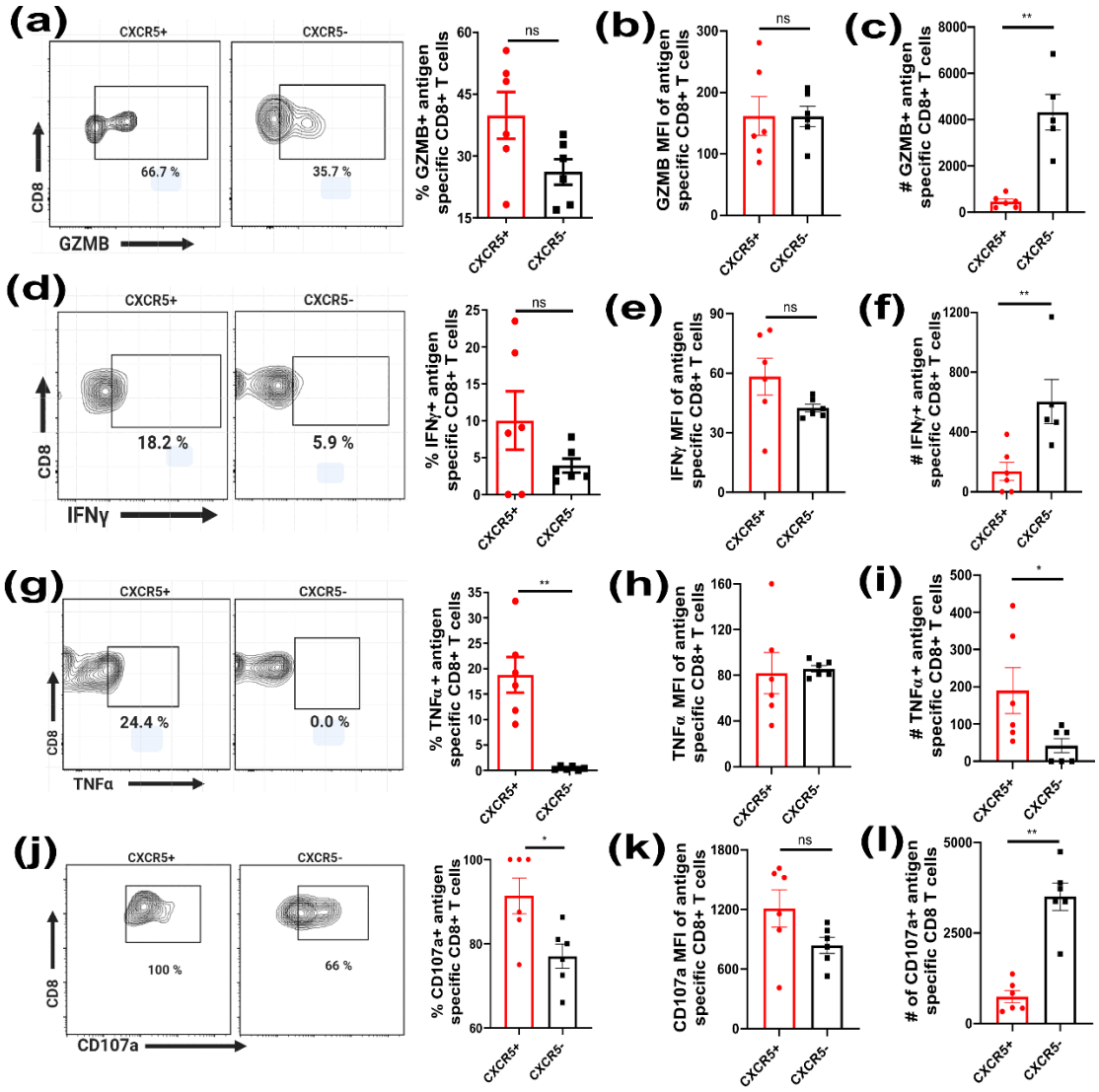

(a -i) High antigen mice were sacrificed 21 days post vaccination with AdOva vector. Splenocytes were isolated, stimulated ex-vivo with PMA/ionomycin for 4-5h in the presence of Brefeldin A for the last 2 hours. Cells were harvested and phenotyped for antigen specific CXCR5+ and CXCR5- CD8+ T cells expressing effector molecules TNFα, IFN-γ and GZMB. Data was analyzed by flow cytometry.

(a) Frequency of GZMB on CXCR5+ and CXCR5- T cells. Representative dot plot (left) and summarized frequency (right) of GZMB.

(b) MFI of GZMB in CXCR5+ and CXCR5- T cells.

(c) Absolute number of GZMB in CXCR5+ and CXCR5- T cell subset.

(d) Frequency of IFN-γ expression in CXCR5+ and CXCR5- T cells. Representative flow plot (left) and summary (right) of IFN-γ expression.

(e) MFI of IFN-γ in CXCR5+ and CXCR5- T cell subsets.

(f) Absolute number of IFN-γ expression in CXCR5+ and CXCR5- T cells.

(g) Frequency of TNFα expression in CXCR5+ and CXCR5- T cells. Representative dot plot (left) and summary (right) of TNFα.

(h) MFI of TNFα in CXCR5+ and CXCR5- T cells.

(i) Absolute numbers of TNFα expression in CXCR5+ and CXCR5- T cells.

(j – k) High antigen mice were vaccinated with AdOva vector. After 21 days, splenocytes were isolated and ex-vivo stimulated with PMA/ionomycin for 4-5h in the presence of anti-CD107a. The cells were phenotyped for antigen specific CXCR5+ and CXCR5- CD8+ T cells. Data was analyzed with flow cytometry.

(j) Frequency of CD107a expression in CXCR5+ and CXCR5- T cells. Representative flow plot (left) and summarized frequency (right) of CD107a expression.

(k) MFI of CD107a in CXCR5+ and CXCR5- T cells.

(l) Absolute number of CD107a in CXCR5+ and CXCR5- T cells.

Figure 5S 7: Improved mitochondria function is associated with CXCR5+ T cell subsets in the spleen

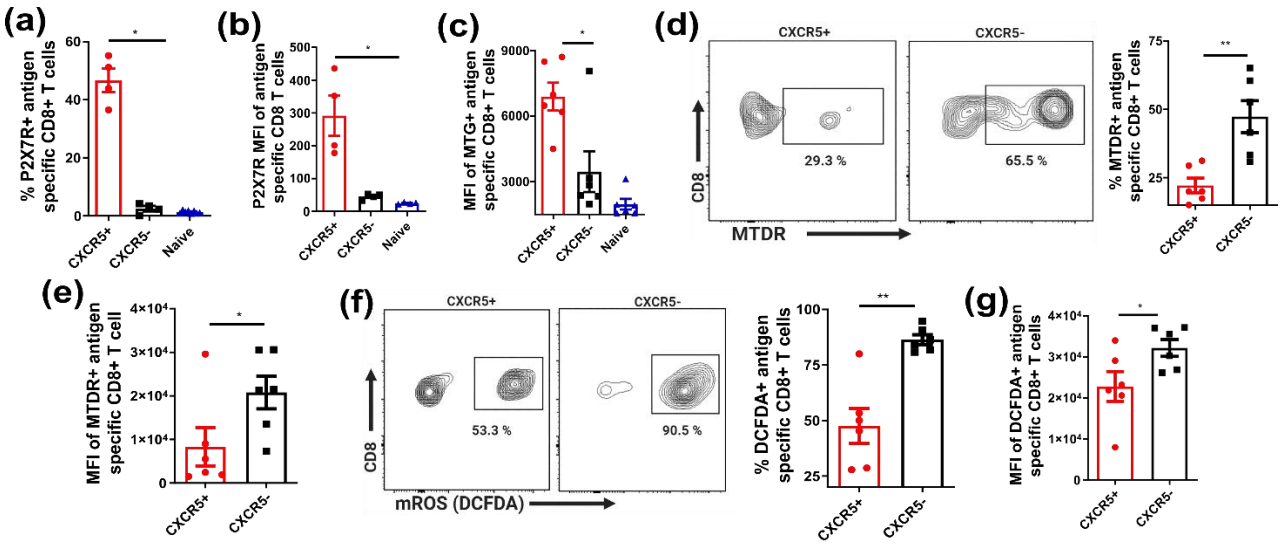

(a) Frequency of P2X7R expression on CXCR5+ and CXCR5- T cells. Splenocytes from high antigen mice were isolated 21 days post vaccination, phenotyped for the expression of P2X7R on antigen specific CXCR5+ and CXCR5- T cells as well as naïve CD8+ T cells. Analysis was done with flow cytometry.

(b) Quantified MFI of P2X7R on CXCR5+ and CXCR5- T cells in (a).

(c – g) Splenocytes were isolated 21 days post AdOva vaccination and were cultured with mitochondria sensitive dyes such as mitotracker green, deep red and mROS dye DCFDA at 37°C for 15 – 30 min. Cells were the harvested and phenotyped for antigen specific CXCR5+ and CXCR5- T cells. Data was analyzed with flow cytometry.

(c) Quantified MFI of MTG (mitochondria mass) in naïve, antigen specific CXCR5+ and CXCR5- T cells.

(d) Frequency of MTDR in antigen specific CXCR5+ and CXCR5- T cells. Representative dot plot (left) and summary (right) of MTDR.

(e) Quantified MFI of MTDR levels in CXCR5+ and CXCR5- T cells in (d).

(f) Frequency of mROS in CXCR5+ and CXCR5- T cells. Representative dot plot (left) and summarized frequency (right) of mROS expression.

(g) Quantified MFI of mROS expression level in CXCR5+ and CXCR5- T cells in (f).

Figure 5S 8: Increased uptake of nutrient is localized to CXCR5+ T cell subset in the spleen

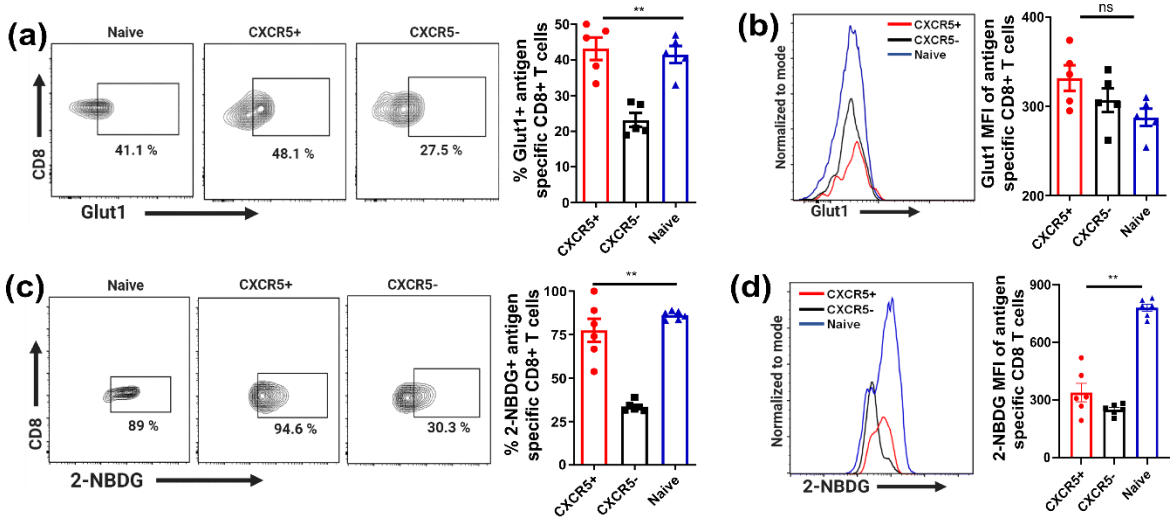

(a) Frequency of Glut-1 expression in naïve, antigen specific CXCR5+ and CXCR5- T cell subsets. Representative dot plot (left) and summarized frequency (right) of Glut-1 expression. Isolated splenocytes from high antigen mice 21 days post AdOva vaccination were stained intracellularly for Glut-1 expression on antigen specific CXCR5+ and CXCR5- T cells. Analysis was done with flow cytometry.

(b) Expression level of Glut-1 in CXCR5+ and CXCR5- T cells in (a). Representative histogram (left) and summarized MFI of Glut-1 expression.

(c) Frequency of 2-NBDG uptake by naïve, antigen specific CXCR5+ and CXCR5- T cells. Representative dot plot (left) and summarized frequency (right) of 2-NBDG uptake. Splenocytes from AdOva vaccinated high antigen mice were cultured with 2-NBDG at 37°C for 30min and phenotyped for the uptake of 2-NBDG in antigen specific CXCR5+ and CXCR5- T cells. Data was then analyzed with flow cytometry.

(d) Expression level of 2-NBDG in naïve, antigen specific CXCR5+ and CXCR5- T cells in (c). Representative histogram (left) and summarized MFI (right) of 2-NBDG uptake.

Figure 5S 9: CXCR5+ T cells in the spleen display enhanced proliferation transcription factor

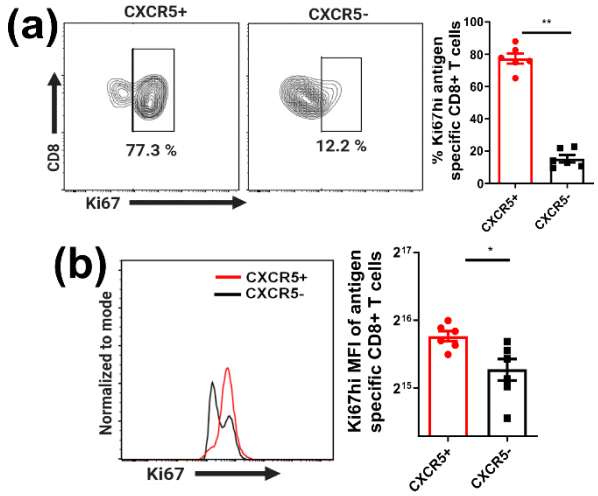

(a) Frequency of Ki67^{hi} expression in CXCR5+ and CXCR5- T cell subsets. Representative dot plot (left) and summarized frequency (right) of Ki67hi expression. Splenocytes were isolated 21 days post vaccination of high antigen mice, phenotyped for antigen specific CXCR5+ and CXCR5- T cells and analyzed with flow cytometry.

(b) Expression level of Ki67^{hi} in CXCR5+ and CXCR5- T cells as in (a). Histogram plot (left) and quantified MFI summary (right) of Ki67 expression.

5 Materials and Methods

5.1 Materials

5.1.1 List of Laboratory Equipment

Name of equipment	**Company**
Centrifuges	Heraeus Biofuge fresco Beckmann GS-15R Sigma 3K20 Heraeus Megafuge 1.0 Thermo Scientific Jouan CR412 Inflexible Rotors GSA, GS3, SS34 Swing Rotor HB4
Autoclave	Belimed steam sterilizer 6-6-6 HS1 FD
Flow Cytometer	BD™LSRII-SORP analyzer BD™LSR Fortessa analyzer BD™ARIA cell Sorter BD™ARIA Fusion cell Sorter
Guava Cell counter	Millipore
Deionized water	Millipore (MilliQ)
Gel electrophoresis	Gibco BRL Horizontal Gel
Tissue Homogenizer	MP FastPrep®-24 Lysing Matrix
Feeding Needle	Heiland Vet GmbH
LightCycler®480 (Real Time PCR)	Roche
PCR cycler	T3 Thermocycler
Nanodrop Spectrophotometer	Peqlab ND-1000
Micropipettes	Gilson
Pipetboy	Eppendorf
Microscopes	Leica Labovert FS, Nikon TMS Olympus BX51TF + camera Color view Illu
pH-meter	Beckman M340
Sterile Benches	Steril-Gard Class II Type A/B3, Baker Company SG 400E

	Heraeus Herasafe, Heraeus HSP 18 Herasafe, Heraeus KS15 BDK-SK 1500
Table-top Centrifuge	Eppendorf 5417C Heraeus Biofuge 13 Heraeus Biofuge PICO 17
Water Bath	GFL
Thermomixer	Eppendorf 5436 Eppendorf Thermomixer compact
Precision scale	Sartorius
Fridge	Liebherr
Freezer (-20^{o}C)	Liebherr
Freezer (-80^{o}C)	Thermo Scientific
CO2 Incubators	Forma Scientific Water Jacketed Incubator 3336 Labotect C200

5.1.2 List of Chemicals

Chemicals	**Manufacturer**	**# Catalog**
Brefeldin A	eBioscience	00-4506
Agarose	Biozym	840004
ClinOleic 20% lipid emulsion for infusion	Baxter	2573668
DirectPCR lysis Buffer	Viagen	102 T
DNase I	Roche	11 284 932 001
Percoll	MP Biomedicals	19536990
Proteinase K	Qiagen	19133
Midori Green	Nippon Genetics	MG04
SIINFEKL peptide	Peptide- and Chemical Synthesis Dr. Werner Tegge	19133

EDTA	Roth	6381-92-6
Glutamine	Serva	G8540-100G
Streptomycin	Serva	
Heparin	Ratiopharm	
Tamoxifen	Ratiopharm	3572257
Nuclease free water	Promega and Qiagen	129117
2-Mercaptoethanol	Gibco	1763054
Fetal Bovine Serum	Sigma	F7524
Ionomycin	Sigma	I0634-1MG
PMA	Sigma	P8139-1MG
Isoflurane	Allbrecht GmbH	701-005-301
CpG-ODN 1668	TIB Molbiol	1973788
Non CpG-ODN 1720	TIB Molbiol	1758088

5.1.3 List of Buffers

Media	**Constituents**
Red blood cell lysis buffer	150 mM NH4Cl 10 mM KHCO3 0.1 mM EDTA pH 7.2-7.4
FACS buffer	PBS 2% FCS
Glutamine (100x)	29.23 mg/ml Glutamine, filter sterilized
HEPES (1 M)	283,3 g, pH 7.2, in 1l H_2O
MACS buffer	PBS

	1% FCS 2mM EDTA
Penicillin/Streptomycin (100x)	6,06 mg/ml ampicillin (10000 U/ml) 10 mg/ml streptomycin pH 7.4 in 1l H_2O Filter sterilized
PBS	140mM NaCl 27mM KCl 7.2mM Na_2HPO_4 in 10l H_2O pH 6.8 – 7.0
RPMI complete media	500ml Roswell Park Memorial Institute medium 1% HEPES 10% FCS 0.1% 2-Mercaptoethanol

5.1.4 List of Kits

Product	**Manufacturer**	**# catalog**
CD8a+ T cell isolation kit II	Miltenyi Biotec	130-095-236
2x Red PCR Master Mix	p.j.k	302004
BD FACS Lysing Solution	BD	349202
FoxP3/transcription factor staining kit	eBiosciences	00 – 5523
CellTrace CFSE Cell Proliferation Kit	Invitrogen	C34554
Live/Dead Blue dead cell stain kit	ThermoFisher Scientific	L23105
Cytofix/Cytoperm™	BD	554714
Live/Dead Fixable Far Red cell stain kit	ThermoFisher Scientific	L10120
RevertAid First Strand cDNA Synthesis Kit	Thermo Scientific	K1622
TMRE-mitochondria Membrane potential assay kit	Abcam	Ab113852
SsoFast EvaGreen Supermix	BIO-RAD	172-5204
RNeasy Mini Kit (250)	Qiagen	74106

QIAshredder	Qiagen	79656
2-NBDG Glucose uptake assay kit	Abcam	Ab235976
MitoTracker Green FM	ThermoFisher	M7514
MitoTracker Deep Red FM	ThermoFisher	M22426
Mouse BLC (CXCL13) ELISA Kit	Thermo Scientific	EMCXCL13

5.1.5 List of Consumables

Product	**Manufacturer**
Cell culture plates (6 well, 24 well, 96 well)	Nunc, Corning
Cell strainer 100 µm Nylon	BD Falcon
Cryogenic vials	CytoOne
Falcon Tubes (15 ml, 50 ml)	Greiner bio-one
Gloves (nitrile, latex)	Microflex
LS columns	Miltenyi Biotec
Lysing matrix D	MP Biomedicals PCR tubes (0,2 ml)
Pipette tips (10 µl, 20 µl, 200 µl, 1000 µl)	StarLab
Reaction Tubes Safe lock (1,5 ml, 2 ml)	Sarstedt
Syringes (1 ml, 2 ml, 5 ml, 10 ml, 20 ml, 50 ml)	Omnifix
Tissue culture flask (25 cm^2, 75 cm^2, 175 cm^2, 300 cm^2)	Nunc,TPP
V-shape micro plate (96 well)	Nunc
PCR tubes	Biozym

5.1.6 List of Primers

Application	**Name**	**Sequence (5’ – 3’)**
RT-PCR	AgFusion1a	CAGGCACTCCTTTCAAGACC
	AgFusion4a	GCGGTTGAGGACAAACTCTT
RT-PCR	mAlbclifwd	GACAAGGAAAGCTGCCTGAC
	mAlbclirev	TTCTGCAAAGTCAGCATTGG
Genotyping	Cre1	GCCTGCATTACCGGTCGATGCAACGA

	Cre2	GTGGCAGATGGCGCGGCAACACCATT
Genotyping	EMCVneo1	AAGAGTCAAATGGCTCTCCTCAAGCGTATT
	EMCVneo2	GTCTGTTGTGCCCAGTCATAGCCGAATAG

5.1.7 Nanobody and Cell line

Name	**Description**
EL4 cells	Mus musculus T lymphoma cell, ATCC TIM-39
ARTC2.2 Nanobody	Binds to toxin-related, GPI-anchored ADP-ribosyltransferase, and helps prevent NAD induced cell death during tissue preparation. Kindly provided by Dr. Björn Rissiek and Prof. Dr. med. Friedrich Koch-Nolte

5.1.8 List of Antibodies

Antigen	**Fluorophore**	**Dilution factor**	**Clone**	**Distributor**
CD8	Percp-Cy5.5	400	53-6.7	Biolegend
CD8	AF647	1600	53-6.7	Biolegend
CD127	FITC	200	A7R34	Biolegend
CD127	PE/Dazzle594	200	A7R34	Biolegend
CCR7	PE/Cy7	50	4B12	Biolegend
TIM-3	BV785	300	RMT3-23	Biolegend
TNFα	APC	300	MP6-XT22	Biolegend
PD-1	FITC	300	J43	eBiosciences
PD-1	PE	300	J43	eBiosciences
Lag-3	APC	300	eBioC9B7W	eBiosciences
CD62L	BV785	300	MEL-14	Biolegend
CXCR5	BV421	100	L138D7	Biolegend
CXCR5	PE/Cy7	100	L138D7	Biolegend
KLRG-1	BV711	400	2F1/KLRG1	Biolegend
Granzyme b(GZMB)	PE/Cy7	200	NGZB	eBiosciences
IFNγ	FITC	300	554411	Biolegend, BD
CD244 (2B4)	AF647	200	M2B4(B6)458.1	Biolegend
CD44	APC	500	IM7	Biolegend
TCF-1/TCF-7	PE	50	S33-966	BD Biosciences
Nur77	AF488	50	12.14	eBiosciences
Glut-1	AF647	300	Ab195020	Abcam
H-2kb SIINFEKL	PE	100	F093-2A-E	ProImmune
CD69	FITC	300	H1.2F3	eBiosciences
CD11a (LFA-1)	AF647	300	M17/4	Biolegend

CD107a	FITC	150	1D4B	Biolegend
P2X7R	PE/Cy7	300	1F11	Biolegend
Ki67	AF647	50	M2B4(B6)458.1	Biolegend
CD28	PE/Cy7	150	37.51	Biolegend
Thy1.1	PE	200	HIS51	eBiosciences
CD19	APC/Cy7	200	ID3	BD Biosciences
Bcl6	AF647	100	IG191E/A8	Biolegend
CD28	PE/Cy7	200	37.51	Biolegend
Thy1.1	APC	200	HIS51	eBiosciences

5.1.9 Mice

Mice used in this study were bred and maintained in the Helmholtz-Zentrum für Infektionsforschung animal facility. The background of all mice was Black 6 from the Jackson laboratory. The animals were bred and maintained under a specific pathogen free (SPF) condition in a single ventilated cage. Mice received all nutrients *ad libitum* and were under a controlled circadian 12h rhythm. Animal experiments were performed according to the animal welfare law of Germany. In addition, the institutional guidelines have been approved by the Lower Saxony local government.

5.1.10 List of mouse strains

Transgenic mouse	**Transgene**	**Description**
Rosa26antiOvaAg	Ova	Ova antigen is integrated at the Rosa26 promotor in an antisense direction, flanked by inversely oriented loxP site [111]
AlbCreER^{T2}	Cre recombinase	Cre recomibinase is under the control albumin locus, and the Cre recombinase is fused to the tamoxifen dependent estrogen receptor [154].
OvaXCre	Ova and Cre	Generated from Rosa26Ova and AlbCreERT2 upon breeding. The Ova and CreER^{T2} double transgenic mice allows for tamoxifen dependent induction of Ova expression exclusively in hepatocytes [111,112]. See Figure 1.9 for details

Thy1.1 OT-1	TCR Vβ5	A transgenic mouse for CD8 T cell, which recognizes Ova peptide expressed on MHC-1. The mice also express a selection marker Thy1.1 (CD90.1) which facilitates the tracking of cells after adoptive transfer, since Bl6/J mice express Thy1.2.
DsRED OT-1	Actin DsRED and TCR Vβ5	A reporter transgenic CD8+ T cell, which recognizes Ova peptide in the context of MHC I. This mouse is bread from homozygote DsRED actin mice and Thy1.1 OT-1 mice.

5.1.11 List of Software

Software	**Version**
FlowJo	V10.6.0
GraphPad Prism	V8

5.2 Methods

5.2.1 Generation of OvaXCre mice harboring low and high antigen in the liver

The transgenic mouse model, OvaXCre used in this study have C57BL6/J genetic background and was bred from two homozygote mice. The Rosa26Ova mice which consists of OVA cassette in an anti-sense orientation to Rosa26 promotor flanked by inversely oriented LoxP sites and homozygous AlbCreERT^2 mice which has Cre recombinase under the albumin promoter. The breeding of Rosa26Ova and AlbCreERT^2 homozygous animals gives rise to heterozygous OvaXCre mice. To achieve high and low level of Ova-antigen in the liver for the purpose of this study, 5 - 8 weeks old OvaXCre mice were fed with and without a single dose of 50µg Tam (Ratiopharm), respectively via gavaging. Tamoxifen was prepared by crushing 10mg Tam into 2ml Clinoleic (Baxter) and then dissolved overnight at 4^{o}C by gentle rotation. The 50µg concentration was then prepared from the initial stock concentration of 5mg/ml.

5.2.2 Genotyping transgenic mice

The transgenic mice used in this study were genotyped for the respective transgene of interest. In this regard, ear biopsies were obtained from 4 weeks old mice and lysed in 150µl of direct PCR lysis buffer supplemented with 2.5µl of Proteinase K. The samples were incubated 2h or overnight in a 55^{o}C heating block at 1050rpm. This process facilitates ear sample digestion. The samples were then heated at 96^{o}C for 15min to stop the enzymatic activity. 1µl of the tissue lysate was added to PCR master mix consisting of 13.5µl 2x PJK PCR buffer, 10pmol/µl forward and reverse primer, and 8.65µl of water. The following PCR program was run for the prepared samples using a thermal cycler, using the program in the table below:

Cycle	**Temperature**	**Time (mm:ss)**
Initial Denaturation	95^{o}C	05:00
	72^{o}C	10:00
Amplification	94^{o}C	00:30
	58^{o}C	00:45
	72^{o}C	01:30
Final Elongation	72^{o}C	10:00
	16^{o}C	forever

After the run, the PCR samples were loaded on 1% agarose gel with Midori Green, according to the manufacturers' protocol. DNA bands were then monitored on the gel for DNA fragment which is indicative for specific transgene of interest.

5.2.3 Adenovirus vaccination of OvaXCre mice

Vaccination of OvaXCre mice were performed with an adenoviral vector encoding OVA antigen referred to as AdOva. The AdOva vector used in this study was based on Ad5 E1-deleted first generation vectors previously described [155,156]. Aliquot of the AdOva viral vector was re-suspended to 2 x 10^7 vp/µl in PBS. The prepared aliquot was kept at 4^{o}C before injection to avoid the loss of viral particle integrity. Mice were made to sleep by narcotizing with Isofloran in IVIS chamber, after which they were vaccinated intramuscularly into the tibialis anterior muscle bilaterally with 50µl of the prepared viral particles. 300µl syringe was used in the vaccination process and each muscle injected with ~25µl of the re-suspended viral particle.

5.2.4 Isolation, purification and adoptive transfer of OT-1 cells

Transgenic Thy1.1+OT-1 or DsRED+Thy1.1+OT-1 mice were used for the purpose of isolating and purifying OT-1 cells for adoptive transfer. Thy1.1+OT-1 or DsRED+Thy1.1 OT-1 mice were euthanized, dissected to obtain the spleen, and the spleen was smashed through a sieve into PBS supplemented with 2% FCS (2% PBS/FCS) in order to obtain the lymphocytes. The lymphocytes were washed by pelleting at 1500rpm, 5min, and re-suspended into ACK red blood cell lysis buffer for 5min at room temperature. After lysis, cells were pelleted at 1500rpm, 5min and re-suspended in 2% PBS/FCS. The cells were then sieved through 100µm cell strainer into 50ml Falcon tube before proceeding to counting using guava machine. Cell counting was carried out by making 1/20 dilution of the isolated cells.

The counted cells were then subjected to Magnetic Cell Separation (MACS) CD8+ T cell isolation procedure according to the manufacturer's protocol (Miltenyi Biotec, Germany). The MACS kit used in this study facilitates the isolation of OT-1 cells by means of negative selection. In brief, 1 x 10^7 splenocytes were pelleted and re-suspended in ice-chilled 40µl MACS buffer, which is made up of 2% PBS/FCS supplemented with 2mM EDTA. After resuspension, 10µl of biotin-labeled antibody was added, re-suspended for homogeneous distribution and then incubated at 4^{o}C for 5min. Furthermore, 30µl of MACS buffer was added and 20µl of anti-biotin MicroBeads were added, mixed thoroughly and incubated at 4^{o}C for 10min. The antibody-biotinylated bead cocktail

allows tagging of all cell types in the spleen except the CD8+ OT-1 cells. The protocol described above can be scaled up for higher numbers of splenocytes. Subsequently the cells were taken through a process of magnetic cell separation, where MACS LS column is placed in the magnetic field of the MACS separator. The LS column was prepared by rinsing with 3ml MACS buffer, and the cell suspension is applied through the column. The flow through which contain the unlabeled cells of interest i.e CD8+ OT-1 cells, were collected. The column was further eluted with 3ml MACS buffer in order to collect the unlabeled cells which may have been trapped in the column. Importantly the maximum number of labeled cells which was loaded on a single column should not exceed 1 X 10^8 cells. The isolated OT-1 cells were then counted to determine numbers for downstream protocols.

In order to be ascertain that MACS purification procedure yielded the required purity of enriched OT-1 cells, OT-1 cells were checked for purity by flow cytometry. In this procedure, the MACS purified cells were stained with antibodies which recognize CD8 and CD3 epitopes. In all the MACS purification processes during this study, the percent purity of OT-1 cells were > 94%. The counted cells were re-suspended into a concentration of 1.5 - 2.5 X 10^6 cell per 100µl of PBS for intravenous injection into recipient mice. Each recipient mice received 3 - 5 X 10^6 OT-1 cells throughout this study, and prior to intravenous injection of T cells, the recipient mice were exposed to red light for ~3.5min. This enhanced the visibility of the tail vein, thereby allowing stress-free injection of T cells into mice.

5.2.5 Isolation of leukocytes from the liver and spleen of OvaXCre mice

Induced OvaXCre mice vaccinated or adoptively transferred with OT-1 cells were sacrificed and the liver microenvironment was perfused with ice cold 2% PBS/FCS to get rid of circulating blood. The liver was taken out of its anatomical position and then shredded in ice cold 2% PBS/FCS. For sorting purposes, the liver of OvaXCre mice were not perfused with 2% PBS/FCS. The shredded liver was smashed through 100µm nylon cell strainer into a 50ml Falcon tube, facilitating the dissociation of liver cells into single cell suspension. The cells suspension was centrifuged 5min at 500rpm, to separate the non-parenchyma cells (NPCs) from hepatocytes. After centrifugation, hepatocytes are loosely pelleted at the bottom of the 50ml tube while the NPCs are in suspension. The NPCs in suspension was decanted into new 50ml Falcon tube. The loosely pelleted hepatocytes were then washed with 50ml of 2% PBS/FCS at 500rpm, 5 min and the cell suspension were then added to the initial NPC suspension. The cell suspension of NPCs was then pelleted at

1500rpm, 5min. In order to get rid of debris, the pelleted NPCs were re-suspended in 40% percol (MP Biological) and centrifuged for 20min at 2000rpm. After centrifugation, the NPC fraction forms a pellet at the bottom of the 15ml falcon tubes while debris are on top of the percol solution. The debris alongside the percol were aspirated gently out leaving the NPCs, and the red blood cells (RBCs) in the pool of NPCs were lysed with ACK buffer at room temperature for 5min. The cells were centrifuged for 5 min at 1500rpm and washed twice with 2% PBS/FCS to stop the activity of the lysis buffer. The isolated NPCs were then utilized in downstream protocol.

In splenocytes isolation, the spleens were smashed through 100µm cell strainer into 50ml Falcon tube and centrifuged for 5min at 1500rpm. The supernatants were decanted off, and the pellet was re-suspended in 5ml ACK buffer for 5 min. The splenocytes in the ACK buffer were centrifuged, washed twice with 2% PBS/FCS and sieved through 100µm cell strainer to get rid of tissue debris. The isolated splenocytes were used for downstream protocols.

5.2.6 Liver tissue sampling

Liver samples from OvaXCre mice were sampled in 2ml Eppendorf tubes in replicates for the purpose of RNA isolation. The sampled liver tissues were initially stored on liquid nitrogen during the sampling process to avoid degradation. After sampling of liver tissues, the samples were then stored at -80^{o}C for downstream analysis.

5.2.7 Purification and storage of RNA

Throughout this study, RNA purification was performed by RNeasy kit (Qiagen), according to the manufacturer's protocol. The purified RNAs were eluted in 30 – 50 µl RNase-free H_2O. All RNA samples were stored at -20°C for short-term use, whereas for long term storage the samples were kept in -80°C.

5.2.8 RNA isolation from liver tissue

Liver samples stored at -80°C were thawed on ice before RNA isolation. The samples were transferred into a FastPrep tube (Lysing matrix D, MP Biomedicals) containing 600µl RLT buffer supplemented with 1% beta-mercaptoethanol. The samples were homogenized 2 times for 10sec. with a tissue homogenizer (MP Biomedicals). After each cycle of homogenization, the samples were kept on ice for 2min. This is to prevent possible enzymatic degradation of RNA. Thereafter, RNA was purified using the RNeasy kit (Qiagen) according to the manufacturer's protocol. In

brief, 400µl of disrupted samples were transferred into shredder column (Qiagen) and centrifuged for 3min at 10000rpm at 25ºC. Afterwards, 400µl of 50% ethanol was added to the flow through, mixed thoroughly and then loaded onto RNeasy elute column (Qiagen). The column was centrifuged for 15sec at 10000 rpm and the flow through was discarded. The column was washed using 350µl RW1 buffer at 10000 rpm for 1 min and the flow through was discarded. To remove DNA contaminants, 80µl of 0.8% prepared DNase (Qiagen) in RDD buffer was directly added to the center of the column. The column was incubated for 15min at 25ºC and washed with 350µl RW1 buffer for 15sec at 10000rpm. The column was washed twice with 500µl RPE buffer for 15sec at 10000rpm. The column was placed onto a new 2ml collection tube with an open lid and centrifuged for 5min at 13000rpm to get rid of any remaining RPE buffer. The collection tube was discarded, and the column was placed in a 1.5ml collection tube. Approximately 30 - 50µl of RNase-free H_2O was added to the center of the column and centrifuged at 13000rpm for 1min to elute the RNA. The concentration of the isolated RNA was determined using 1µl of the eluate on a Nanodrop machine. The isolated RNA was stored at -80°C for downstream cDNA synthesis protocols.

5.2.9 Complementary DNA (cDNA) synthesis and quantitative RT-PCR

The synthesis of cDNA from isolated RNA was performed using RevertAid First strand cDNA synthesis kit (Thermo Scientific) according to the manufacturer's protocol. In brief, 2µg of isolated RNA was added to 1µl of 18-mer oligo dT primer. The volume of the reaction mixture was made up to 12µl with RNase free water. A master mix of the RevertAid cDNA synthesis kit was made consisting of 4µl of 5x reaction buffer, 1µl of RiboLock RNase inhibitor, 2µl of 10mM dNTP Mix and 1µl of RevertAid M-MuLV RT (200 U/µl). The RNA-oligo dT primer mix was added to the RevertAid cDNA synthesis master mixed prepared, to make a total volume of 20µl. Each tube was centrifuged briefly and incubated at 42ºC for 1h. The reaction was terminated after 1h at 70ºC for 5min and the synthesized cDNA was stored at -20ºC for downstream qRT-PCR.

For quantitative RT-PCR analysis of expressed Ova-antigen, the synthesized cDNA was 1:20 diluted with RNase-free water and 5µl was added to RT-PCR reaction mix consisting of 10µl EVAGreen (BioRad), 1µl each of forward and reverse Ova-antigen primers and 3µl of RNase-free water. The same reaction mix was prepared for primers targeting the housekeeping gene, albumin. The albumin quantification was used for normalization purposes for the expressed Ova-antigen. Each sample was prepared in triplicates on 96 well LightCycler 480 Multiwell plate (Roche) for

the Ova-antigen and albumin primers. The samples were run on LightCycler 480 Real Time PCR instrument (Roche) using the following cycling conditions in the table below:

Cycles	**Steps**	**Temperature**	**Time (mm:ss)**
Pre-incubation (1X)		95^{o}C	15:00
Amplification (45X)	Denaturation	95^{o}C	00:15
	Annealing	58^{o}C	00:20
	Elongation	72^{o}C	00:30
Melting curve (1X)		95^{o}C	00:05
		70^{o}C	01:00
		95^{o}C	Continuous
Cooling		40^{o}C	00:30

5.2.10 Isolation of serum samples for CXCL13 ELISA assay

To quantify the expression of CXCL13 chemokine, blood samples were drawn with a 1ml syringe from the liver using the portal vein D14 post vaccination. The treatment groups consist of AdOva vaccinated OvaXCre and wildtype (WT) mice as well as OvaXCre without AdOva vaccination. Equal volume of blood (200µl) from each treated condition was deposited in a 1.5ml Eppendorf tube. They were then allowed to clot at room temperature for 15 - 35 min. The samples were centrifuged for 10min at 13000rpm, 25^{o}C. This facilitates the separation of the serum samples on top of the whole blood components. Immediately after centrifugation, the serum is aspirated into a new 2ml Eppendorf tube for storage at -20 for short-term or -80 for long-term downstream CXCL13 quantification protocol.

To facilitate the quantification of the concentration of CXCL13 levels in the serum samples, murine BLC (CXCL13) ELISA kit (Thermo Scientific) was used in accordance to the manufacturer's protocol. Briefly, 100µl of each standard and serum sample were placed into appropriate wells, in triplicate. The serum samples were diluted 1:20 in double deionized water. The ELISA plate was incubated overnight with gentle shaking at 4^{o}C. The solution was discarded afterwards and washed 4 times with 1X wash buffer. Washing was done by filling each well with 300µl of the buffer. After the last wash, the plate was blotted on a tissue paper to get rid of residual

wash buffer, and 100µl of 1X biotinylated antibody was added to each well. This was incubated for 1h at room temperature with gentle shaking. The biotinylated solution was discarded, and the wells washed 4x with 1X wash buffer, followed by blotting, after the last washing. Furthermore, 100µl of prepared streptavidin-HRP solution was added to each well and incubated at room temperature for 45min, after which the streptavidin solution was discarded. Wells were washed 4x with wash buffer. The wells were then incubated for 30min with 100µl TMB substrate at room temperature in the dark with gentle shaking and the plates were evaluated within 30min after stopping the reaction. The absorbance was measured with an ELISA plate reader at 450nm. Standard curve was plotted, and the concentration of the serum samples were interpolated from the standard curve plotted.

5.2.11 Multiparametric flow-cytometry

Phenotypic characteristics of isolated cells from the liver and the spleen were performed at the Flow Cytometry Core Facility of the Helmholtz-Zentrum für Infektionsforschung GmbH using either Becton Dickinson LSRII or LSR Fortessa. On the other hand, Aria II SORP and Aria Fusion were used for sorting purposes.

5.2.12 Ex vivo re-stimulation

For intracellular cytokine quantification, isolated cells from the liver or the spleen were re-stimulated ex vivo with PMA/Ionomycin or SIINFEKL peptide depending on the experimental setup.

For adoptive OT-1 transfer studies, isolated cells were re-stimulated ex vivo in RPMI complete media (5% FCS, 1% Pen/Strep, 1% Glutamine, 1mM HEPES) supplemented with 2.5µg/ml SIINFEKL peptide. Briefly, isolated cells were plated in U-bottom (liver cells) or flat bottom (splenocytes) in 96 well plate at a concentration of 2 $x10^5$ cell/well and 5 $x10^5$ cells/well respectively in 100µl RPMI complete media. The plate was incubated at 37ºC for 6-7h in a CO_2 incubator. For the last 4h of incubation, 100µl of 1/500 diluted Brefeldin A (eBiosciences) was added to block cytokine secretion. The cells were harvested after re-stimulation period for downstream intracellular and extracellular staining protocol.

In the case of AdOva vaccination, isolated cells (liver and spleen) were re-stimulated in RPMI complete media supplemented with 10ng/ml PMA and 1µg/ml Ionomycin for 4-5 h in a 37C, 5% CO_2 incubator. The cell concentration was the same as in OT-1 transfer experiment above. For the

last 2h of incubation, 100µl of 1/500 diluted Brefeldin A (eBiosciences) was added to block cytokine secretion. The cells were harvested after re-stimulation period for downstream intracellular and extracellular staining protocols.

5.2.13 Extracellular marker staining

For extracellular marker quantification on antigen specific CD8+ T cells, 5 x 10^5 - 1 x 10^6 LNPCs or splenocytes per sample were used. The cells were incubated with fluorescently labeled antibodies for specific extracellular marker (table of extracellular marker) in V-bottom 96 well plate, in the dark at 4^{o}C for 1h. After which the cells were washed 2x with 2% PBS/FCS to remove any unbound antibodies before proceeding to downstream protocol.

5.2.14 Intracellular cytokine staining

After re-stimulation and phenotyping for extracellular markers, the cells were fixed and permeabilized with BD cytofix/Cytoperm kit (BD Biosciences) according to the manufacturers' protocol. In brief, the cells were fixed with the Cytofix buffer at 4^{o}C for 30 min in the dark, after which the cells were permeabilized with Cytoperm buffer at 4^{o}C for 10min. Fluorescent antibodies specific to Granzyme B (GZMB), Interferon gamma (IFNγ) and tumor necrosis factor α (TNFα) were re-suspended in Cytoperm buffer. The cells were incubated with the antibody cocktail at 4^{o}C for at least 30 min. After the incubation period, cells were washed twice with permeabilization buffer for flow cytometry analysis. Gates for positive marker expression of interest were defined using internal florescence minus one (FMO) controls.

5.2.15 Transcription factor staining

Transcription factors TCF-1, Nur77 and Bcl6 were stained with the help of FoxP3/transcription factor staining Buffer set (eBiosciences), according to the manufacturers' instruction. Briefly, 0.5 - 1 x10^6 cells were fixed with Fixative/Permeabilization buffer at 4^{o}C for 30 min and then permeabilized with the permeabilization buffer for 10min at 4^{o}C. Antibody cocktails consisting of fluorescently tagged TCF-1, Nur77 and Bcl6 were made with the permeabilization buffer. The cells were incubated with the antibody cocktail for 30 min at 4^{o}C. Cells were then washed twice with permeabilization buffer for downstream analysis. Gates were defined as previously stated.

5.2.16 Fluorescent glucose (2-NBDG) uptake

RPMI media (without nutrient supplementation) was reconstituted with 50 – 100µM of fluorescent glucose (2-NBDG). Using a flat bottom 96 well plate, 5 x 10^5 cells/well were cultured with 150µl of 2-NBDG supplemented RPMI media for 45 - 60min in CO_2 incubator at 37^{o}C. Cells were then harvested, washed and phenotypically characterized extracellularly for flow cytometry, and gates were defined as previously described.

5.2.17 Mitochondria staining

To elucidate the characteristics status of mitochondria, Mitotracker Green (MTG), Mitotracker Deep Red (MTDR), TMRE and 2′, 7′-Dichlorofluorescin diacetate (DCFDA) were used. In all these experiments a concentration of 5 x 10^5 cells/well in 150 µl co-culturing media was used. Staining for the purpose of assessing mass of mitochondria was performed with 50nM of MTG whereas the mitochondria membrane potential was assessed with 25nM of MTDR and 300nM of TMRE. The level of mitochondria reactive species (mROS) were measure with 5uM DCFDA. All the stainings were done by reconstituting each staining reagent in nutrient/protein free RPMI media, for 30 min in a CO_2 incubator at 37^{o}C. After the incubation period, cells were harvested, washed and phenotypically characterized extracellularly for flow cytometry. Gates were defined as previously stated.

5.2.18 Sorting liver resident CXCR5+ and CXCR5- T cells

Liver NPCs were isolated as described in **2.2.5**. The isolated cells were extracellularly phenotyped for antigen specific CXCR5+ T cells as described in **2.2.13**. The stained cells were sorted on Aria II or Aria Fusion FACS sorters.

5.2.19 CFSE labelling

CFSE (CellTrace CFSE cell proliferation kit) labelling was performed in order to track T cell proliferation in vivo as well as to evaluate the rate of EL4 (Murine T lymphoma cell line; ATCC TIM-39) killing by T cells. To track the in vivo proliferation of CXCR5+ and CXCR5- T cells, 3 x 10^5 – 6 x 10^5 cells were stained with 2.5uM CFSE at for 15min (25^{o}C) or 10min (37^{o}C) in PBS. CFSE labeling was stopped with 2x volume of 100% FCS addition to sequester the CFSE dye. The cells were washed and re-suspended in PBS for intravenous injection into recipient mice. 0.7 – 1 x 10^5 cells/mouse were injected into high antigen mouse.

In case of EL4 cell labelling with CFSE for downstream protocol, 6 x 105 EL4 cells were labeled with 5uM CFSE ($CFSE^{hi}$) and 0.5uM CFSE ($CFSE^{lo}$) for 10min in a water bath. After this period the labelling was stopped with 2x volume of 100% FCS. The cells were washed for downstream protocol.

5.2.20 In vitro killing assay

The functionality of CXCR5+ and CXCR5- T cells were assessed using in vitro killing assay. Pursuant to this, EL4 cells were exploited for this purpose. In brief, 6 x 10^5 EL4 cells were labelled with high ($CFSE^{hi}$) and low ($CFSE^{lo}$) intensities of CFSE. The $CFSE^{hi}$ labelled EL4 cells were pulsed with 1µg/ml SIINFEKL peptide in 3 x 10^5 EL4 cells/ml for 1.5 h on a 37ºC water bath. The pulsed EL4 cells serve as target cell. The $CFSE^{lo}$ cells were also incubated for the same time period without peptide pulsing. 4000 EL4 cells each from the $CFSE^{hi}$ and $CFSE^{lo}$ labelling were aliquated into U-bottom 96 well plate. The EL4 cells were co-cultured in RPMI complete media with sorted CXCR5+ and CXCR5- T cells isolated from the liver D14 post adoptive OT-1 transfer using an effector: target ratio of 2:1 and 5:1. The co-cultured cells were incubated in a 5% CO2 incubator at 37ºC for 24h. The cells were harvested, washed and analyzed by flow cytometry. The rate of killing induced in EL4 cells by T cells were normalized to the $CFSE^{lo}$ EL4 cells in each well.

5.2.21 Statistical analysis

In this study, 5-7 mice were analyzed per group and statistical analysis was made with GraphPad Prism 8. Statistical significance was calculated using Mann-Whitney's test.

6 References

1. Cui, W. & Kaech, S. M. Generation of effector CD8+ T cells and their conversion to memory T cells. *Immunol. Rev.* **236**, 151–166 (2010).

2. Masopust, D. & Schenkel, J. M. The integration of T cell migration, differentiation and function. *Nat. Rev. Immunol.* **13**, 309–320 (2013).

3. McLane, L. M., Abdel-Hakeem, M. S. & Wherry, E. J. CD8 T Cell Exhaustion During Chronic Viral Infection and Cancer. *Annu. Rev. Immunol.* **37**, 457–495 (2019).

4. McLane;Abdel;Wherry. CD8 T cell exhustion during chronic viral infection and cancer. 1–75 (2018).

5. Hashimoto, M. *et al.* CD8 T Cell Exhaustion in Chronic Infection and Cancer: Opportunities for Interventions. *Annu. Rev. Med.* **69**, 301–318 (2018).

6. Wherry, E. J. T cell exhaustion. *Nat. Immunol.* **12**, 492–499 (2011).

7. Yi, J. S., Cox, M. a. & Zajac, A. J. T-cell exhaustion: Characteristics, causes and conversion. *Immunology* **129**, 474–481 (2010).

8. Wherry, E. J. & Kurachi, M. Molecular and cellular insights into T cell exhaustion. *Nat. Rev. Immunol.* **15**, 486–499 (2015).

9. Nemeth, E., Baird, A. W. & O'Farrelly, C. Microanatomy of the liver immune system. *Semin. Immunopathol.* **31**, 333–343 (2009).

10. Crispe, I. N. The liver as a lymphoid organ. *Annu. Rev. Immunol.* **27**, 147–63 (2009).

11. MacPhee, P. J., Schmidt, E. E. & Groom, A. C. Intermittence of blood flow in liver sinusoids, studied by high-resolution in vivo microscopy. *Am. J. Physiol. - Gastrointest. Liver Physiol.* **269**, (1995).

12. Fraser, R., Dobbs, B. R. & Rogers, G. W. T. Lipoproteins and the liver sieve: The role of the fenestrated sinusoidal endothelium in lipoprotein metabolism, atherosclerosis, and cirrhosis. *Hepatology* **21**, 863–874 (1995).

13. Bogdanos, D. P., Gao, B. & Gershwin, M. E. Liver immunology. *Compr. Physiol.* **3**, 567–98 (2013).

14. Grimm, D., Heeg, M. & Thimme, R. Hepatitis B virus: from immunobiology to immunotherapy. *Clin. Sci.* **124**, 77–85 (2012).

15. Zhigang, T., Cai, Z. & Zhe-Xiong, L. The liver and immune tolerance. *Liver Immunol.* (2013) doi:10.1007/978-3-319-02096-9.

16. MacPhee, P. J., Schmidt, E. E. & Groom, A. C. Evidence for Kupffer cell migration along liver sinusoids, from high- resolution in vivo microscopy. *Am. J. Physiol. - Gastrointest. Liver Physiol.* **263**, (1992).

17. Hines, I. N., Son, G. & Kremer, M. Contribution of gut bacteria to liver pathobiology. *Gastroenterol. Res. Pract.* **2010**, (2010).

18. Berg, R. D. Bacterial translocation from the gastrointestinal tract. *Adv. Exp. Med. Biol.* **473**, 11–30 (2000).

19. Wisse, E., de Zanger, R. B., Charels, K., van der Smissen, P. & McCuskey, R. S. The liver sieve: Considerations concerning the structure and function of endothelial fenestrae, the sinusoidal wall and the space of disse. *Hepatology* **5**, 683–692 (1985).

20. Racanelli, V. & Rehermann, B. The liver as an immunological organ. *Hepatology* **43**, (2006).

21. Protzer, U., Maini, M. K. & Knolle, P. a. Living in the liver: hepatic infections. *Nat. Rev. Immunol.* **12**, 201–213 (2012).

22. Crispe, I. N. Immune tolerance in liver disease. *Hepatology* **60**, 2109–17 (2014).

23. Dunham, R. M. *et al.* Hepatic stellate cells preferentially induce Foxp3+ regulatory T cells by production of retinoic acid. *J. Immunol.* **190**, 2009–16 (2013).

24. Thomson, A. W. & Knolle, P. A. Antigen-presenting cell function in the tolerogenic liver environment. *Nat. Rev. Immunol.* **10**, 753–766 (2010).

25. Doherty, D. G. Immunity, tolerance and autoimmunity in the liver: A comprehensive review. *J. Autoimmun.* **66**, 60–75 (2016).

26. Grakoui, A. & Crispe, I. N. Presentation of hepatocellular antigens. *Cell. Mol. Immunol.* 1–8 (2016) doi:10.1038/cmi.2015.109.

27. Heymann, F. *et al.* Liver Inflammation Abrogates Immunological Tolerance Induced by Kupffer Cells. *Hepatology* **62**, 279–291 (2015).

28. Wong, Y. C., Tay, S. S., McCaughan, G. W., Bowen, D. G. & Bertolino, P. Immune outcomes in the liver: Is CD8 T cell fate determined by the environment? *J. Hepatol.* **63**, 1005–1014 (2015).

29. Berg, M. *et al.* Cross-presentation of antigens from apoptotic tumor cells by liver sinusoidal endothelial cells leads to tumor-specific CD8+ T cell tolerance. *Eur. J. Immunol.* **36**, 2960–2970 (2006).

30. Limmer, A. *et al.* Cross-presentation of oral antigens by liver sinusoidal endothelial cells leads to CD8 T cell tolerance. *Eur. J. Immunol.* **35**, 2970–2981 (2005).

31. Kubes, P. & Jenne, C. Immune Responses in the Liver. *Annu. Rev. Immunol.* **36**, (2018).

32. Franco, A. *et al.* Expression of class I and class II major histocompatibility complex antigens on human hepatocytes. *Hepatology* **8**, 449–454 (1988).

33. Wahl, C., Bochtler, P., Chen, L., Schirmbeck, R. & Reimann, J. B7-H1 on Hepatocytes Facilitates Priming of Specific CD8 T Cells But Limits the Specific Recall of Primed Responses. *Gastroenterology* **135**, 980–988 (2008).

34. Guidotti, L. G. *et al.* Immunosurveillance of the liver by intravascular effector CD8+ T cells. *Cell* **161**, 486–500 (2015).

35. Tiegs, G. & Lohse, A. W. Immune tolerance: What is unique about the liver. *J. Autoimmun.* **34**, 1–6 (2010).

36. Robinson, M. W., Harmon, C. & O'Farrelly, C. Liver immunology and its role in inflammation and homeostasis. *Cell. Mol. Immunol.* **13**, 267–276 (2016).

37. Knoll, P. *et al.* Human Kupffer cells secrete IL-10 in response to lipopolysaccharide (LPS) challenge. *J. Hepatol.* **22**, 226–229 (1995).

38. You, Q., Cheng, L., Kedl, R. M. & Ju, C. Mechanism of T cell tolerance induction by murine hepatic Kupffer cells. *Hepatology* **48**, 978–990 (2008).

39. Bilzer, M., Roggel, F. & Gerbes, A. L. Role of Kupffer cells in host defense and liver

disease. *Liver Int.* **26**, 1175–1186 (2006).

40. Huang, L.-R. R. *et al.* Intrahepatic myeloid-cell aggregates enable local proliferation of CD8(+) T cells and successful immunotherapy against chronic viral liver infection. *Nat. Immunol.* **14**, 1–12 (2013).

41. Wieland, S. *et al.* Simultaneous detection of hepatitis C virus and interferon stimulated gene expression in infected human liver. *Hepatology* **59**, 2121–2130 (2014).

42. Knolle, P. a. & Thimme, R. Hepatic immune regulation and its involvement in viral hepatitis infection. *Gastroenterology* **146**, 1193–1207 (2014).

43. Thimme, R. *et al.* Viral and immunological determinants of hepatitis C virus clearance, persistence, and disease. *Proc. Natl. Acad. Sci. U. S. A.* **99**, 15661–15668 (2002).

44. Thimme, R. *et al.* Determinants of viral clearance and persistence during acute hepatitis C virus infection. *J. Exp. Med.* **194**, 1395–1406 (2001).

45. Rehermann, B. Pathogenesis of chronic viral hepatitis: Differential roles of T cells and NK cells. *Nat. Med.* **19**, 859–868 (2013).

46. Klenerman, P. & Thimme, R. T cell responses in hepatitis C: The good, the bad and the unconventional. *Gut* **61**, 1226–1234 (2012).

47. Hatzi, K. *et al.* BCL6 orchestrates Tfh cell differentiation via multiple distinct mechanisms. *J. Exp. Med.* **212**, 539–553 (2015).

48. Kahan, S. M., Wherry, E. J. & Zajac, A. J. T cell exhaustion during persistent viral infections. *Virology* **479–480**, 180–193 (2015).

49. Sun, J. Immune and non-immune responses to hepatitis C virus infection. *World J. Gastroenterol.* **21**, 10739 (2015).

50. Callendret, B. *et al.* T-cell immunity and hepatitis C virus reinfection after cure of chronic hepatitis C with an interferon-free antiviral regimen in a chimpanzee. *Hepatology* **60**, 1531–1540 (2014).

51. Shin, E.-C., Sung, P. S. & Park, S.-H. Immune responses and immunopathology in acute and chronic viral hepatitis. *Nat. Rev. Immunol.* (2016) doi:10.1038/nri.2016.69.

52. Maini, M. K. & Burton, A. R. Restoring, releasing or replacing adaptive immunity in chronic hepatitis B. *Nat. Rev. Gastroenterol. Hepatol.* **16**, 662–675 (2019).

53. Matloubian, M., Concepcion, R. J. & Ahmed, R. CD4+ T cells are required to sustain CD8+ cytotoxic T-cell responses during chronic viral infection. *J. Virol.* **68**, 8056–63 (1994).

54. Mueller, S. N. & Ahmed, R. High antigen levels are the cause of T cell exhaustion during chronic viral infection. *Proc. Natl. Acad. Sci. U. S. A.* **106**, 8623–8628 (2009).

55. Shin, H., Blackburn, S. D., Blattman, J. N. & Wherry, E. J. Viral antigen and extensive division maintain virus-specific CD8 T cells during chronic infection. *J. Exp. Med.* **204**, 941–949 (2007).

56. Wherry, E. J. *et al.* Molecular Signature of CD8+ T Cell Exhaustion during Chronic Viral Infection. *Immunity* **27**, 670–684 (2007).

57. Reignat, S. *et al.* Escaping high viral load exhaustion: CD8 cells with altered tetramer binding in chronic hepatitis B virus infection. *J. Exp. Med.* **195**, 1089–1101 (2002).

58. Goepfert, P. A. *et al.* A Significant Number of Human Immunodeficiency Virus Epitope-Specific Cytotoxic T Lymphocytes Detected by Tetramer Binding Do Not Produce Gamma Interferon. *J. Virol.* **74**, 10249–10255 (2000).

59. Zajac, A. J. *et al.* Viral immune evasion due to persistence of activated T cells without effector function. *J. Exp. Med.* **188**, 2205–2213 (1998).

60. Angelosanto, J. M., Blackburn, S. D., Crawford, A. & Wherry, E. J. Progressive Loss of Memory T Cell Potential and Commitment to Exhaustion during Chronic Viral Infection. *J. Virol.* **86**, 8161–8170 (2012).

61. Brooks, D. G., McGavern, D. B. & Oldstone, M. B. A. Reprogramming of antiviral T cells prevents inactivation and restores T cell activity during persistent viral infection. *J. Clin. Invest.* **116**, 1675–1685 (2006).

62. Curtsinger, J. M. & Mescher, M. F. Inflammatory cytokines as a third signal for T cell activation. *Curr. Opin. Immunol.* **22**, 333–340 (2010).

63. Stelekati, E. *et al.* Bystander chronic infection negatively impacts development of CD8+ T cell memory. *Immunity* **40**, 801–813 (2014).

64. Li, M. O., Wan, Y. Y., Sanjabi, S., Robertson, A.-K. L. & Flavell, R. A. Transforming Growth Factor-B Regulation of Immune Responses. *Annu. Rev. Immunol.* **24**, 99–146 (2006).

65. Couper, K. N., Blount, D. G. & Riley, E. M. IL-10: The Master Regulator of Immunity to Infection. *J. Immunol.* **180**, 5771–5777 (2008).

66. Buck, M. D., O'Sullivan, D., Pearce, E. L., O'Sullivan, D. & Pearce, E. L. T cell metabolism drives immunity. *J. Exp. Med.* **212**, 1345–1360 (2015).

67. O'Sullivan, D. & Pearce, E. L. Targeting T cell metabolism for therapy. *Trends Immunol.* **36**, 71–80 (2015).

68. van der Windt, G. J. W. *et al.* Mitochondrial Respiratory Capacity Is a Critical Regulator of CD8 + T Cell Memory Development. *Immunity* **36**, 68–78 (2012).

69. Patsoukis, N. *et al.* PD-1 alters T-cell metabolic reprogramming by inhibiting glycolysis and promoting lipolysis and fatty acid oxidation. *Nat. Commun.* **6**, (2015).

70. Bengsch, B. *et al.* Bioenergetic Insufficiencies Due to Metabolic Alterations Regulated by the Inhibitory Receptor PD-1 Are an Early Driver of CD8+ T Cell Exhaustion. *Immunity* **45**, 358–373 (2016).

71. Blackburn, S. D. *et al.* Coregulation of CD8+ T cell exhaustion by multiple inhibitory receptors during chronic viral infection. *Nat. Immunol.* **10**, 29–37 (2009).

72. Schildberg, F. A., Klein, S. R., Freeman, G. J. & Sharpe, A. H. Coinhibitory Pathways in the B7-CD28 Ligand-Receptor Family. *Immunity* **44**, 955–972 (2016).

73. Patsoukis, N. *et al.* Selective effects of PD-1 on Akt and ras pathways regulate molecular components of the cell cycle and inhibit T cell proliferation. *Sci. Signal.* **5**, (2012).

74. Chemnitz, J. M., Parry, R. V., Nichols, K. E., June, C. H. & Riley, J. L. SHP-1 and SHP-2 Associate with Immunoreceptor Tyrosine-Based Switch Motif of Programmed Death 1 upon Primary Human T Cell Stimulation, but Only Receptor Ligation Prevents T Cell Activation. *J. Immunol.* **173**, 945–954 (2004).

75. Youngblood, B. *et al.* Cutting Edge: Prolonged Exposure to HIV Reinforces a Poised Epigenetic Program for PD-1 Expression in Virus-Specific CD8 T Cells. *J. Immunol.* **191**,

540–544 (2013).

76. Youngblood, B. *et al.* Chronic Virus Infection Enforces Demethylation of the Locus that Encodes PD-1 in Antigen-Specific CD8+ T Cells. *Immunity* **35**, 400–412 (2011).

77. Odorizzi, P. M., Pauken, K. E., Paley, M. A., Sharpe, A. & John Wherry, E. Genetic absence of PD-1 promotes accumulation of terminally differentiated exhausted CD8+ T cells. *J. Exp. Med.* **212**, 1125–1137 (2015).

78. Frebel, H. *et al.* Programmed death 1 protects from fatal circulatory failure during systemic virus infection of mice. *J. Exp. Med.* **209**, 2485–2499 (2012).

79. Barber, D. L. *et al.* Restoring function in exhausted CD8 T cells during chronic viral infection. *Nature* **439**, 682–687 (2006).

80. Pentcheva-Hoang, T., Corse, E. & Allison, J. P. Negative regulators of T-cell activation: Potential targets for therapeutic intervention in cancer, autoimmune disease, and persistent infections. *Immunol. Rev.* **229**, 67–87 (2009).

81. Hodi, F. S. *et al.* Improved survival with ipilimumab in patients with metastatic melanoma. *N. Engl. J. Med.* **363**, 711–723 (2010).

82. Nakamoto, N. *et al.* Synergistic reversal of intrahepatic HCV-specific CD8 T cell exhaustion by combined PD-1/CTLA-4 blockade. *PLoS Pathog.* **5**, (2009).

83. Chen, D. S. & Mellman, I. Oncology meets immunology: The cancer-immunity cycle. *Immunity* **39**, 1–10 (2013).

84. Frauwirth, K. A. *et al.* The CD28 Signaling Pathway Regulates Glucose Metabolism of metabolism in response to changes in cellular condi- tions. However, it has recently been shown that signals from cell surface receptors are required to control the ability of resting cells to tak. *Immunity* **16**, 769–777 (2002).

85. Esensten, J. H., Helou, Y. A., Chopra, G., Weiss, A. & Bluestone, J. A. CD28 Costimulation: From Mechanism to Therapy. *Immunity* **44**, 973–988 (2016).

86. Kamphorst, A. O. *et al.* Rescue of exhausted CD8 T cells by PD-1 – targeted therapies is CD28-dependent. **1427**, 1423–1427 (2017).

87. Vezys, V. *et al.* 4-1BB Signaling Synergizes with Programmed Death Ligand 1 Blockade To Augment CD8 T Cell Responses during Chronic Viral Infection. *J. Immunol.* **187**, 1634–1642 (2011).

88. Penaloza-MacMaster, P. *et al.* Opposing Effects of CD70 Costimulation during Acute and Chronic Lymphocytic Choriomeningitis Virus Infection of Mice. *J. Virol.* **85**, 6168–6174 (2011).

89. Paley, M. A. *et al.* Progenitor and terminal subsets of CD8+ T cells cooperate to contain chronic viral infection. *Science (80-.).* **338**, 1220–1225 (2012).

90. Doering, T. a. *et al.* Network Analysis Reveals Centrally Connected Genes and Pathways Involved in CD8+ T Cell Exhaustion versus Memory. *Immunity* **37**, 1130–1144 (2012).

91. Intlekofer, A. M. *et al.* Effector and memory CD8+ T cell fate coupled by T-bet and eomesodermin. *Nat. Immunol.* **6**, 1236–1244 (2005).

92. Banerjee, A. *et al.* Cutting Edge: The Transcription Factor Eomesodermin Enables CD8 + T Cells To Compete for the Memory Cell Niche . *J. Immunol.* **185**, 4988–4992 (2010).

93. Pearce, E. L. *et al.* Control of Effector CD8+ T Cell Function by the Transcription Factor Eomesodermin. *Science (80-.).* **302**, 1041–1043 (2003).

94. Fan, R. *et al.* T-bet expression in CD8+ T cells associated with chronic hepatitis B virus infection. *Virol. J.* **13**, 1–10 (2016).

95. Zhou, X. *et al.* Differentiation and Persistence of Memory CD8+ T Cells Depend on T Cell Factor 1. *Immunity* **33**, 229–240 (2010).

96. Utzschneider, D. T. T. *et al.* T Cell Factor 1-Expressing Memory-like CD8+ T Cells Sustain the Immune Response to Chronic Viral Infections. *Immunity* **45**, 415–427 (2016).

97. Wu, T. *et al.* The TCF1-Bcl6 axis counteracts type I interferon to repress exhaustion and maintain T cell stemness. (2016) doi:10.1002/dev.21214.Developmental.

98. Buenrostro, J. D., Wu, B., Chang, H. Y. & Greenleaf, W. J. ATAC-seq: A method for assaying chromatin accessibility genome-wide. *Curr. Protoc. Mol. Biol.* **2015**, 21.29.1-21.29.9 (2015).

99. Sen, D. R. *et al.* The epigenetic landscape of T cell exhaustion. *Science (80-.).* **0491**, 1165–1169 (2016).

100. Pauken, K. E. *et al.* Epigenetic stability of exhausted T cells limits durability of reinvigoration by PD-1 blockade. *Science (80-.).* **354**, 1160–1165 (2016).

101. Scott-Browne, J. P. *et al.* Dynamic Changes in Chromatin Accessibility Occur in CD8+ T Cells Responding to Viral Infection. *Immunity* **45**, 1–14 (2016).

102. Ghoneim, H. E. *et al.* De Novo Epigenetic Programs Inhibit PD-1 Blockade-Mediated T Cell Rejuvenation. *Cell* **170**, 142-157.e19 (2017).

103. Im, S. J. *et al.* Defining CD8 + T cells that provide the proliferative burst after PD-1 therapy. *Nature* **537**, 417–421 (2016).

104. He, R. *et al.* Follicular CXCR5-expressing CD8(+) T cells curtail chronic viral infection. *Nature* **537**, 1–20 (2016).

105. Mylvaganam, G. H. *et al.* Dynamics of SIV-specific CXCR5+ CD8 T cells during chronic SIV infection. *Proc. Natl. Acad. Sci.* **114**, 1976–1981 (2017).

106. Chu, F. *et al.* CXCR5 + CD8 + T cells are a distinct functional subset with an antitumor activity. *Leukemia* (2019) doi:10.1038/s41375-019-0464-2.

107. Miller, B. C. *et al.* Subsets of exhausted CD8 + T cells differentially mediate tumor control and respond to checkpoint blockade. *Nat. Immunol.* **20**, 326–336 (2019).

108. Xu, L. *et al.* The transcription factor TCF-1 initiates the differentiation of TFH cells during acute viral infection. *Nat. Immunol.* **16**, 991–999 (2015).

109. Im, S. J. *et al.* Defining CD8 + T cells that provide the proliferative burst after PD-1 therapy. *Nature* **537**, 417–421 (2016).

110. Ochel, A. *et al.* Effective intrahepatic CD8+ T-cell immune responses are induced by low but not high numbers of antigen-expressing hepatocytes. *Cell. Mol. Immunol.* 1–11 (2015) doi:10.1038/cmi.2015.80.

111. Sandhu, U. *et al.* Strict control of transgene expression in a mouse model for sensitive biological applications based on RMCE compatible ES cells. *Nucleic Acids Res.* **39**, 1–13

(2011).

112. Cebula, M. *et al.* An Inducible Transgenic Mouse Model for Immune Mediated Hepatitis Showing Clearance of Antigen Expressing Hepatocytes by CD8+ T Cells. *PLoS One* **8**, 1–9 (2013).

113. Imayoshi, I., Ohtsuka, T., Metzger, D., Chambon, P. & Kageyama, R. Temporal regulation of Cre recombinase activity in neural stem cells. *Genesis* **44**, 233–238 (2006).

114. Cebula, M. *et al.* TLR9-Mediated Conditioning of Liver Environment Is Essential for Successful Intrahepatic Immunotherapy and Effective Memory Recall. *Mol. Ther.* **25**, 2289–2298 (2017).

115. Mueller, S. N. & Mackay, L. K. Tissue-resident memory T cells: Local specialists in immune defence. *Nat. Rev. Immunol.* **16**, 79–89 (2016).

116. Masopust, D. & Soerens, A. G. Tissue-Resident T Cells and Other Resident Leukocytes. *Annu. Rev. Immunol.* **37**, 521–546 (2019).

117. Jiang, Y., Li, Y. & Zhu, B. T-cell exhaustion in the tumor microenvironment. *Cell Death Dis.* **6**, 1–9 (2015).

118. Danilo, M., Chennupati, V., Silva, J. G., Siegert, S. & Held, W. Suppression of Tcf1 by Inflammatory Cytokines Facilitates Effector CD8 T Cell Differentiation. *Cell Rep.* **22**, 2107–2117 (2018).

119. Shi, J. *et al.* PD-1 Controls Follicular T Helper Cell Positioning and Function. *Immunity* **49**, 264-274.e4 (2018).

120. McNamara, H. A. *et al.* Up-regulation of LFA-1 allows liver-resident memory T cells to patrol and remain in the hepatic sinusoids. *Sci. Immunol.* **2**, (2017).

121. Chen, Z. *et al.* TCF-1-Centered Transcriptional Network Drives an Effector versus Exhausted CD8 T Cell-Fate Decision. *Immunity* 1–16 (2019) doi:10.1016/J.IMMUNI.2019.09.013.

122. Milner, J. J. *et al.* Runx3 programs CD8+T cell residency in non-lymphoid tissues and tumours. *Nature* **552**, 253–257 (2017).

123. Skon, C. N. *et al.* Transcriptional downregulation of S1pr1 is required for the establishment of resident memory CD8+ T cells. *Nat. Immunol.* **14**, 1285–1293 (2013).

124. Li, C. *et al.* The Transcription Factor Bhlhe40 Programs Mitochondrial Regulation of Resident CD8+ T Cell Fitness and Functionality. *Immunity* **51**, 491-507.e7 (2019).

125. MacIver, N. J., Michalek, R. D. & Rathmell, J. C. Metabolic Regulation of T Lymphocytes. *Annu. Rev. Immunol.* **31**, 259–283 (2013).

126. Borges Da Silva, H. *et al.* The purinergic receptor P2RX7 directs metabolic fitness of long-lived memory CD8+ T cells. *Nature* **559**, 264–268 (2018).

127. Bantug, G. R. *et al.* ER contact sites are immunometabolic hubs that orchestrate the rapid recall response of memory CD8 + T cells. **48**, 542–555 (2018).

128. Desdín-Micó, G., Soto-Heredero, G. & Mittelbrunn, M. Mitochondrial activity in T cells. *Mitochondrion* **41**, 51–57 (2018).

129. Sena, L. A. *et al.* Mitochondria Are Required for Antigen-Specific T Cell Activation through Reactive Oxygen Species Signaling. *Immunity* **38**, 225–236 (2013).

130. Dan Dunn, J., Alvarez, L. A. J., Zhang, X. & Soldati, T. Reactive oxygen species and mitochondria: A nexus of cellular homeostasis. *Redox Biol.* **6**, 472–485 (2015).

131. Klein Geltink, R. I. *et al.* Mitochondrial Priming by CD28. *Cell* **171**, 385-397.e11 (2017).

132. Pauken, K. E. & Wherry, E. J. Overcoming T cell exhaustion in infection and cancer. *Trends Immunol.* **36**, 265–276 (2015).

133. Zahm, C. D., Colluru, V. T., McIlwain, S. J., Ong, I. M. & McNeel, D. G. TLR stimulation during T-cell activation lowers PD-1 expression on CD8 + T cells. *Cancer Immunol. Res.* **6**, 1364–1374 (2018).

134. Knolle, P. a., Böttcher, J. & Huang, L. R. The role of hepatic immune regulation in systemic immunity to viral infection. *Med. Microbiol. Immunol.* **204**, 21–27 (2015).

135. Chen, Z. *et al.* TCF-1-Centered Transcriptional Network Drives an Effector versus Exhausted CD8 T Cell-Fate Decision. *Immunity* **51**, 840-855.e5 (2019).

136. Pradervand, S. *et al.* Intratumoral Tcf1+PD-1+CD8+ T Cells with Stem-like Properties

Promote Tumor Control in Response to Vaccination and Checkpoint Blockade Immunotherapy. *Immunity* **50**, 195-211.e10 (2019).

137. Wu, T. *et al.* The TCF1-Bcl6 axis counteracts type I interferon to repress exhaustion and maintain T cell stemness. *Sci. Immunol.* **1**, 54–60 (2016).

138. Bertoletti, A. & Ferrari, C. Adaptive immunity in HBV infection. *J. Hepatol.* **64**, S71–S83 (2016).

139. Leong, Y. A. *et al.* CXCR5 + follicular cytotoxic T cells control viral infection in B cell follicles. (2016) doi:10.1038/ni.3543.NATURE.

140. Kazanietz, M. G., Durando, M. & Cooke, M. CXCL13 and its receptor CXCR5 in cancer: Inflammation, immune response, and beyond. *Front. Endocrinol. (Lausanne).* **10**, 1–15 (2019).

141. Li, Y. *et al.* CXCL13-mediated recruitment of intrahepatic CXCR5+CD8+T cells favors viral control in chronic HBV infection. *J. Hepatol.* (2019) doi:10.1016/j.jhep.2019.09.031.

142. Nicolas W. Cortes-Penfield, Barbara W. Trautner, R. J. Endogenous Nur77 is a specific indicator of antigen receptor signaling in human T and B cells. *Physiol. Behav.* **176**, 139–148 (2017).

143. Jin, X. *et al.* Dramatic rise in plasma viremia after CD8+ T cell depletion in simian immunodeficiency virus-infected macaques. *J. Exp. Med.* **189**, 991–998 (1999).

144. Schmitz, J. E. *et al.* Control of viremia in simian immunodeficiency virus infection by CD8+ lymphocytes. *Science (80-.).* **283**, 857–860 (1999).

145. Wieland, D. *et al.* TCF1+ hepatitis C virus-specific CD8+ T cells are maintained after cessation of chronic antigen stimulation. *Nat. Commun.* **8**, 1–13 (2017).

146. Almeida, L., Lochner, M., Berod, L. & Sparwasser, T. Metabolic pathways in T cell activation and lineage differentiation. *Semin. Immunol.* **28**, 1–11 (2016).

147. Mills, E. L., Kelly, B. & O'Neill, L. A. J. Mitochondria are the powerhouses of immunity. *Nat. Immunol.* **18**, 488–498 (2017).

148. Klein Geltink, R. I., Kyle, R. L. & Pearce, E. L. Unraveling the Complex Interplay Between

T Cell Metabolism and Function. *Annu. Rev. Immunol.* **36**, 461–488 (2018).

149. Buck, M. D. D. *et al.* Mitochondrial Dynamics Controls T Cell Fate through Metabolic Programming. *Cell* **166**, 63–76 (2016).

150. Lang, P. A. *et al.* Reactive oxygen species delay control of lymphocytic choriomeningitis virus. *Cell Death Differ.* **20**, 649–658 (2013).

151. Schieber, M. & Chandel, N. S. ROS function in redox signaling and oxidative stress. *Curr. Biol.* **24**, R453–R462 (2014).

152. Scharping, N. E. *et al.* The Tumor Microenvironment Represses T Cell Mitochondrial Biogenesis to Drive Intratumoral T Cell Metabolic Insufficiency and Dysfunction. *Immunity* **45**, 701–703 (2016).

153. Huang, Z. *et al.* IL-27 promotes the expansion of self-renewing CD8 + T cells in persistent viral infection . *J. Exp. Med.* **216**, 1791–1808 (2019).

154. Schuler, M., Dierich, A., Chambon, P. & Metzger, D. Efficient temporally controlled targeted somatic mutagenesis in hepatocytes of the mouse. *Genesis* **39**, 167–172 (2004).

155. Schirmbeck, R., Reimann, J., Kochanek, S. & Kreppel, F. The immunogenicity of adenovirus vectors limits the multispecificity of CD8 T-cell responses to vector-encoded transgenic antigens. *Mol. Ther.* **16**, 1609–1616 (2008).

156. Wortmann, A. *et al.* Fully detargeted polyethylene glycol-coated adenovirus vectors are potent genetic vaccines and escape from pre-existing anti-adenovirus antibodies. *Mol. Ther.* **16**, 154–162 (2008).

7 Appendix

7.1 Abbreviations

2-NBDG	Florescent glucose
AdOva	Adenoviral vector encoding Ovalbumin
ATP	Adenosine triphosphate
Bcl	B cell lymphoma
APCs	Antigen presenting cells
ATACseq	Assay for Transposase-accessible chromatin using sequencing
CCR	Chemokine receptor
CD	Cluster of differentiation
CpG ODN	CpG oligodeoxynucleotide
Cre	Cyclic recombinase
CTLA-4	cytotoxic T-lymphocyte antigen 4
CXCR	Chemokine receptor
CXCL	Chemokine ligand
DAAs	Direct acting antivirals
DCs	Dendritic cells
DCFDA	2′, 7′-Dichlorofluorescin diacetate
DNMT3A	DNA methyltransferase 3A
Eomes	Eomesodermin
Glut	Glucose transporter
GZMB	Granzyme b
HBV	Hepatitis B virus

HCV	Hepatitis C virus
HIV	human immunodeficiency virus
IDO	Indole-amine 2, 3-dioxygenase
IL	Interleukin
IRs	Inhibitory receptors
ICAM	Intracellular adhesion molecule
ICOS	Inducible T cell costimulator
IFNα/β	Interferon α/β
IFNγ	Interferon gamma
ITIM	Immunoreceptor tyrosine-based inhibitory motif
ITSM	immunoreceptor tyrosine-based switch motif
KCs	Kupffer cells
KLRG-1	Killer cell lectin like receptor G1
LCMV	Lymphocytic choriomeningitis virus
Lag-3	Leukocyte activating gene 3
LFA	Lymphocyte function associated antigen
LPS	Lipopolysaccharide
LNPCs	Liver non-parenchyma cells
LSECs	Liver sinusoidal endothelial cells
mDCs	Myeloid-derived DCs
mRNA	Messenger ribonucleotide acid
mTOR	mammalian target of rapamycin
MFI	Median florescence intensity
MHC I & II	Major histocompatibility molecule I & II

MTDR	Mitotracker Deep Red
mROS	Mitochondria reactive oxygen species
MTG	Mitotracker Green dye
MPECs	Memory precursor cells
NK cells	Natural killer cells
NKT cells	Natural Killer T cells
Nur	Nuclear receptor
OXPHOS	oxidative phosphorylation
Ova	Ovalbumin
PD-L	Programmed death ligand
pDCs	Plasmacytoid DCs
PAMPs	Pathogen associated molecular patterns
PD-1	Programmed death 1
PI3K	phosphoinositide 3-kinase
PGC-1α	Peroxisome proliferator-activated receptor γ coactivator 1α
P2X7R	Purinergic receptor
TIM-3	T cell immunoglobulin molecule 3
RT-PCR	Reverse transcriptase polymerase chain reaction
Tex	Exhausted T cells
TGF-β	Transforming growth factor β
TCR	T cell receptor
TCF-1	T cell factor 1
T-bet	T-box factors
Tfh	follicular helper T cells

TLR	Toll like receptor
TMRE	Tetramethylrhodamine ethyl ester, perchlorate
Teff	Effector T cell
Tmem	Memory T cell
TNFα	Tumor necrosis factor α

7.2 List of Figures

7.3 Acknowledgement

First and foremost, I would like to appreciate my supervisor Prof. Dr. Dagmar Wirth for her immense support during my research work. I am extremely grateful for her guidance. I would like to thank Dr. Marcin Cebula for his tutelage on planning animal experiments. Many thanks to Dr. Mario Köster for his thought-provoking questions, they were very much appreciated.

Secondly, I would like to thank my thesis committee members Prof. Dr. Ingo Schmitz, Dr. Hansjörg Hauser and Prof. Dr. Nikolaus Gaßler for their excellent scientific contribution during this project. Not forgetting Dr. Björn Rissiek for his suggestions on isolating healthy liver resident T cells for adoptive transfer.

I also want to thank all members of MSYS and InSCREENeX, for the special atmosphere shared during the brainstorming events, thank you all. Most importantly, my special appreciation goes to Petra Buhr for genotyping all my mice, and Sara Behme for helping me in various aspects of this project. In addition, I would like to thank Dr. Ivana Kutle, Dr. Natascha Gödeke, Dr. Aileen Bleisch, Anne Dittrich, Artur Wilhelm and Sabrina Herrmann for all their contribution and the great moments we shared together. Enormous gratitude to Sami Ullah for being a wonderful but annoying buddy, surely, those time spent together will be missed.

Finally, I would like to thank my family for their wonderful support and believing in my potential.

7.4 Curriculum Vitae

PERSONAL INFORMATION

Kingsley G. Kumashie

Siedlerstraße 26, 38124 Braunschweig, Germany

E-Mail: gideonkumashie88@gmail.com

D.O.B: 04-04-1988 **Gender**: Male

EDUCATION & RESEARCH EXPERIENCE

2016 - Date **Ph.D. student in Biology**

Model Systems for Infection and Immunity Lab

Helmholtz Centre for Infection Research, Braunschweig

Chronic liver infections: New in-situ insights into the dynamic regulation of exhausted CD8+ T cell subsets (PhD Project)

2013 - 2015 **MSc in Molecular Medicine**

Centre of Molecular Inflammation Research, CEMIR

Norwegian University of Science and Technology (NTNU)

Flow-cytometric analysis of autophagy in activated primary human CD4+ T cells (Master project)

2008 - 2012 **BSc in Biochemistry**

Department of Biochemistry, Cell and Molecular Biology

University of Ghana

WORK EXPERIENCE

2015 - 2016 West African Centre for Cell Biology of Infectious Pathogens, WACCBIP

Profiling immune cell function in malaria infected patients